TECHNISCHE UNIVERSITÄT WIEN
Vienna University of Technology

D I P L O M A R B E I T

NEUROSCIENCE MEETS PHOTOPHARMACOLOGY:

SCALE-UP AND OPTIMIZATION OF THE SYNTHESIS OF PHOTOSWITCHABLE PAROXETINE BASED SEROTONIN REUPTAKE INHIBITORS

ausgeführt zum Zwecke der Erlangung des akademischen Grades eines Diplomingenieurs der technischen Wissenschaften unter der Leitung von

Univ. Prof. Dipl.-Ing. Dr. techn. Marko D. Mihovilovic

Institut für Angewandte Synthesechemie (E163)

eingereicht an der

Fakultät für Technische Chemie

von

Philipp Mikšovsky, BSc

Arnikaweg 27, 1220 Wien

Wien, am 18. 06. 2019

Das Ergebnis einer einjährigen, sehr lehrreichen Reise.

Vielen Dank an euch alle!

Table of Contents

Danksagung

Zuallererst möchte ich Dir, Marko, für die Möglichkeit danken, meine Diplomarbeit in Deiner Forschungsgruppe praktisch zu absolvieren und schlussendlich auch zu Papier zu bringen. Diese oder ähnliche Sätze mögen Dir schon das eine oder andere Mal im Zuge deiner beruflichen Laufbahn untergekommen sein und mitunter auch schon etwas „abgedroschen“ klingen, jedoch ist es für mich keineswegs eine Selbstverständlichkeit eine Diplomarbeit unter Deiner Leitung absolvieren zu dürfen. Ganz besonders möchte ich Dir in diesem Zusammenhang für die ehrlichen aber auch klaren Worte bei dem einen oder anderen Gespräch danken, die, unterstützt durch Verständnis und Rücksicht Deinerseits, mir geholfen haben, weiter- und voranzukommen. Des weiteren ist es mir ein Anliegen, Dir für die Diversität der Forschungsgruppe zu danken, wodurch es zwar manchmal nicht einfach erscheinen mag, alle verschiedenen Meinungen „unter einen Hut zu bringen“, im Endeffekt jedoch zu einem tieferen Verständnis füreinander führt, das in jeder Hinsicht für den weiteren Werdegang eines jeden von uns von immenser Bedeutung sein kann.

Dieser Dank gilt auch Euch, Michael und Flo, die ihr ebenfalls euren einzigartigen Beitrag zum Zusammenhalt sowie der Diversität der Gruppe beisteuert, nicht zuletzt durch eure komplett unterschiedlichen Fachgebiete. Ebenso der „group retreat“ samt Aktivitäten und der „Feedbackbox“ seien in diesem Zusammenhang erwähnt.

Ebenso möchte ich Dir, Christian, danken, von dem ich sowohl aus chemischer als auch persönlicher Sicht sehr viel lernen konnte. Du schaffst es, jedem das zu geben was er braucht um weiterzukommen und zwar, unabhängig von Person und „Anforderungen“, auf eine respektvolle Art und Weise.

Auch Dir, Dominik, gilt mein Dank, es war mir eine Ehre Dein Projekt fortsetzen zu dürfen und auf solider Basis weiterarbeiten zu können. Ebenso möchte ich mich für die Möglichkeit bedanken, an zwei Deiner Papers mitzuwirken.

Angekommen bei euch, liebe Kollegen des G20, möchte ich mich bei jedem von euch für die Atmosphäre im Labor bedanken, der wahre Grund, warum man sich der chemikalienangereicherten Atmosphäre überhaupt aussetzt. Spaß beseite, von der Hilfe bei chemischen sowie technischen Fragen über Messung unzähliger NMR bis hin zu persönlichen Gesprächen war echt alles dabei. Vielen lieben Dank an euch,

Clemens, Markus, Hubert, Sebastian und Laszlo sowie Kathi, Antonio, Jesse und Matthias!

Auch euch, Charlie, David, David, Martin, Resi, Dani, Blanca, Rafaela, Sarah, Viktor, Hamid, Erna und Alex, möchte ich für jegliche Hilfe chemisch-technischer sowie persönlicher Natur danken. Auch euch ein großes Dankeschön für euren Beitrag zum Klimawandel innerhalb der Gruppe!

Ebenfalls danken möchte ich den weiteren Forschungsgruppen des Instituts für Hilfe sowie Aufeinandertreffen jeglicher Art und sei es nur im Zuge des Syntheselabors gewesen, das mir in diesem Zusammenhang ebenfalls sehr positiv in Erinnerung bleiben wird.

Ein ganz großes Dankeschön auch an Dich, Irena, die Du mir weit über das normale Maß für meine Messungen inklusive Methodenentwicklung zur Verfügung gestanden bist. Du warst mir eine große Hilfe!

Dem anschließend möchte ich mich bei allen weiteren Mitarbeitern des Instituts bedanken, im Speziellen bei Florian Untersteiner, Gerhard Seebauer, Thomas, Martin, Isolde, Emiliya und Danko. Vielen Dank für euren Beitrag!

Zu guter Letzt möchte ich mich bei euch, Mama, Papa, Christoph, Bernhard und Michael, sowie Freunden, im Speziellen bei Christian, Marion und Laura, aber auch meinem gesamten Umfeld für die nötige Unterstützung jeglicher Art bedanken, die diese Arbeit erst möglich gemacht hat. Ich danke jedem Einzelnen von euch von ganzem Herzen!

In diesem Sinne bleibt mir nur noch eins zu sagen, und zwar:

Es war mir eine Ehre!

Vielen Dank an jeden Einzelnen von euch!

Abstract

In the future, multidisciplinary co-operations in science will be of more value and importance than ever due to proceeding differentiation into different research areas.

One of the most important examples of multidisciplinary science is the field of brain research. Ongoing research in the field of neurotransmission led to the establishment of a new multidisciplinary field, called photopharmacology.

Photophamacology deals, amongst others, with the synthesis of photo-dependent inhibitors, which allow the control of the reuptake of neurotransmitters by transporter proteins via light. The advantages of using light as stimulus are obvious. Light allows a temporal, contactless and especially a spacial control. This should enable neuroscientists in the future to study the neural activity in different brain areas separately.

Developing such a photo-dependent inhibitor for the serotonin transporter (SERT) is of high interest. A malfunction of the transporter leads, for example, to depressive disorders. Today such disorders are treated with selective serotonin reuptake inhibitors (SSRI), commonly known as antidepressants.

Recently azo-paroxetine, such a photo-dependent inhibitor, was developed. It is based on paroxetine, a widely described SSRI, and azobenzene, one representative of the best studied class of photoswitches.

This work focused on the optimization and the scale-up of the 7-step synthesis to the azo precursor. High quantities of the azo precursor allow the derivatization with substituted azobenzenes in order to find more potent azo-paroxetine based photoswitchable SSRIs with a more efficient switch between the biological active and inactive state in the future.

Additionally the optimized synthesis, developed for azo-paroxetine, was successfully applied to the entirely different HTI-paroxetine based SSRI. Hemithioindigo (HTI) as photoswitchable moiety shows a red-shift in comparison to azobenzenes, which is desirable for biological applications.

Kurzfassung

In Zukunft werden multidisziplinäre Kooperationen in der Wissenschaft aufgrund der fortschreitenden Differenzierung in verschiedene Forschungsbereiche von größerem Wert als je zuvor sein.

Eines der wichtigsten Beispiele für multidisziplinäre Wissenschaft ist die Hirnforschung. Laufende Forschungen auf dem Gebiet der Neurotransmission führten zur Etablierung eines neuen multidisziplinären Bereichs, der sogenannten Photopharmakologie.

Die Photopharmakologie befasst sich u.a. mit der Synthese von lichtabhängigen Inhibitoren, die die Kontrolle der Wiederaufnahme von Neurotransmittern durch Transporterproteine über Licht ermöglichen. Die Vorteile der Verwendung von Licht als Stimulus liegen auf der Hand. Licht ermöglicht eine zeitliche, kontaktlose und vor allem lokale Kontrolle. Damit sollen Neurowissenschafter künftig in der Lage sein, die neuronale Aktivität verschiedener Hirnareale getrennt voneinander zu untersuchen.

Die Entwicklung eines solchen lichtabhängigen Inhibitors für den Serotonintransporter (SERT) ist von großem Interesse. Eine Fehlfunktion des Transporters führt beispielsweise zu depressiven Störungen. Heutzutage werden diese mit selektiven Serotonin-Wiederaufnahmehemmern (SSRI) behandelt, die allgemein als Antidepressiva bekannt sind.

Vor kurzem wurde mit Azo-Paroxetin ein solcher lichtabhängiger Inhibitor entwickelt. Es basiert auf Paroxetin, einem weit verbreiteten SSRI, und Azobenzol, einem Vertreter der am besten untersuchten Klasse von Photoschaltern.

Diese Arbeit konzentrierte sich auf die Optimierung und den Scale-up der 7-stufigen Synthese zum Azo Vorläufer. Hohe Mengen des Azo Vorläufers ermöglichen die Derivatisierung mit substituierten Azobenzolen, um zukünftig wirksamere photoschaltbare SSRIs auf Azo-Paroxetin-Basis mit einem effizienteren Wechsel zwischen dem biologisch aktiven und dem inaktiven Zustand zu finden.

Außerdem wurde die für Azo-Paroxetin entwickelte, optimierte Synthese erfolgreich auf den grundlegend verschiedenen HTI-Paroxetin basierten SSRI umgelegt. Hemithioindigo (HTI) als photoschaltbarer Teil zeigt im Vergleich zu Azobenzolen eine Rotverschiebung, die für biologische Anwendungen erstrebenswert ist.

1 General Scheme

1.1 Key

All compounds synthesized in this thesis or used as starting materials are labeled with bold Arabic numbers. Compounds taken from the literature or from other theses conducted in this research group are numbered in bold Roman numbers. Literature citations are indicated by subscript Arabic numbers.

1.2 Azo Series

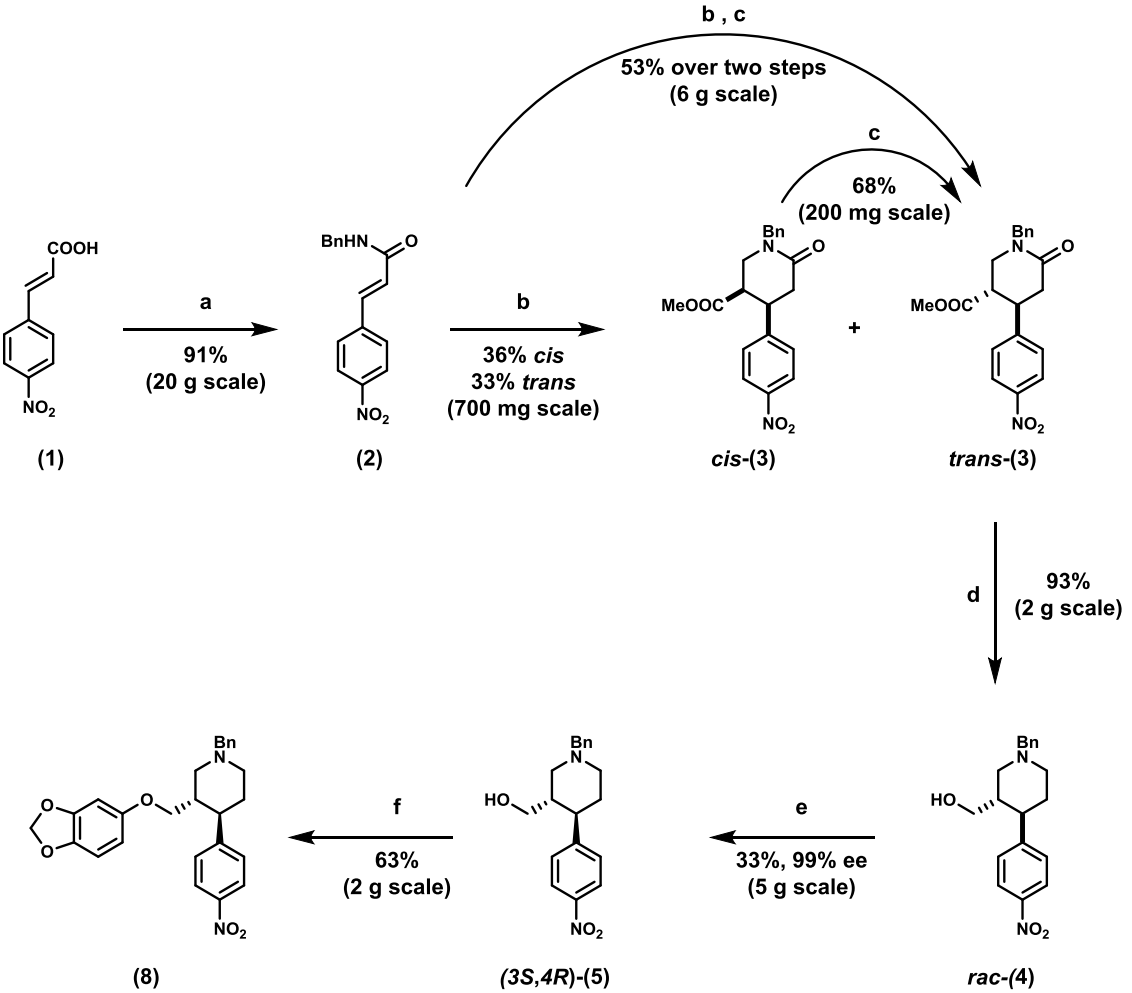

Conditions and reagents:

a) 1.) $(COCl)_2$, DMF (cat.), DCM, rt, 1 h 2.) benzylamine, NEt_3, DCM, rt, 20 h

b) methyl acrylate, NEt_3, TBSOTf, *t*-BuOH, DCE, rt, 20 h

c) Na, MeOH, rt, 30 min

d) 1.) $NaBH_4$, BF_3•OEt_2, THF, 0 °C - 50 °C, 15 h 2.) MeOH, 50 °C, 1.5 h

e) vinyl acetate, Amano Lipase PS, MTBE, rt, 47 h

f) 1.) mesyl chloride, NEt_3, DCM, 0 °C - rt, 10 min 2.) sesamol, NaH, DMF, 90 °C, 2 h

g) H_2, Pd/C, MeOH/EtOAc (4/1), 60 °C, 24 h

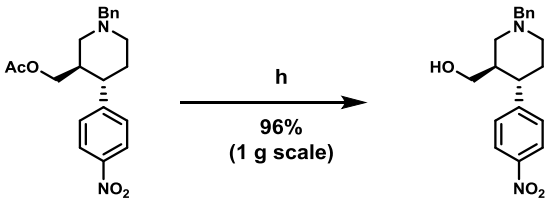

(*3R,4S*)-(6) *(3R,4S)*-(7)

Conditions and reagents:

h) NaOMe (cat.), MeOH, rt, 6 h

1.3 HTI Series

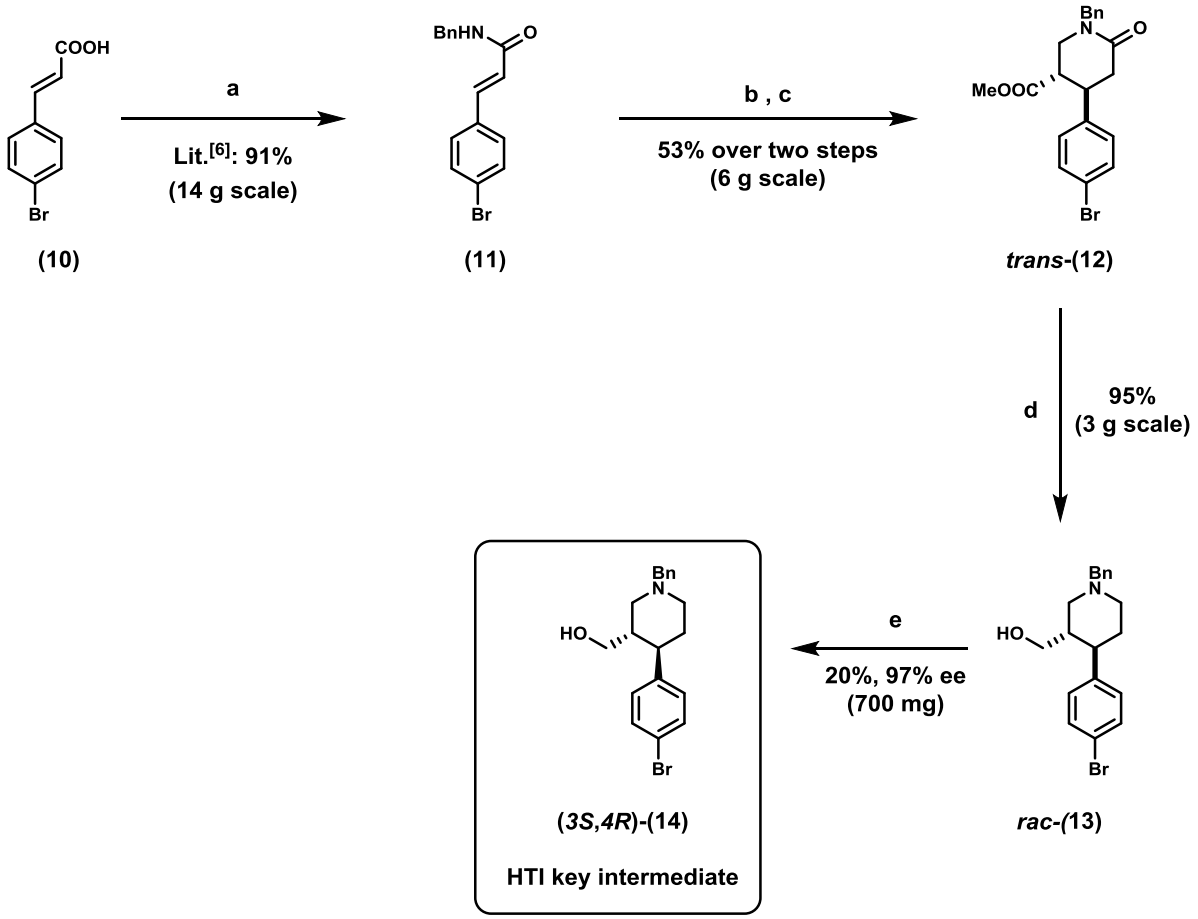

Conditions and reagents:

a) 1.) $(COCl)_2$, DMF (cat.), DCM, rt, 1 h 2.) benzylamine, NEt_3, DCM, rt, 16 h

b) methyl acrylate, NEt_3, TBSOTf, *t*-BuOH, DCE, rt, 16 h

c) Na, MeOH, rt, 30 min

d) 1.) $NaBH_4$, BF_3•OEt_2, THF, 0 °C - 50 °C, 16 h 2.) MeOH, 50 °C, 1 h

e) vinyl acetate, Amano Lipase PS, MTBE, rt, 67 h

2 Introduction

2.1 The Brain: A Complex Organ Requires Multidisciplinary Studies

"How our brains work is one of the major unsolved problems of biology."

Sir Francis Crick (1999)[1]

In 1999, none other than Sir Francis Crick pointed out with this statement that the scientific understanding of our brain, one of the most complex organs or maybe the most complex one, is one of the greatest challenges which will be solved *hopefully some time in the 21st century*[1].

Today, twenty years later, we are far away from saying that we know what is really going on. However, scientists like biologists, chemists, neuroscientists and physicians are interested in solving this multidisciplinary problems and therefore working together all over the world in different research areas is of high importance in order to come one step closer to the declared goal.

In this context, one important research area is the understanding of the signal transduction between neurons, called neurotransmission, as a malfunction is linked to many serious diseases[2] as elaborated in the following.

2.2 Neurotransmission: The Communication Between Neurons

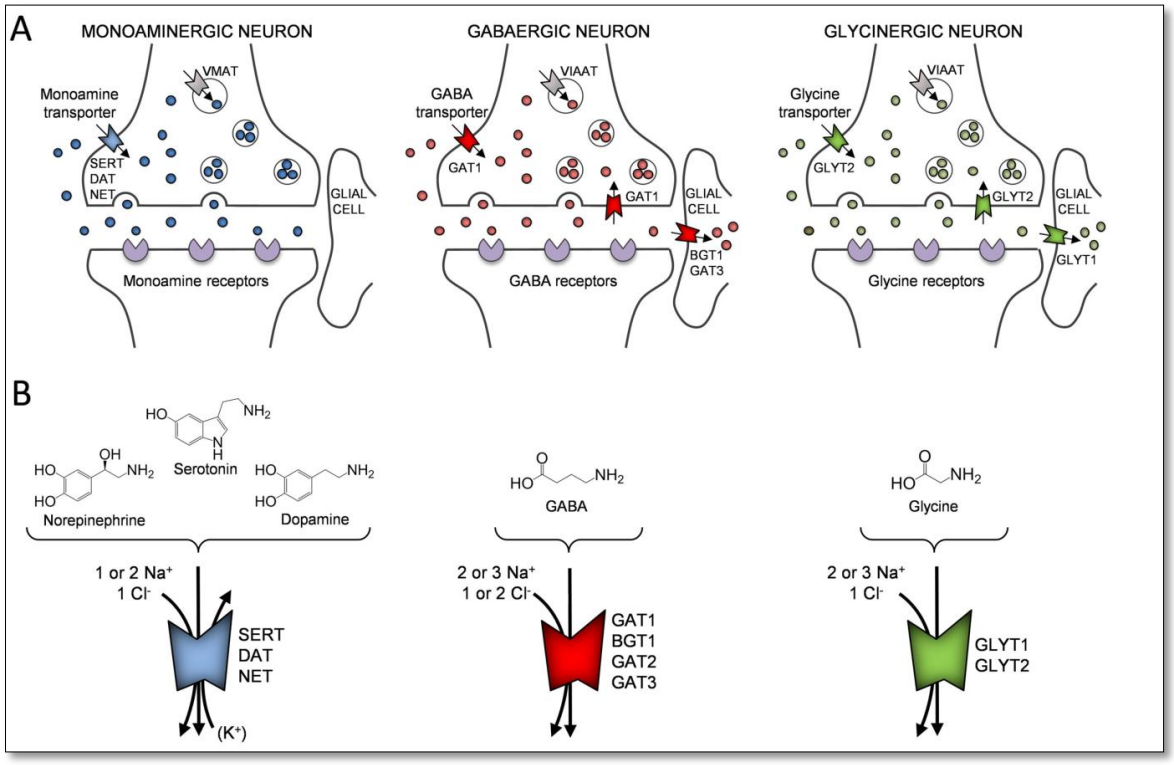

Figure 1: Neurotransmission between different neurons occur via release and reuptake of the corresponding neurotransmitter. [2]

Neurotransmission is the decisive process in the communication between neurons. The neurons can be divided into monoaminergic, gabaergic and glycinergic neurons (**Figure 1**). All of them have in common that the transduction of the electric signal from one neuron to the post neuron occurs via release of neurotransmitter into the synaptic cleft. Vice versa, the transformation of this chemical signal into an electric signal occurs via binding of the neurotransmitter to the particular receptor. The regulation of the concentration occurs via reuptake of the neurotransmitters in the presynaptic neuron. The reuptake is the task of the transporter proteins, which are named according to the transported neurotransmitters (monoamine-, GABA-, and glycine transporter).

A malfunction of these transporters leads to more than 20 completely different clinical patterns like anxiety disorders, depressions, epilepsy or cardiovascular diseases, to mention only a few. For further reading, the review of Kristensen et al.[2] is recommended.

In order to manipulate the neural activity of different neurons, a couple of inhibitors for each class of transporter was developed in the recent years. The mode of action of such inhibitors (**Figure 2**) is based on the inhibition of the reuptake of the neurotransmitters back into the nerve cell, causing an increase of the concentration of the neurotransmitter in the synaptic cleft which is directly linked to the mentioned diseases[2].

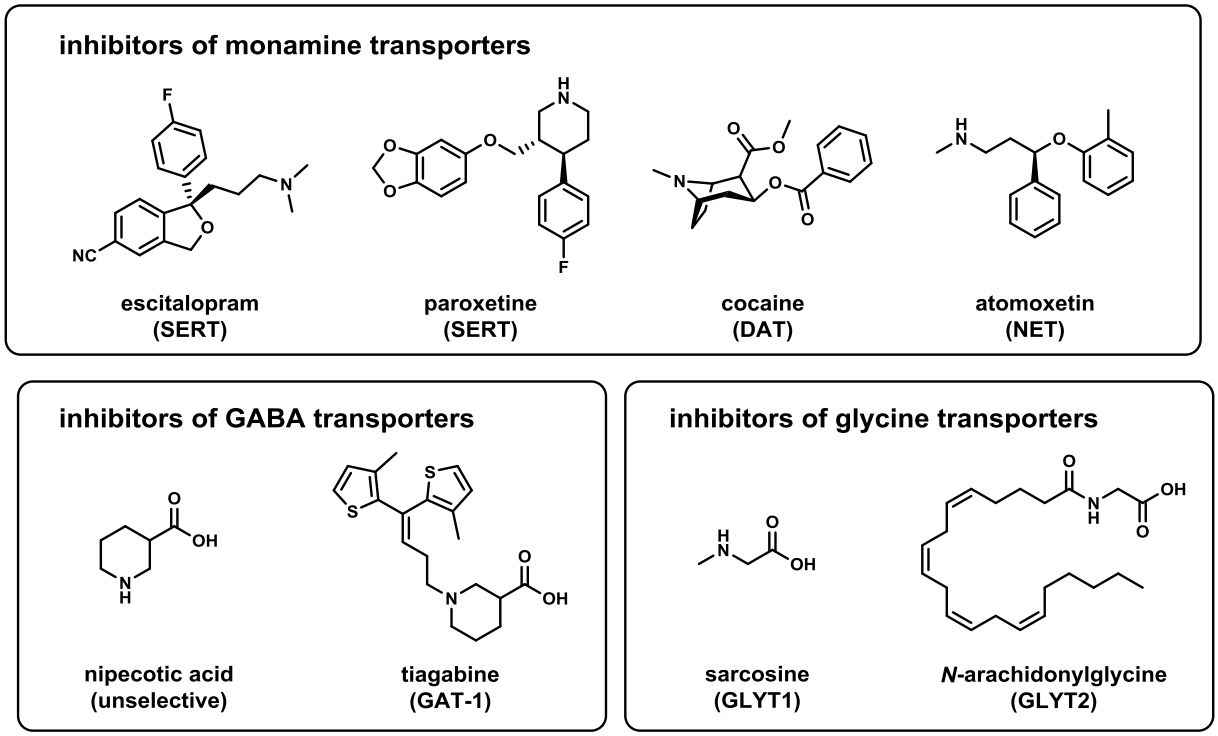

Figure 2: Examples for inhibitors of the mentioned transporters, which can serve as base for the synthesis of new tools for the research of neurotransmission.

The synthesis of new tools, based on these inhibitors can help in the future to understand the processes of neurotransmission in more detail in order to develop better methods for the treatment or even the prevention of the mentioned diseases.

Therefore, first and foremost the control of the reuptake of neurotransmitters into the cell is of great importance. However, the feature of controlling the reuptake has to be combined with a suitable stimulus in order to enable neuroscientists to manipulate the neural activities from outside.

2.3 Light: The Ideal Stimulus for Studying Neurotransmission

"The ideal signal would be light, probably at an infrared wavelength to allow the light to penetrate far enough."

Sir Francis Crick (1999)[1]

As already pointed out by Sir Francis Crick, light would be the ideal signal for the study of brain and neurotransmission related questions.

The advantages of using light as stimulus are first and foremost the spatial precision and the temporal control in addition to contactlessness and the ability to modulate the intensity of light within femtoseconds[3].

Sir Francis Crick also stated the requirements, being necessary for further studies regarding neurotransmission, more precisely as cited in the following.

"A major first step, then, is to identify the many different types of neuron existing (…) in the brain. One of the next requirements (…) is to be able to turn the firing of one or more types of neuron on and off in the alert animal in a rapid manner."

Sir Francis Crick (1999)[1]

The identification of different neurons[2] (monoaminergic, gabaergic, glycinergic) is already achieved to some extent. However, the ability to turn off and on neurons, even from the same type, would lead to a more precise study of neurotransmission today.

In combination with light as stimulus, today we are aiming for new tools, which enable scientists to turn off and on neurons of the same type but in different areas of the brain for example for studying the contribution of a small area of the brain to the whole complex system.

2.4 Photopharmacology: The Way to Photo-Dependent Inhibitors

"The tendency in neuroscience (and I'm hoping this will change) is to say,'Yes, I'd love to have new tools, but will someone else please develop them?' "

Sir Francis Crick (1999)[1]

Today neuroscientists with their desires of having new tools for brain research and the need of turning neurons on and off in order to study neurotransmission in more detail, inspired chemists and lead to a new research area called photopharmacology[3-5].

Photopharmacology deals with the development of photo-dependent tools, which enable the control of the activity of biological targets via light. With regard to neurotransmission, the control of the activity of neurons, represented by the reuptake of neurotransmitter, can be controlled by a photo-dependent inhibitor.

There are two different types of photo-dependent inhibitors, those with photocleavable ligands and those with photoswitchable ligands.

Photocleavable inhibitors are caged inhibitors which are activated by the cleavage of a certain kind of protecting group, induced by light. The disadvantage of such tools is the irreversibility of the cleavage and the release of potentially toxic protecting groups.

In contrast, photoswitchable inhibitors can switch between two configurations being induced by light and therefore trigger the desired biological effect in a reversible fashion (**Figure 3**).

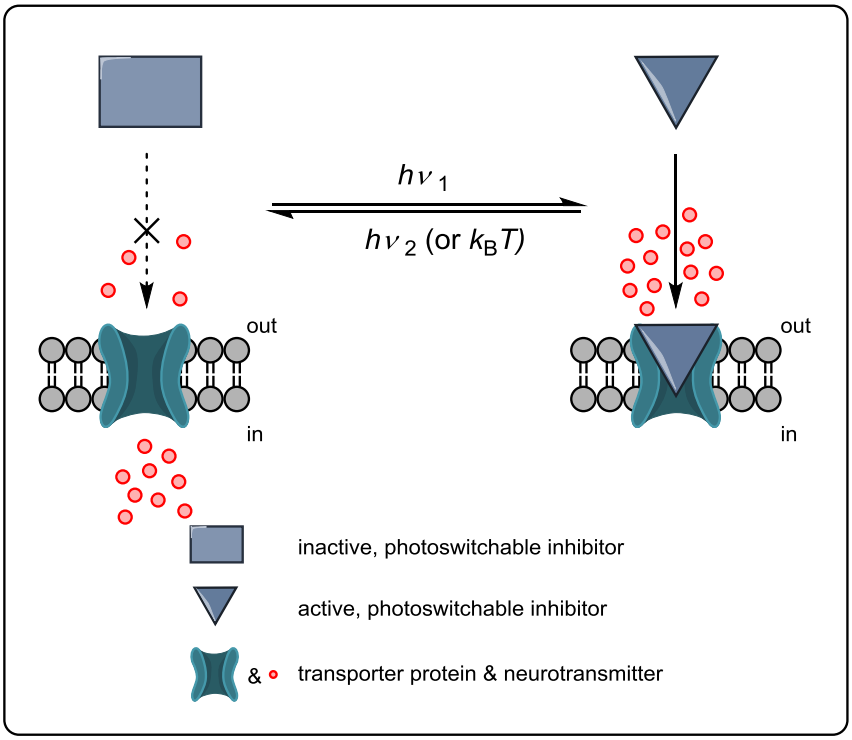

Figure 3: The mode of action of a photoswitchable inhibitor. The reversible switch between the active and the inactive state of the inhibitor is triggered by light. Modified figure from reference[6].

The switch can be chemically provided either by a *(E)/(Z)* photoisomerization or a reversible photoinduced ring-closure and ring-opening reaction.[7]

The most widespread molecular photoswitches, undergoing *(E)/(Z)* photoisomerization, are without any doubt, azobenzenes[8-11], because of their high photostability as well as their high extinction coefficients and quantum yields, leading to a highly efficient absorption of light[3, 12].

The absorbance of light in the π-π* region and the ensuing rotation of the N-N bond[13] leads to the formation of the less stable *(Z)*-isomer, causing different biological effects[9] due to a significant change in geometry, numerically expressed in a change of the end-to-end distance of 3.5 Å of the two photoisomers[14].

Besides azobenzenes, there exist also other well studied classes of photoswitches undergoing *(E)/(Z)* photoisomerization, like stilbenes[15], hemiindigos[16-17] and hemithioindigos[16, 18].

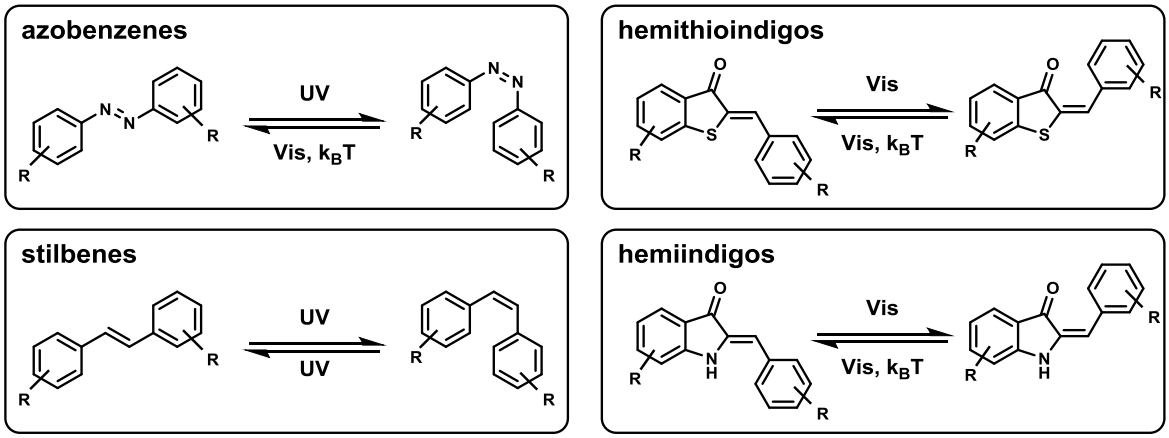

Figure 4: Different photoswitches which undergo *(E)/(Z)* photoisomerism. Modified figure from reference[6].

As shown in **Figure 4,** in case of azobenzenes and stilbenes, the isomerization of the thermodynamically more stable *(E)*-isomer to the less stable *(Z)*-isomer occurs via irradiation with light in the UV region whereas hemithioindigos as well as hemiindigos show a red-shift to visible light. In contrast, the switch back can be triggered thermally or by light in the UV-Vis region. The thermally induced switch is represented by the corresponding half-life period of the less stable (*Z)*-isomer.

Especially for photopharmacology and related biological applications, a red-shift is desirable because of the deeper penetration depth and the feature of being less harmful for any kind of tissue.

With regard to photopharmacology, recently the synthesis of azo-paroxetine, a photoswitchable selective serotonin reuptake inhibitor (SSRI) for the research of the serotonin transporter was developed in our research group in a previous work[6].

2.5 Azo-Paroxetine: A Photopharmacological Tool for the Serotonin Transporter

Azo-paroxetine is a photopharmacological tool based on paroxetine and azobenzene (**Figure 5**). Paroxetine is a widely described selective serotonin reuptake inhibitor (SSRI) and is well established as antidepressant. The photoswitchable part derives from azobenzene, the unsubstituted derivative of the best studied class of photoswitches undergoing *(E)/(Z)* photoisomerism.

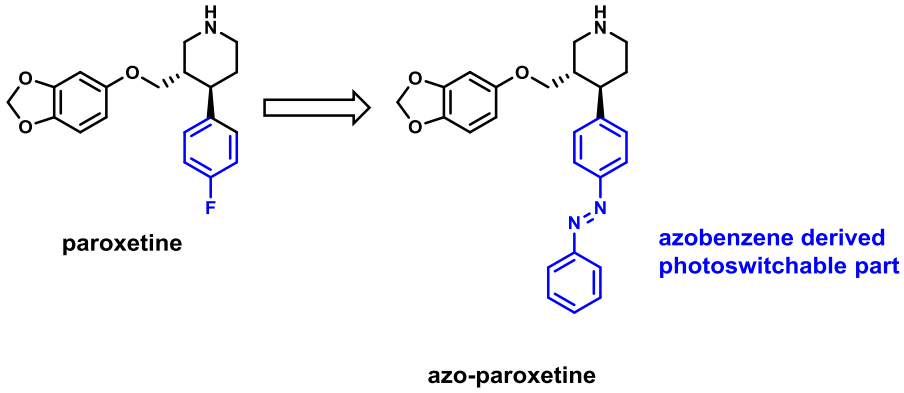

Figure 5: Azo-paroxetine as a photoswitchable SSRI derived from paroxetine and azobenzene.

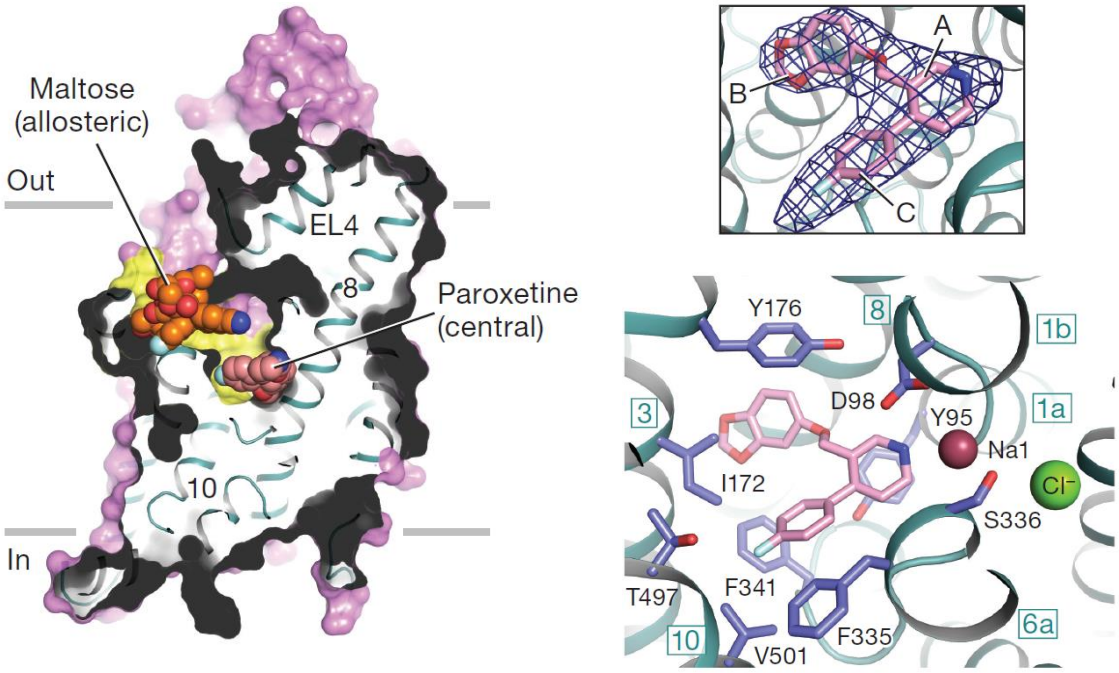

Figure 6: Left: X-Ray structure of the hSERT and paroxetine which bound to the central binding pocket. The maltose head group derived from detergents. Right: Sub-pocket C hosted the fluorophenyl moiety of paroxetine, pointing out of the central binding pocket.

In 2016 and 2018, Gouaux et al.[19-20] published the first X-ray structures of the human serotonin transporter (hSERT). Additionally they were able to co-crystallize paroxetine amongst other SSRIs.

Paroxetine is bound to the central binding pocket, as shown in **Figure 6**. Sub-Pocket A hosted the secondary amine of paroxetine, whereas in sub-pocket B the benzodioxol fragment is located. In sub-pocket C the fluorophenyl moiety can be found, which protrudes from the central binding pocket.

With regard to the design of the photoswitchable inhibitor azo-paroxetine, it was of great importance to install the azobenzene derived photoswitchable part at a position, where hSERT offered enough space for switching but not too much in order to see a difference in activity between the two photoisomers.

As the fluorophenyl moiety of paroxetine complied best with the mentioned requirements, the installation of the azobenzene derived photoswitchable part was performed via exchange of the fluorine substituent as shown before (**Figure 5**). The photoswitchable azobenzene derived part of azo-paroxetine was installed via Mills reaction (**Figure 7**).

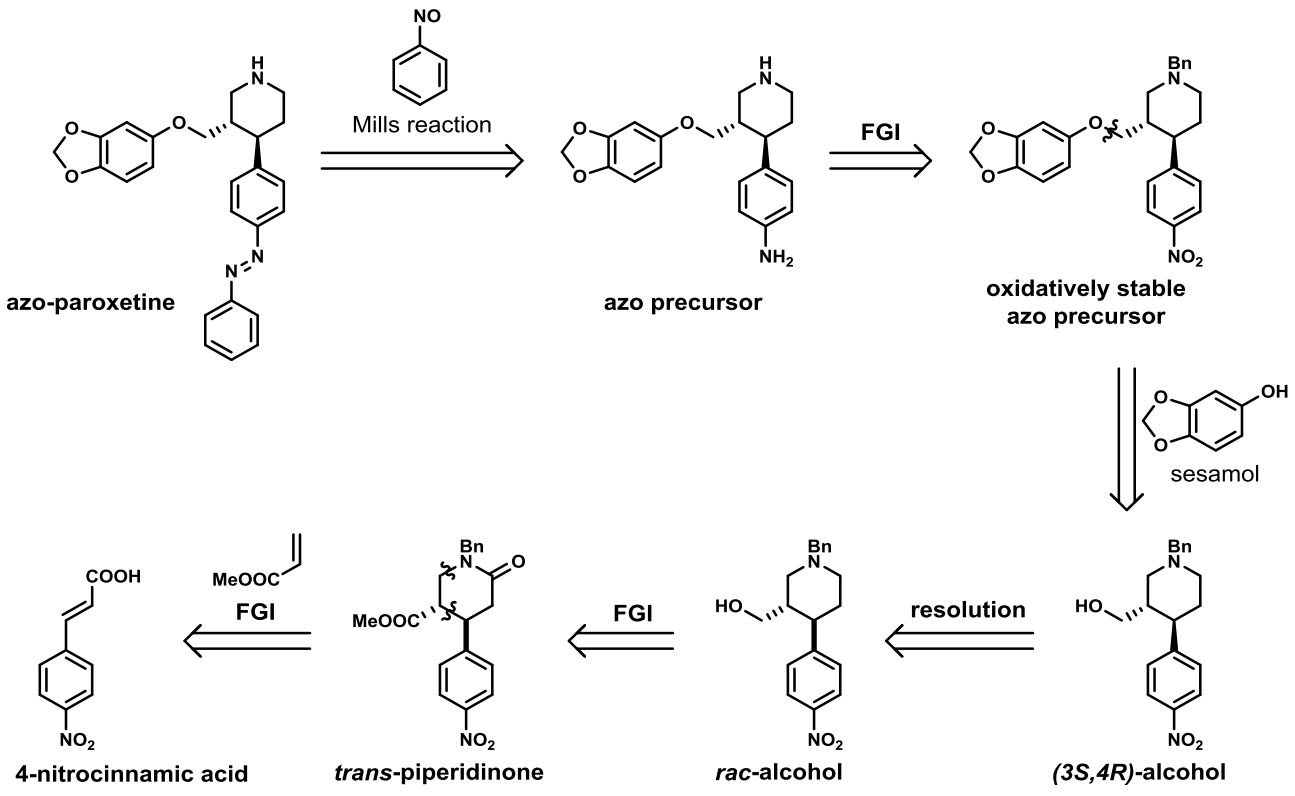

Figure 7: Retrosynthetic analysis of azo-paroxetine.

As shown in **Figure 7**, the Mills reaction required the aniline derivative of paroxetine as azo precursor. The oxidative labile aniline was transformed into the corresponding nitro derivative, showing higher oxidative stability. The oxidatively stable azo precursor was prepared via etherification of sesamol with the corresponding alcohol. The enantiopure alcohol was obtained via resolution. After functional group interconversion to the corresponding methyl ester, *trans*-piperidinone was prepared via cyclization of methyl acrylate and the secondary *N*-benzyl protected amine. After functional interconversion of the secondary amine to the corresponding acid, 4-nitrocinnamic acid was found to be a suitable and commercially available starting material.

Concluding, azo-paroxetine as photopharmacological tool, based on paroxetine and azobenzene, was synthesized successfully starting from 4-nitrocinnamic acid. The photophysical characterization and biological of azo-paroxetine evaluation will be elaborated in the following chapter.

2.6 Azo-Paroxetine: Photophysical Characterization and Biological Evaluation

The photophysical characterization (**Figure 8**), being performed in the previous work[6], lead to the discovery that light in the UV-range (365 nm) triggered the switch between the thermodynamically preferred *(E)*-configuration to the excited *(Z)*-configuration.

In contrast, the switch of the exited *(Z)*-isomer back to the stable *(E)*-isomer was triggered by light of 400 nm and 460 nm. The thermal relaxation is represented by half-life periods ($\tau_{1/2}$) between 6.5 and 8.5 days, dependent on the solvent.

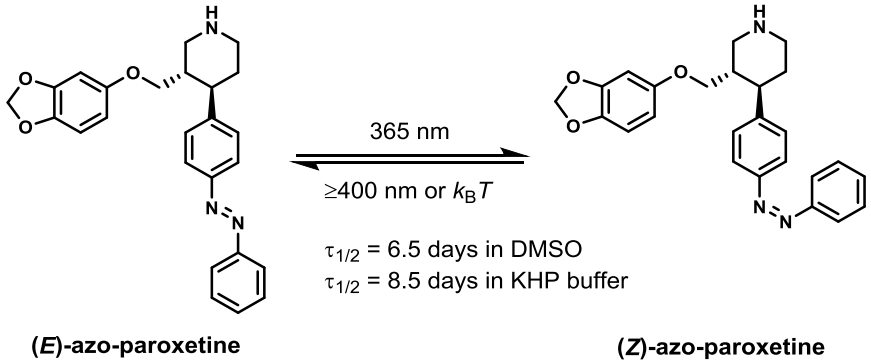

Figure 8: Azo-Paroxetine showed an effective switch with light of 365 nm and showed half-life periods in the range of days.[6]

Additionally an in-vitro assay was carried out in order to evaluate the photo-dependent ability of azo-paroxetine to inhibit the reuptake of serotonin by the human serotonin transporter (hSERT). As shown in **Figure** 9, the irradiation of azo-paroxetine with light of 365 nm resulted in a photo-dependent inhibition. Whereas the *(E)*-isomer showed an IC_{50} of 8.7 µM, irradiation with light of 365 nm resulted in the excited (*Z)*-isomer, which led to an increase in potency by one order of magnitude to an IC_{50} of 0.8 µM. Furthermore, the fact of a difference in potency between the two photoisomers was confirmed by computational studies.

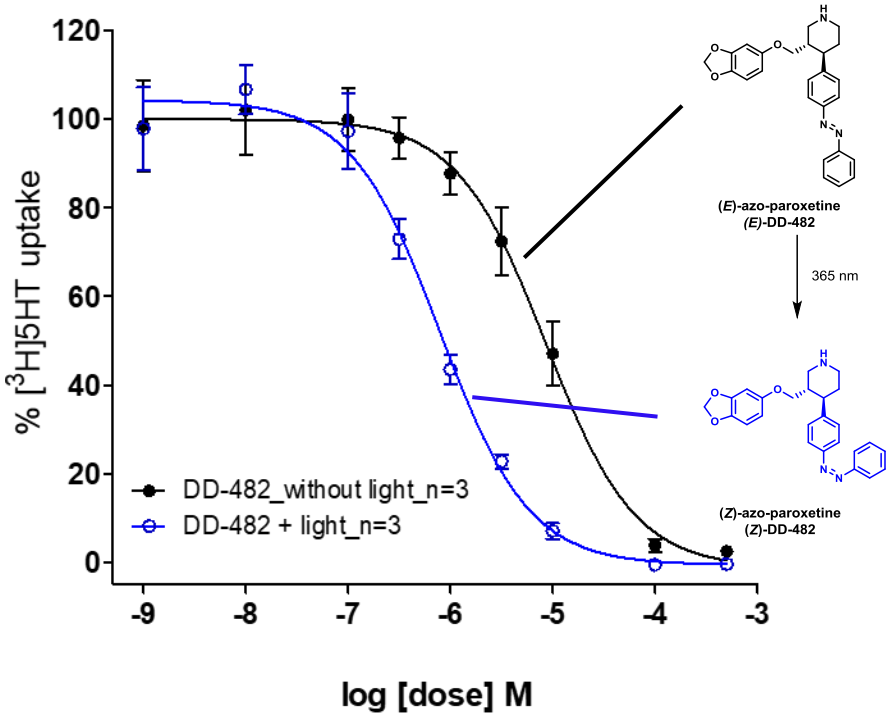

Figure 9: The IC_{50} increased from 8.7 µM for the *(E)*-isomer to 0.8 µM for the *(Z)*-isomer by one order of magnitude when azo-paroxetine was irradiated with light of 365 nm.[6]

Concluding, a photo-dependent inhibitor for the hSERT was developed in the previous work[6] by the synthesis of azo-paroxetine.

However, the irradiation with visible light instead of 365 nm would lead to a deeper penetration and to less damage of the tissue. Furthermore, a higher difference of the IC_{50} between the two states is desirable in order to make this photopharmacological tool ready for future neuroscientific studies.

3 Results and Discussion

3.1 This Project: Starting Point and Objective

3.1.1 Starting Point: The Synthesis of Azo-Paroxetine

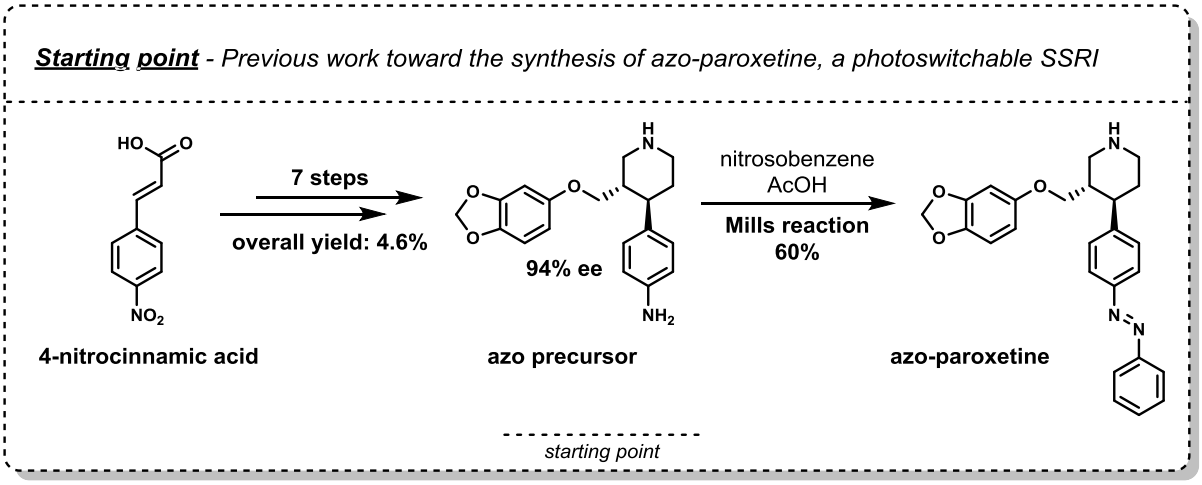

As mentioned in the introduction, azo-paroxetine was described in the previous work[6] in this research group to be a selective serotonin reuptake inhibitor (SSRI) with photoswitchable properties.

In this previous work[6], azo-paroxetine was synthesized starting from commercially available 4-nitrocinnamic acid. After 7 steps, the precursor, an aniline derivative, was obtained in 4.6% overall yield and an enantiomeric excess of 94% ee.

This aniline served as a nucleophile in the following Mills reaction step. The nucleophilic precursor reacted with the electrophilic nitrosobenzene under acidic conditions and formed the desired azo-paroxetine. Acidic conditions were also necessary for the protonation of the secondary amine of the paroxetine moiety, in order to suppress its nucleophilicity which will lead to side reactions.

Concluding, azo-paroxetine as a photoswitchable SSRI, was successfully synthesized in the previous work[6].

3.1.2 The Derivatization: The Way to More Potent Photoswitchable SSRIs

As mentioned in the introduction, the performance of azo-paroxetine as photoswitchable SSRI has to be improved in order to have a more valuable photopharmacological tool in hand.

Regarding the performance, the two main aims are the possibility of irradiation with visible light in order to increase the penetration depth and being less harmful to tissue. The second aim which is desirable, is the increase of the difference in potency between the two photoisomers (up to three orders of magnitude) in order to being able to photoinhibit the serotonin uptake in a reliable manner.

In order to reach both aims, the derivatization of azo-paroxetine seemed to be the first promising approach.

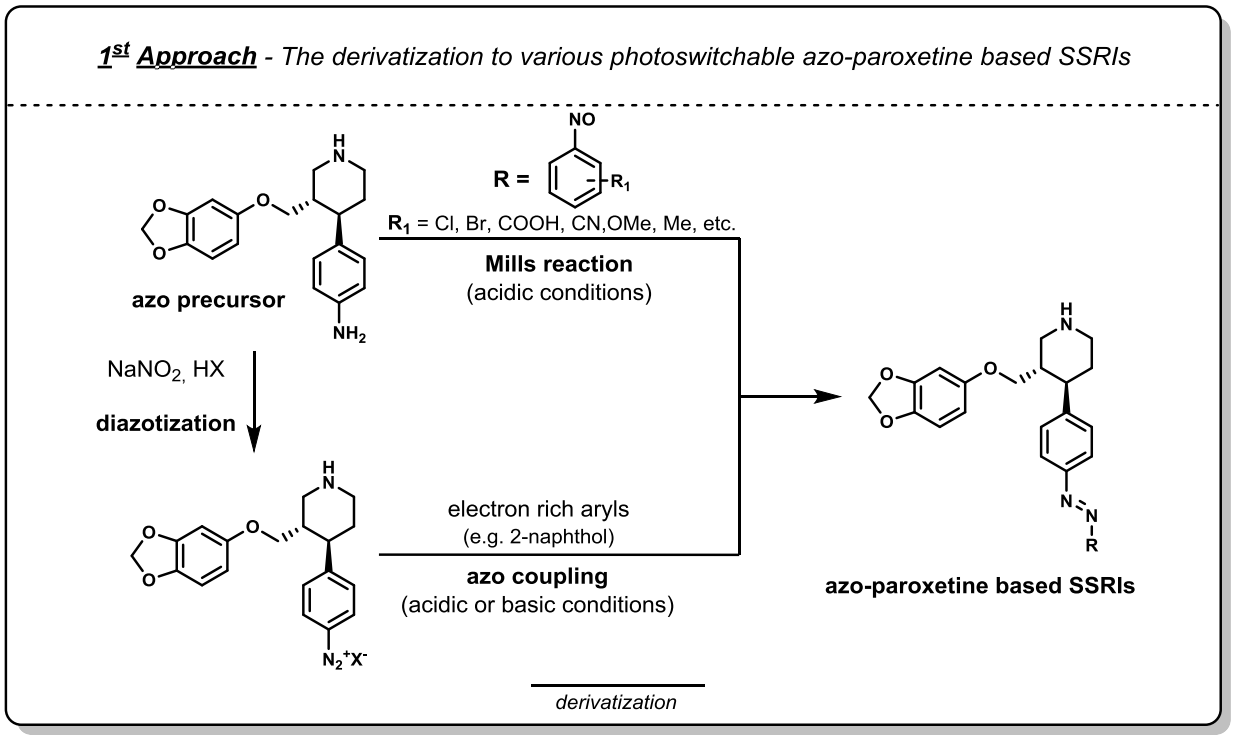

In this approach, the derivatization is performed via introduction of different azo based photoswitchable moieties, which can be synthesized via various synthesis pathways[21]. However, the Mills reaction as well as the azo coupling are the best studied pathways.

In the Mills reaction, the nucleophilic aniline precursor would react with various electrophilic nitrosobenzene derivatives under acidic conditions in order to obtain azo-paroxetine based SSRIs with different properties regarding the photoinhibition of the SERT.

In contrast, in case of the azo coupling, the precursor has to be converted to the appropriate diazonium salt under acidic conditions using $NaNO_2$ followed by the azo coupling, an electrophilic aromatic substitution. The reaction with electron rich and sterically demanding aromatic systems like naphthol would lead to a photoswitchable SSRIs with a completely different behavior on the SERT.

Concluding, electronically and sterically completely diverse azo-paroxetine based SSRIs can be made accessible via Mills reaction as well as via azo coupling.

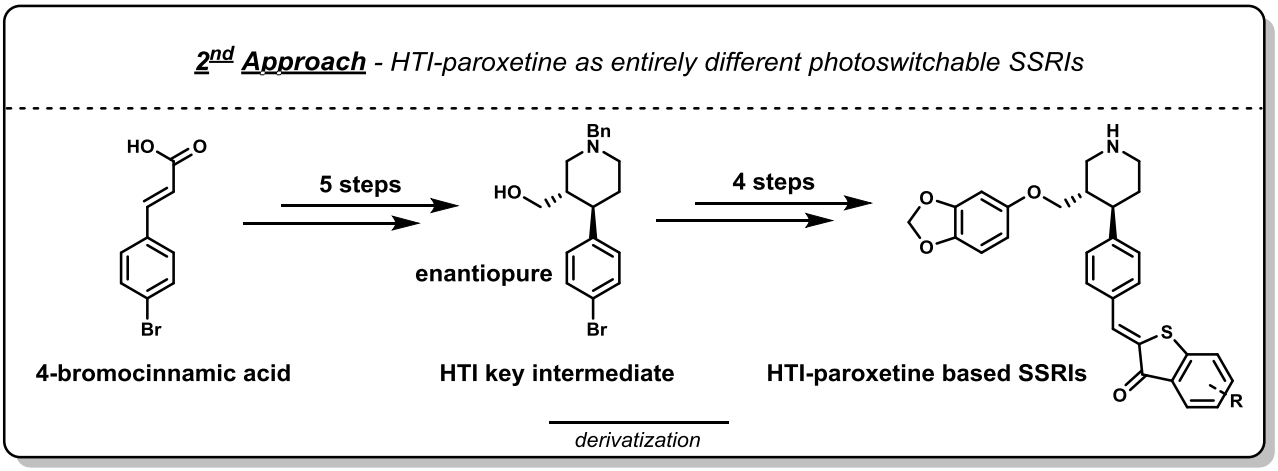

In order to extend the diversity of paroxetine based SSRIs, a completely different paroxetine derivative with a hemithioindigo (HTI) substituent as photoswitchable moiety seemed to be a second promising target. The racemic form of the HTI-paroxetine based SSRI was already synthesized in the previous work[6].

In contrast to azo-paroxetine, where the synthesis started from 4-nitrocinnamic acid, the synthesis of the HTI-paroxetine was performed starting from commercially available bromo substituted cinnamic acid. After 5 steps, which were similar to steps for the azo-paroxetine, an alcohol was obtained as key intermediate in a racemic form. After etherification and metal halogen exchange of the bromo substituent followed by quenching with DMF, the appropriate aldehyde was obtained. In the following step, the aldehyde served as a precursor for the condensation with substituted benzothiophenone.

Concluding, besides the derivatization of the azo-paroxetine via Mills reaction and the azo coupling, also the photoinhibiting properties of HTI-paroxetine can be varied by using benzothiophenones of a different substitution pattern.

3.1.3 Objective: Optimization and Scale-up of Enantioselective Syntheses

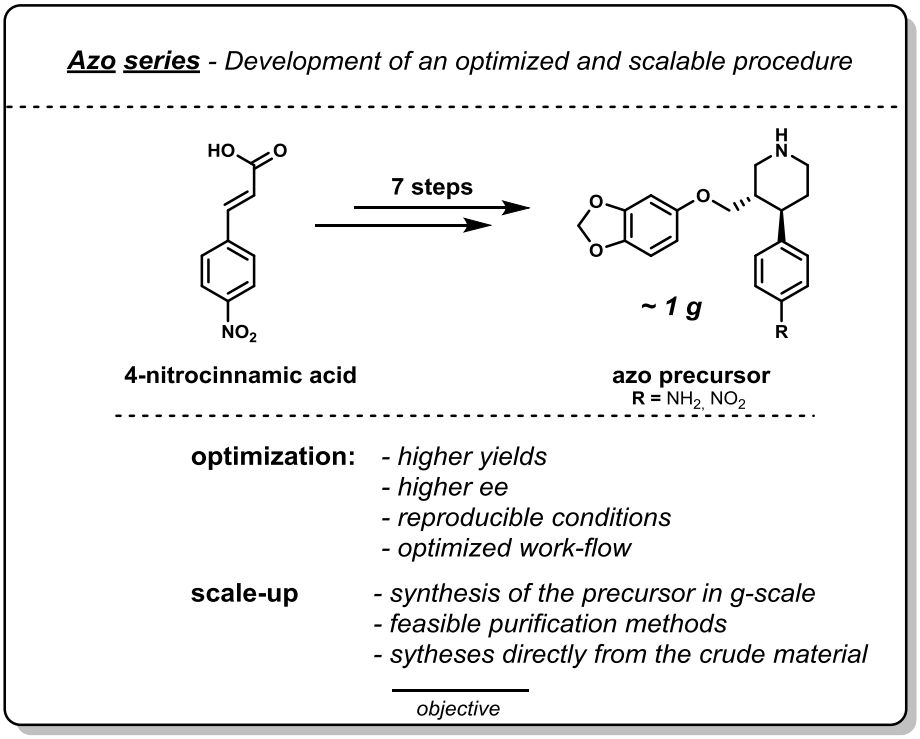

In order to open the door for the screening of various azo-paroxetine based SSRIs and to find more potent candidates, first and foremost the azo precursor has to be synthesized in high quantities. According to the oxidatively labile aniline derivative, the scale-up will be performed to the oxidatively stable nitro derivative (6th step). However, the optimization will be performed for all 7 steps.

Therefore, the challenge of this thesis is the development of an optimized and scalable protocol for the 7-step synthesis pathway in order to obtain around 1 g of the oxidativlely stable azo precursor in the end.

With regard to the optimization, it is necessary to develop procedures for each step with high yields (Lit.[6]: 4.6% over 7 steps), an increased enantiomeric excess (Lit.[6]: 94% ee) as well as reproducible conditions in combination with an optimized work-flow.

In view of the scale-up, the azo precursor has to be synthesized in quantities around 1 g (Lit.[6]: 37 mg). For such high quantities, feasible purification methods, or, even better, protocols, where the crude materials can be used directly, have to be developed.

HTI series *- Scalable and optimized synthesis of the enantiopure key intermediate*

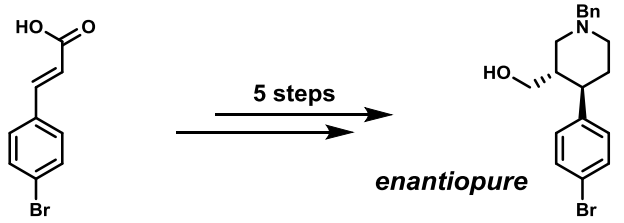

4-bromocinnamic acid **HTI key intermediate**

enantioselectivity: *- via enzymatic kinetic resolution of the racemate*

optimization: *- modification of the procedures of the azo series*

scalability: *- adaption of the purification protocols of the azo series*

objective

With regards to HTI-paroxetine, emphasis was put especially to the enantioselective synthesis in this thesis due to the fact that in the previous work[6], the HTI-paroxetine was only synthesized in a racemic form. In view of the synthesis of various HTI-paroxetine based SSRIs, the enantiopure form of this key intermediate is of high interest.

Furthermore, the optimized and scaled procedures coming from the azo-paroxetine should be modified and adapted in a way that they are also feasible for the synthesis of the HTI key intermediate.

Concluding, the optimization, the up-scale as well as the enantioselective synthesis are the three cornerstones of this thesis, which will be the door openers for the synthesis and screening of sterically and electronically different paroxetine based photoswitchable SSRIs in future projects in order to find more potent candidates for a photo induced inhibition of the SERT.

3.2 Azo Series

3.2.1 Synthesis: The Azo Precursor

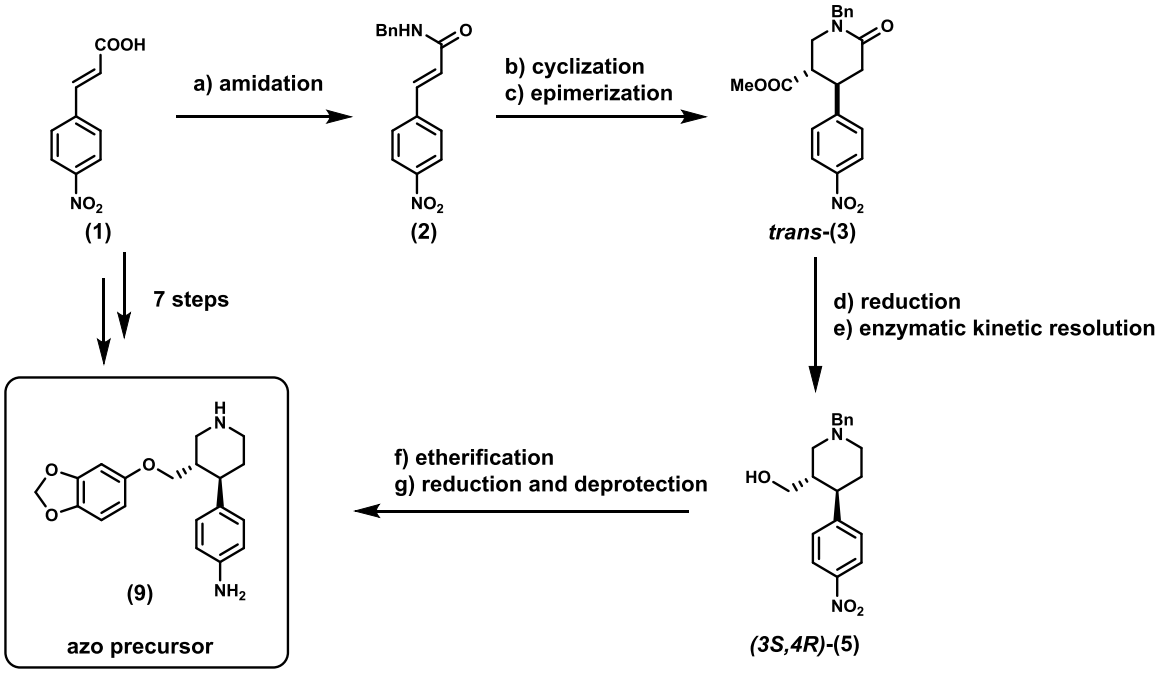

Figure 10: The synthesis of the precursor for the azo-paroxetine based SSRIs

The synthesis of the enantiopure azo precursor was performed via 7-step synthesis starting from commercially available 4-nitrocinnamic acid **(1)**.

In the first step, 4-nitrocinnamic acid **(1)** was converted to *N*-benzyl protected intermediate **(2)** via amidation. The cyclization via double Michael addition resulted in a diastereomeric mixture of piperidinones **(3)**. The enrichment of desired *trans*-piperidinone ***trans*-(3)** was achieved via epimerization. The reduction of the ester functionality to the alcohol and the subsequent enzymatic kinetic resolution resulted in enantiopure alcohol **(*3S,4R*)-(5)**. Azo precursor **(9)** was obtained after etherification with sesamol, deprotection of *N*-benzyl protected amine and reduction of the nitro group to the aniline.

3.2.2 Amidation: Synthesis of *N*-Benzyl Protected Amide (2)

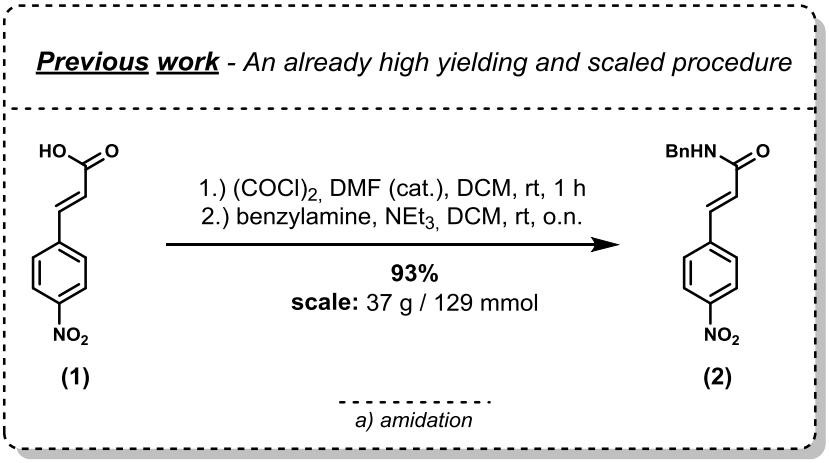

In the previous work[6], an already high yielding and scaled procedure for the amidation was developed.

Commercially available 4-nitrocinnamic acid **(1)** was converted to the acid chloride under argon atmosphere, using freshly distilled oxalyl chloride as reagent, dry DMF as catalyst and dry DCM as solvent. After 1 h hour, TLC analysis (MeOH quench) indicated full conversion. After removal of the volatiles, the isolated acid chloride was dissolved in dry DCM and was converted again to *N*-benzyl protected amide **(2)** under argon atmosphere using freshly distilled benzylamine as reagent and dry NEt_3 as acid scavenger. After filtration of the formed precipitate, a washing step with 1 N NaOH and 1 N HCl followed. The additionally performed recrystallization of the concentrated mother liquor in toluene resulted in an overall yield of 93%.

Concluding, an already high yielding and scaled procedure was developed in the previous work[6].

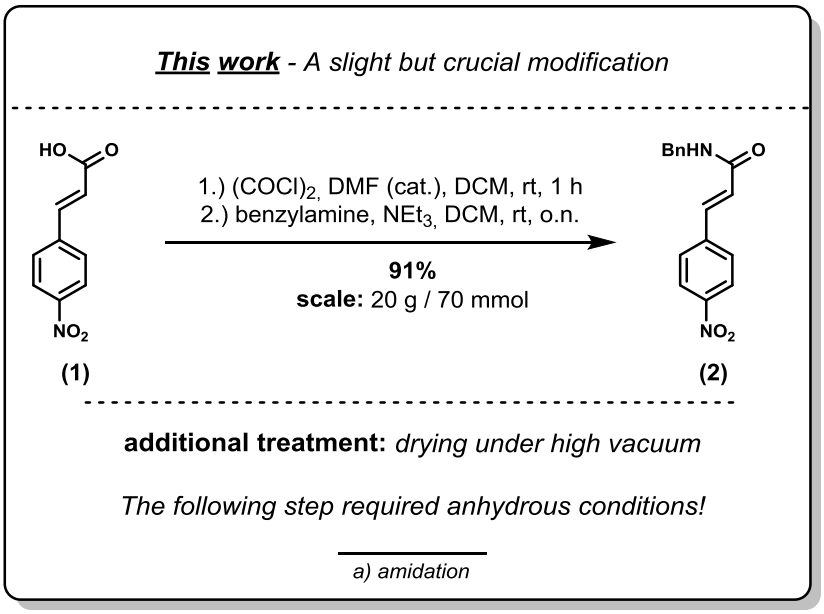

In this work, the reproducibility of the already high yielding and scaled amidation protocol of previous work[6] was proven obtaining a comparable yield of 91% in a 20 g scale (Lit[6]: 93%, 37 g scale).

Furthermore, one crucial modification was implemented. Amide **(2)** was dried after work-up under high vacuum, which was necessary for reproducibility of the next step, as it will be elaborated in detail in the following chapter.

3.2.3 Cyclization: Synthesis of Piperidinones *cis*-(3) and *trans*-(3)

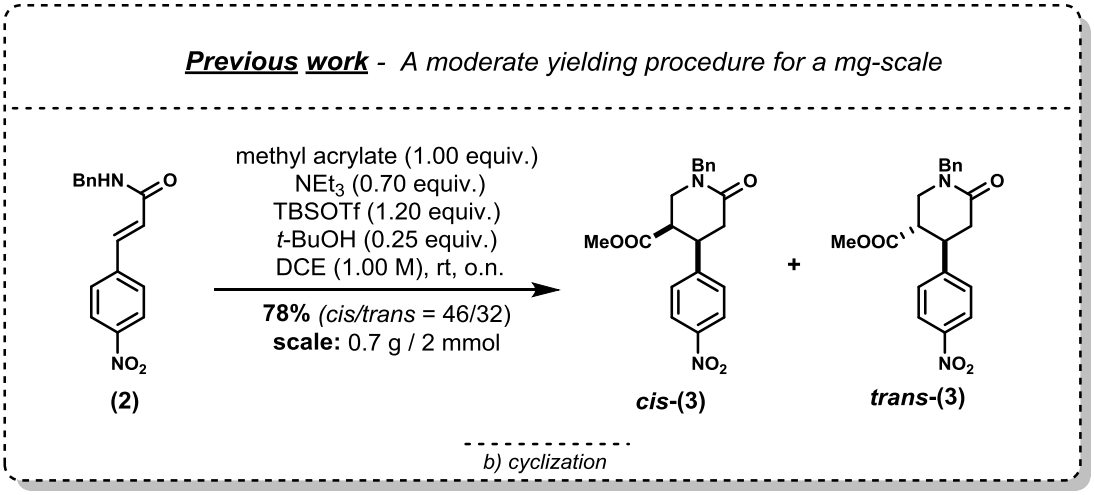

In the previous work[6], the cyclization to piperidinones ***cis*-(3)** and ***trans*-(3)** was performed referring to a literature protocol toward the synthesis of paroxetine[22].

The cyclization to a diasteriomeric mixture of desired piperidinones **(3)** proceeded via double Michael addition, starting from *N*-benzyl protected amide **(2)** and methyl acrylate as building blocks. The mechanism is shown in **Figure 11**.

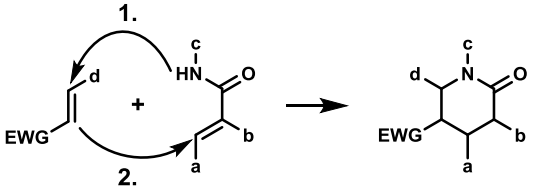

Figure 11: The piperidinones are formed via double Michael addition[6]

The nitrogen of the amide act as the nucleophile and attacked the α,β-unsaturated olefin, which is activated by the electron withdrawing group (*EWG*), represented by the methyl ester in this specific case. The intramolecular attack of the formed enolate on the double bond of the α,β-unsaturated amide resulted in the formation of stable six-membered ring systems, the desired piperidinones **(3)**.

Figure 11 also points out that many different piperidinones can be formed via this pathway by variation of the substituents (a-d) and the electron withdrawing group (*EWG*). But this requires primarily a reproducible protocol. Therefore, the reproduction of the procedure, developed in the previous work[6], was performed in the following.

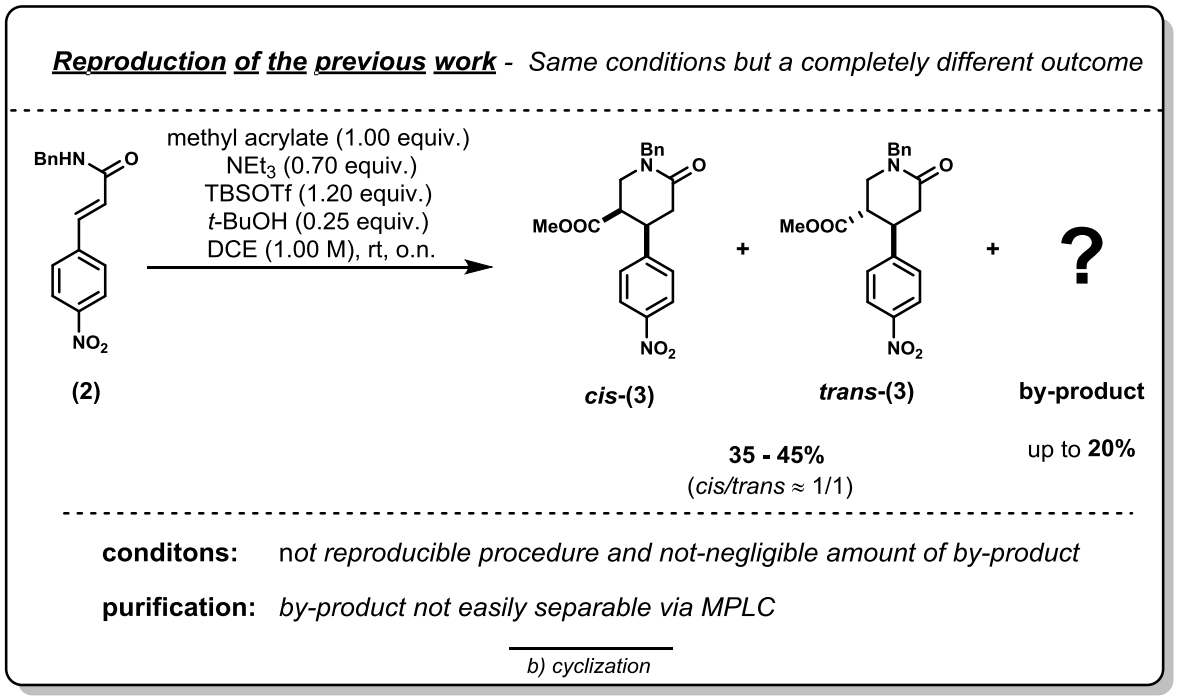

The reproduction of the procedure, developed in the previous work[6], resulted in a completely different outcome, meaning a lower yield of 35 - 45% and the formation of a by-product in a not-negligible amount of up to 20%. Due to the high amount of by-product and the unfeasible separation from one desired piperidinone ***trans*-(3)**, the structure of the by-product had to be determined in order to find a suitable way for its suppression.

As assumed in the literature[22], a third Michael addition between piperidinones **(3)** and methyl acrylate can lead to the formation of a triple Michael adduct (**Figure 12**).

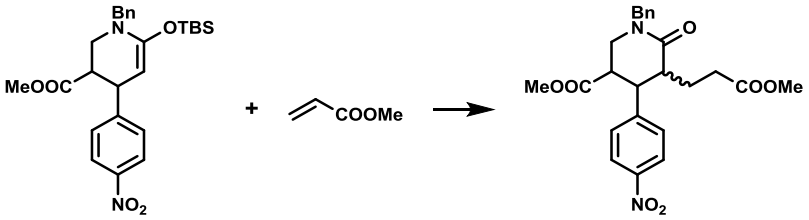

Figure 12: The formation of a triple Michael adduct as prominent side reaction

In this work, the structure of the by-product was analyzed via HPLC/MS and 2D NMR and led to the confirmation of the assumed structure. Furthermore, the stereochemistry of the triple Michael adduct was determined using NOESY. A correlation between H3 and H6' as well as between H5 and H2' led to the conclusion that all substituents had to be in *trans*-configuration to each other.

Analysis of the by-product

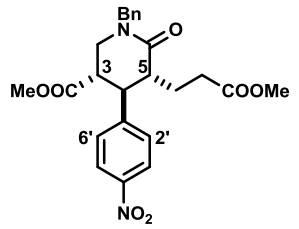

triple Michael adduct (16)

analysis: *HPLC/MS, 2D NMR*

stereochemistry: *NOESY*

The fact that only this specific stereoisomer out of four possible stereoisomers was formed, led to the conclusion that triple Michael adduct **(16)** was formed only from *trans*-piperidinone ***trans*-(3)** whereas *cis*-piperidinone ***cis*-(3)** remained unconverted. This was expected to some extent due to the fact that the formed stereoisomer of **(16)** represents the energetically favored stereoisomer. However, the exclusive formation of this stereoisomer has to be pointed out from a synthetic point of view because the remarkable stereocontrol of the triple Michael addition can be used for synthetic applications of this compound.

However, this work focused on the suppression of triple Michael adduct **(16)** in order to increase the yield of desired piperidinones **(3)**. According to the literature[22], a small amount of triflic acid, coming from partly decomposed TBSOTf, led to a lower amount of triple Michael adduct **(16)**. Due to a lack in reproducibility when employing "partly decomposed" reagents, the addition of *t*-BuOH (0.25 equiv.) should suppress the formation of triple Michael adduct **(16)** completely even if using freshly distilled TBSOTf as published in the literature[22] .

As these conditions using *t*-BuOH as suppressing agent were not reproducible and led, in contrast to the literature report[22], to the formation of up to 20% of triple Michael adduct (**16)**, this reaction has to be studied in more detail in order to find reproducible conditions.

Optimization *- The development of reproducible conditions*

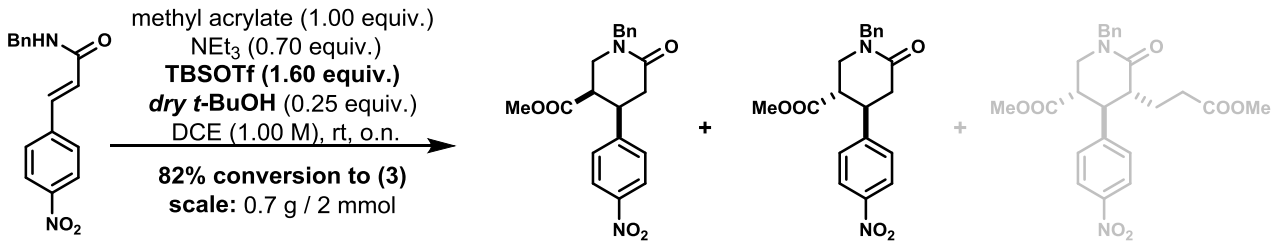

conditons: **-** r*eproducible*
- higher conversion (1.6 equiv. TBSOTf)
- no formation of the triple Michael adduct (dry t-BuOH)

b) cyclization

The first idea regarding the suppression of the intermolecularly formed triple Michael adduct **(16)** was to perform the reaction in a more diluted fashion. But this led to no conversion according to previous work[6].

Due to the fact that the reaction started after the addition of TBSOTf, it would be better to add the *t*-BuOH before TBSOTf so that the *t*-BuOH can act as suppressing agent right from the beginning. Unfortunately, this attempt led to a decrease in conversion of 10%.

Cooling the reaction mixture during the addition of the reagents in order to decrease the reaction rate until all reagents were added was also no option because of the low melting point of *t*-BuOH of 26 °C.

The decisive step in order to find reproducible conditions and to suppress triple Michael adduct **(16)** completely was identified when it was found that only dry *t*-BuOH was able to suppress the formation of triple Michael adduct **(16)** completely, even if fresh TBSOTf was used.

In addition, a screening of different amounts of methyl acrylate (1.30 equiv.), NEt_3 (1.20 equiv.) and TBSOTf (1.60 equiv.) led to the conclusion that a higher amount of TBSOTf led to the highest conversion.

With these reproducible conditions, a conversion of 82% to piperidinones **(3)** and the complete suppression of triple Michael adduct **(16)** were observed. Additionally it is worth mentioning that the maximum of conversion was reached after 4 h. However, due to the presence of unconverted starting material after 4 h, the reaction mixture was always stirred over night. Nevertheless, a longer reaction time resulted in no further conversion or reaction according to GC/MS analysis.

The reaction was monitored via TLC analysis (LP/EtOAc = 1/2; R_f = 0.71 **(2)**, 0.49 **(16)**, 0.45 ***trans*-(3)**, 0.25 ***cis*-(3)**; visualized by ultraviolet light) and GC/MS (Note: The triple Michael adduct **(16)** was not detectable via GC/MS measurements). The conversion to piperidinones ***cis*-(3)** and ***trans*-(3)** was calculated by comparison of the integrals of the ^{1}H-NMR measurement of the crude mixture (**Table 1**).

Table 1: The signals of the ^{1}H-NMR measurements used for the calculations of the conversion

parameters	***cis*-(3)**	**(2)**	***trans*-(3)**	**(16)**
protons	H3' & H5'	Ar-C<u>H</u>=CH-	H3	H2' & H6'
δ [ppm]	8.08	7.72	3.05	7.16
integral	2	1	1	2

The calculation of the ratio of the integrals of compounds ***cis*-(3)** and ***trans*-(3)** to the sum of all compounds resulted in the conversion of the starting material **(2)** to the desired piperidinones **(3)**.

Finally, with the optimized conditions and a reliable reaction monitoring in hand, the scale-up of the reaction had to be performed.

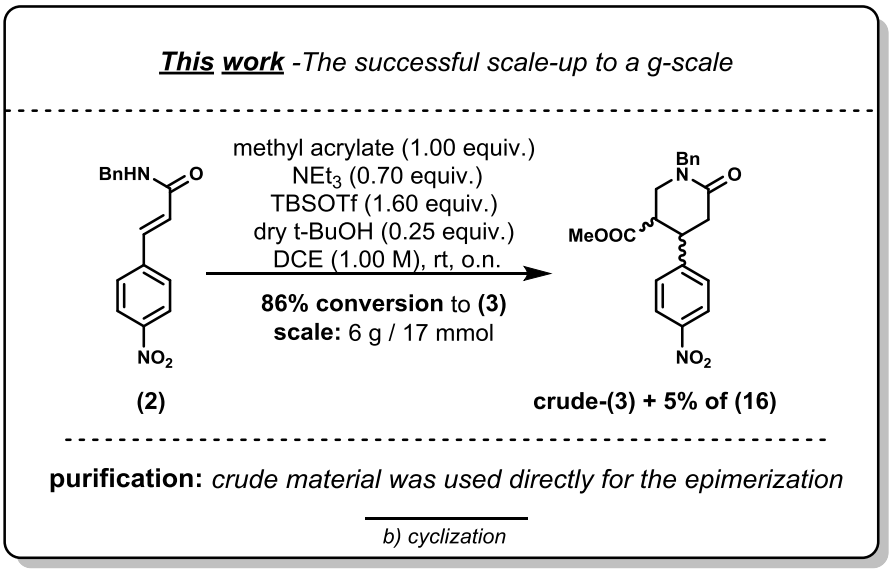

The scale-up of the optimized conditions from the 0.7 g scale to a 6 g scale led to a similar conversion of 86% to piperidinones **(3)** like in small scale (82%) and a formation of triple Michael adduct **(16)** of only 5%. The formed species (**(2)**, ***cis*-(3)**, ***trans*-(3)** and **(16)**) can be separated via MPLC, which is only suitable for a small scale. Even there, ***trans*-(3)** and **(16)** are not easily separable due to similar R_f-values of **(16)** and ***trans*-(3)**.

In addition, in case of a g-scale, a 500 g column had to be used. This led to a time and solvent consuming separation. According to the fact that only *trans*-piperidinone ***trans*-(3)** ends up in the final target molecule, the crude material was used directly for the epimerization, wherein the enrichment of the desired *trans*-piperidinone ***trans*-(3)** was performed.

3.2.4 Epimerization: Enrichment of *trans*-Piperidinone *trans*-(3)

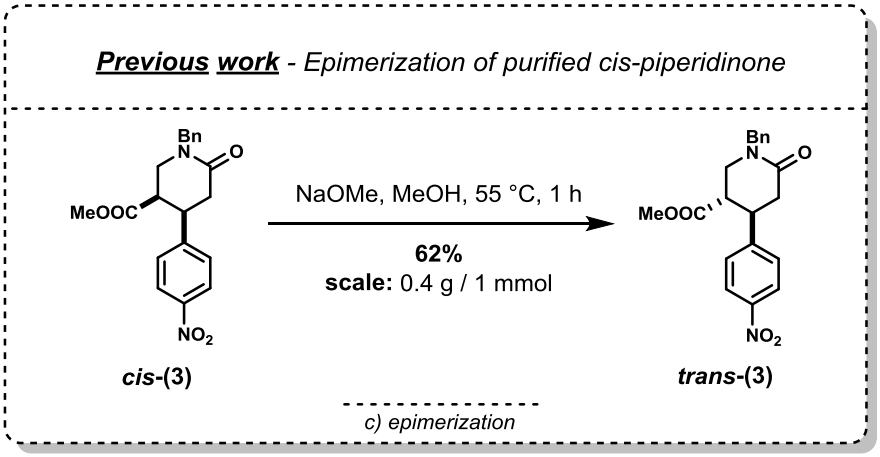

In the previous work[6], the epimerization was performed referring to a literature protocol toward the synthesis of paroxetine[22].

In those procedures, the enrichment of *trans*-piperidinone ***trans*-(3)** was performed via deprotonation of the stereocenters followed by a twist of the molecule into the thermodynamically favored *trans*-configuration.

NaOMe, used as the base, was added to a suspension of compound ***cis*-(3)** under argon counter stream. After stirring the reaction mixture for 1 h at 55 °C, TLC analysis indicated no further conversion to ***trans*-(3)**. The reaction mixture was quenched with a satd. aqu. solution of NH_4Cl and extracted with EtOAc. The combined organic phases were washed with a satd. aqu. solution of $NaHCO_3$ and brine followed by drying over $MgSO_4$. After removal of the volatiles, the crude mixture was purified via MPLC, where a yield of 62% of ***trans*-(3)** was obtained.

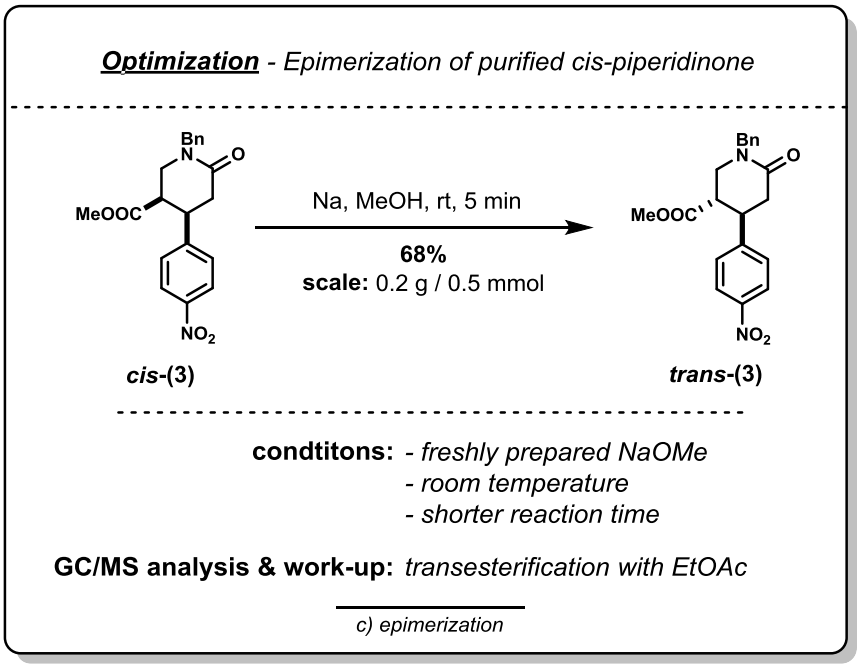

During the optimization of the reaction, it was realized that NaOMe contained NaOH to some extent, which can hydrolyze the ester functionality and which would lead to decrease in yield. Therefore, NaOMe was prepared freshly from sodium in dry MeOH.

Accordingly, a solution of *cis*-piperidinone ***cis*-(3)** in dry MeOH was added to the freshly prepared solution of NaOMe in dry MeOH. At this point it is worth mentioning that piperidinone ***cis*-(3)** showed a low solubility in MeOH. By means of an ultrasonic bath a solution of a concentration (0.04 mg/mL or lower, dependent on the scale) which could be transferred via syringe could be prepared.

The reaction was monitored via TLC and GC/MS analysis. GC/MS analysis indicated that the equilibrium between the two diastereomers **(3)** (*cis*/*trans* = 15/85) was reached after stirring the reaction mixture for 5 min at room temperature. In contrast, in the previous work[6], the reaction mixture was stirred at 55 °C for 1 h.

The reaction mixture was quenched with a satd. aqu. solution of NH_4Cl. In case of insufficient quenching and the subsequent extraction with EtOAc, a transesterification to the appropriate ethyl ester occurred according to ^{1}H-NMR measurements. Therefore the extracting agent as well as the solvent for GC/MS samples was exchanged from EtOAc to DCM. After removal of the solvent and the purification via MPLC, ***trans*-(3)** was obtained in a higher yield of 68% (Lit.[6]: 62%). With this optimized conditions, a scale-up can be performed.

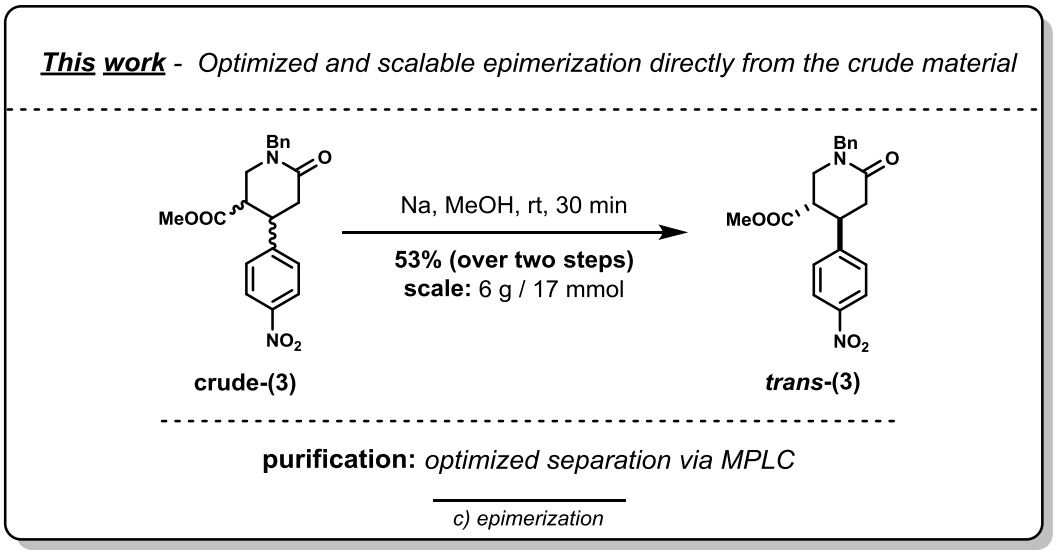

In case of the scale-up of the 0.2 g scale to a 6 g scale, the crude material of the cyclization was used in order to avoid one time and solvent consuming purification step via MPLC.

The crude mixture, which showed a better solubility in MeOH (0.1 g/mL) than purified ***cis*-(3)**, was added to a solution of freshly prepared NaOMe in dry MeOH. The equilibrium of piperidinones **(3)** was reached according to GC/MS analysis after 30 min. Therefore, the reaction mixture was quenched with a satd. aqu. solution of NH_4Cl followed by the optimized extractive work-up with DCM.

The further purification was done via MPLC. A mixture of acetone in LP was used instead of the commonly used eluents because of a better separation and a faster elution.

The only disadvantage of the use of acetone as eluent is its absorption of light of 254 nm, which can, dependent on the scale, overlap with the signal of the separated compounds. However, the problem can be solved easily by choosing a wavelength were the absorption of the separated compounds is higher than the absorption of acetone.

After purification, a yield of 53% over two steps was obtained. In case of the epimerization of purified ***cis*-(3)**, an insignificantly higher yield over two steps of 57% (Lit.[6]: 61%) was obtained.

Concluding, the direct epimerization of the crude material is definitely the better choice especially for a g-scale.

3.2.5 Reduction: Synthesis of Alcohol *rac*-(4)

Previous work *- The intermediate formation and cleavage of a borane-amine complex*

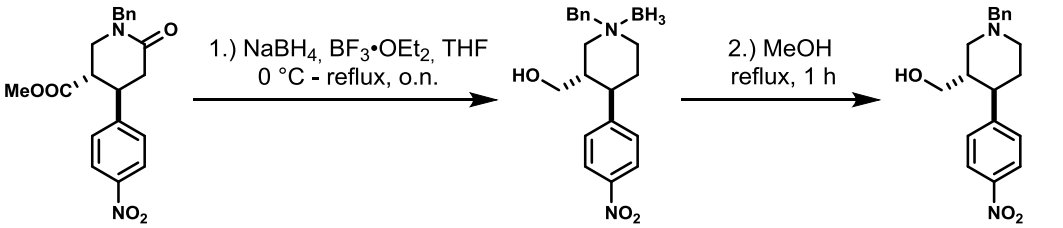

***trans*-(3)** | **complex-(4) borane-amine complex** | ***rac*-(4)**

83%
scale: 2 g / 6 mmol

condtitons: *1.) formation of a stable borane-amine complex*
2.) cleavage via methanolysis

purification: *via MPLC (silica gel/crude material = 100/1)*

d) reduction

In this step, the ester and the amide functionality had to be reduced. According to previous work[6], the reduction with $LiAlH_4$ was incompatible with the nitro substituent.

Therefore, by reviewing the literature, a suitable procedure[23] was found, where the reduction of an amide in the presence of a nitro substituent was described.

Following this procedure, the reducing species were formed in situ from four equivalents of $NaBH_4$ and four equivalents of BF_3•OEt_2 at 0 °C in dry THF as solvent.

$$4\ NaBH_4 + 4\ BF_3 \rightarrow 4\ BH_3 + NaBH_4 + 3\ NaBF_4$$

In accordance with this equation, four equivalents of BH_3 were formed in situ and one equivalent of $NaBH_4$ remained unconverted in order to reduce both functional groups.

After the formation of the reducing species at 0 °C, a solution of piperidinone ***trans*-(3)** in dry THF was added. The reaction mixture was stirred at reflux temperature over night followed by quenching and extractive work-up.

After removal of the solvent, a borane-amine complex[24] was obtained. The conversion of this borane-amine complex to alcohol ***rac*-(4)** was performed via methanolysis referring to a modified literature protocol[25]. After stirring the borane-amine complex for 1 h at reflux temperature in MeOH, volatiles were removed in vacuo. The purification via MPLC resulted in a yield of 83%.

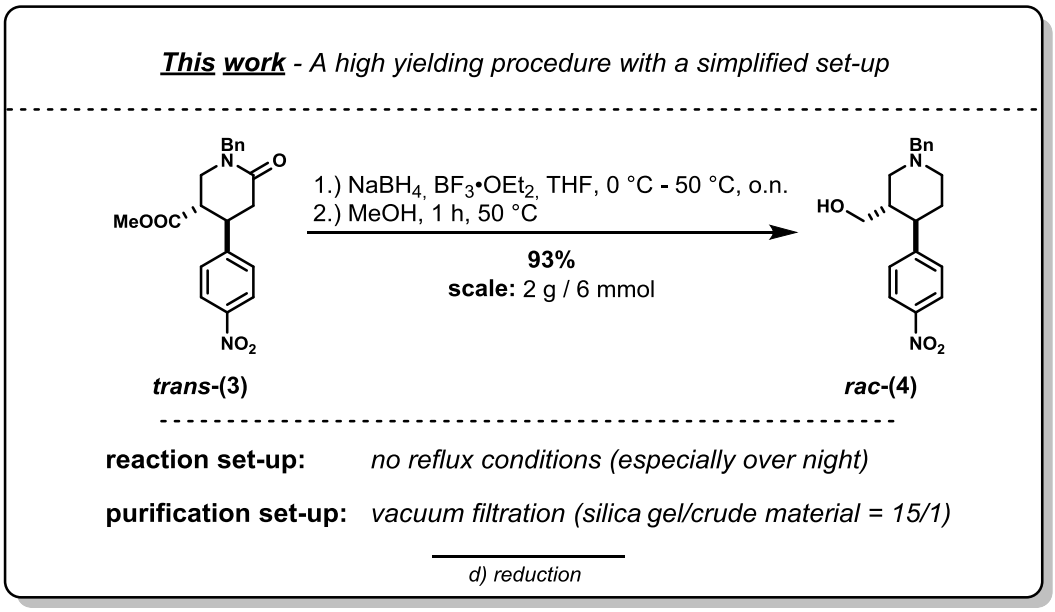

In this work, the formation of the reducing species using $NaBH_4$ and BF_3•OEt_2 was performed accordingly. After the addition of the solution of piperidinone ***trans*-(3)** in dry THF, the reaction mixture was stirred at 50 °C instead of reflux temperature ($b_{p\ (MeOH)}$ = 65 °C) in order to avoid reflux conditions, especially over night.

The reaction was monitored via TLC (DCM/MeOH = 100/10; R_f = 0.81 ***trans*-(3)**, 0.69 **complex-(4)**, 0.52 ***rac*-(4)**; visualized via ultraviolet light). A monitoring via HPLC/MS was not possible because of undetectable compounds.

In addition to the reaction monitoring via TLC it is worth mentioning that the TLC showed a <u>less</u> polar spot (R_f = 0.88) directly after the addition of starting material ***trans*-(3)**. Due to the fact that the spot disappeared in course of the reaction, it can either be a partly reduced species or the borane complex of starting material ***trans*-(3)**. Due to the fact that the ester functionality is more reactive than the amide, the partly reduced species would be the alcohol which would lead to a <u>more</u> polar spot. Therefore, the spot had to refer to the borane complex of starting material ***trans*-(3)**.

After stirring the reaction over night at 50 °C, the reaction mixture was quenched and the borane-amine complex was obtained after extractive work-up. The methanolysis of the borane-amine complex was also performed at 50 °C and not at reflux temperature. After removal of volatiles in vacuo, the crude material was obtained.

For further purification, vacuum filtration was used instead of MPLC in order to make the purification more suitable for the g-scale. Furthermore, the loading capacity was increased by using a ratio of silica gel to crude material of 15/1 instead of 100/1. With this improved set-up, a significantly higher yield of 93% (Lit.[6]: 83%) was obtained.

3.2.6 Enzymatic Kinetic Resolution: Enantiopure Alcohol (*3S,4R*)-(5)

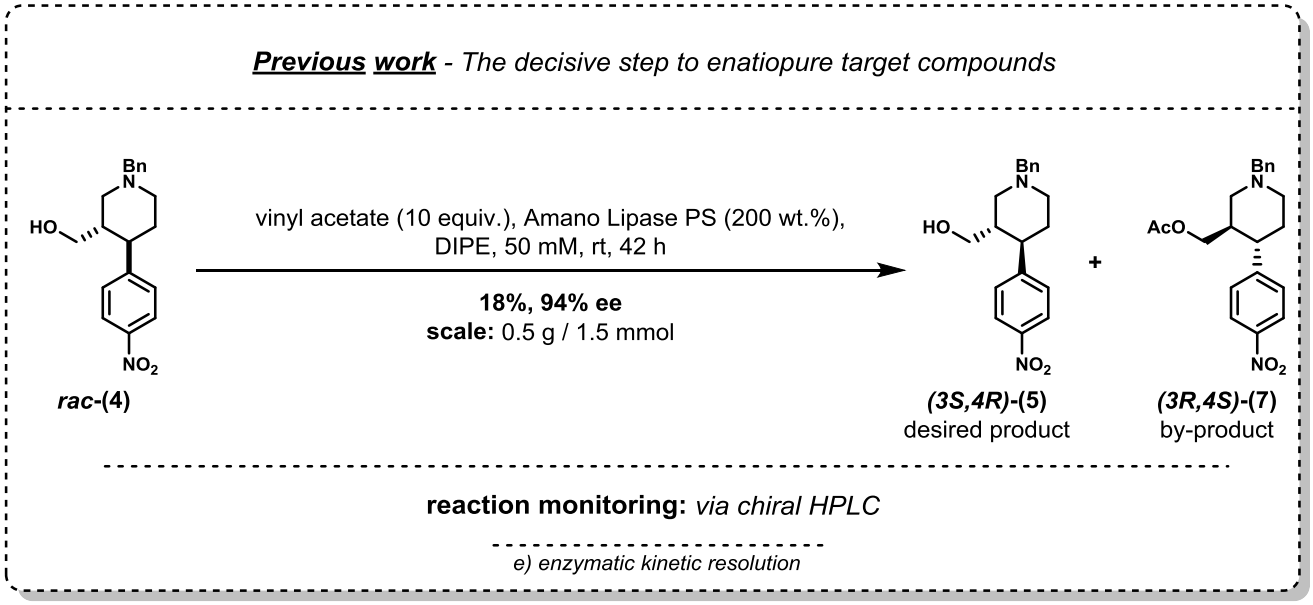

The enzymatic kinetic resolution of racemic alcohol ***rac*-(4)** was developed in the previous work[6], in order to provide enantioselctive access to azo-paroxetine.

The enzymatic kinetic resolution was performed using a lipase as catalyst. The active center of the lipase had to be acetylated with vinyl acetate and resulted in the formation of an enolate as leaving group which tautomerized to the corresponding ketone which could not act as nucleophile any more. In the following, the acetylated lipase catalyzed preferentially the acetylation of the (*3R,4S*)-enantiomer. In contrast, the (*3S,4R*)-enantiomer remained unconverted and was used for the synthesis of the following intermediates.

For the indirect determination of the absolute configuration of the alcohol, enantiomerically enriched alcohol (56% ee) was converted to the corresponding paroxetine analog of the alcohol in the previous work[6] (**Figure 13**).

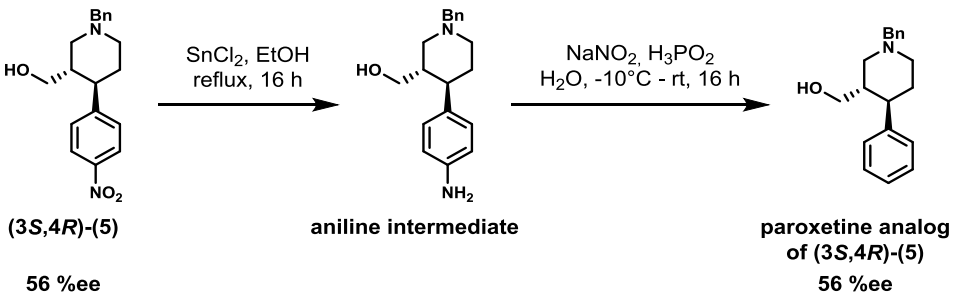

Figure 13: Determination of the absolute configuration of the alcohol.

The comparison of literature values[26] for the (*3R*,*4S*)-enantiomer of the paroxetine analog of the alcohol ($[\alpha]_D^{23}$ = +15.1, c = 1.0, $CHCl_3$, 90% ee), with the determined values[6] ($[\alpha]_D^{23}$ = -8.2, c = 1.0, $CHCl_3$, 56% ee), led to the conclusion that **(*3S,4R*)-(5)** was formed under the chosen reaction conditions, which will be elaborated in the following.

In the previous work[6], the enzymatic kinetic resolution was performed at room temperature with Amano Lipase PS (200 wt.%) as catalyst and MTBE as solvent. The reaction was stopped after 47 h and the catalyst was removed via filtration through a pad of celite. After removal of the solvent, alcohol **(*3S,4R*)-(5)** was obtained in a yield of 18% and a selectivity of 94% ee.

In order to stop the reaction at the point where alcohol **(*3S,4R*)-(5)** showed a selectivity around 95% ee, the reaction was monitored via chiral HPLC (ChiralPak AS-H column) using mixtures of EtOH in hexane as eluents (for details see chapter **4.1.8**).

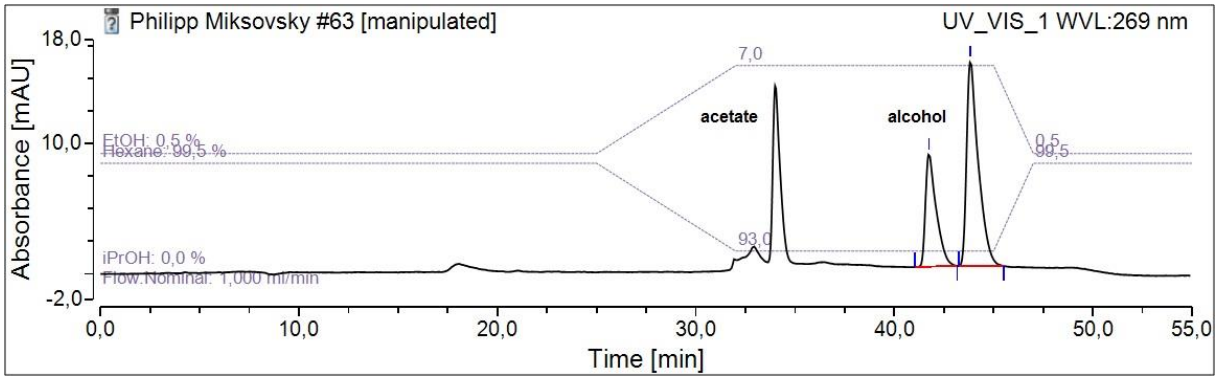

Figure 14: The monitoring of the enzymatic kinetic resolution in the previous work[6].

As shown in **Figure 14**, one peak of the acetate was not resolved from a gradient peak, not compromising a reliable evaluation. Furthermore, one run took 55 min, which could be optimized as shown in the following.

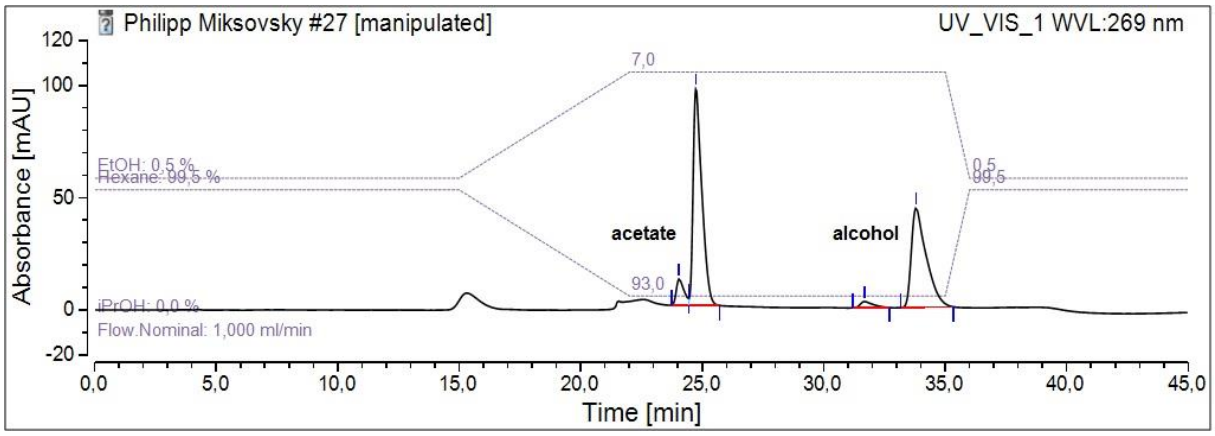

Figure 15: The optimization of the HPLC method in this work led to reliable measurements.

By optimizing the HPLC method (**Figure 15**) in this work, the measurement time was shortened to 45 min and the gradient peak was resolved from the acetate peak.

This resulted in reliable measurements for monitoring the enzymatic kinetic resolution. The decisive data, which had to be evaluated in order to monitor the reaction, were the enantiomeric excess of the alcohol and the absolute peak area of the alcohol and the acetate. The ratio of the absolute peak areas of both species represented the approximate expectable yield, provided that both species show a similar absorbance at the deployed wavelength, which is the case according to the spectral data.

With this optimized HPLC method at hand, a screening was performed in order to obtain higher yields (Lit.[6]: 18%) and selectivities higher than 95% ee (Lit.[6]: 94% ee).

Optimization via a screening *- High yields and very good selectivities in a meaningful time*

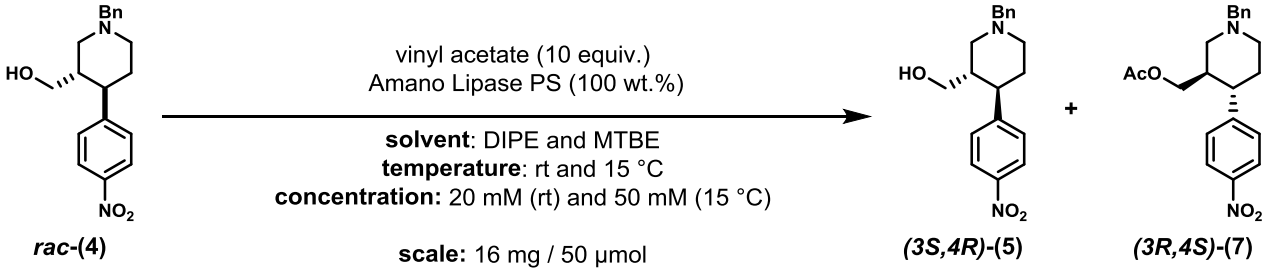

best conditions: *MTBE, rt, 20 mM, 141 h (38% exp. yield, 98% ee)*

accelarated reaction: *200 wt.% Amano Lipase PS, 44 h (41% exp. yield, 97% ee)*

e) enzymatic kinetic resolution

A screening of different lipases and different solvents was performed already in the previous work[6] referring to a literature procedure[27] toward the synthesis of paroxetine.

The screening of the enzymes showed that only Amano Lipase PS led to the desired acetylation of the (*3R,4S*)-enantiomer. In contrast, the enzymes CAL-A and CAL-B showed the opposite enantioselectivity and led to the acetylation of the (*3S,4R*)-enantiomer.

The screening of different solvents indicated that MTBE, DIPE or toluene are the solvents of choice regarding the selectivity but, regarding the reaction time, only MTBE and DIPE were suitable.

For these reasons, Amano Lipase PS as enzyme as well as MTBE and DIPE as solvents were used for further screenings performed in this work.

The screening of different solvents, temperatures and concentrations as well as different amounts of lipase should lead to higher yields (Lit.[6]: 18%), selectivities higher than 95% ee (Lit.[6]: 94% ee) but also to reaction times around 2 - 3 days.

The enantiomeric excess and expectable yields for alcohol **(*3S,4R*)-(5)**, determined via screening are summarized in **Table 2**.

Table 2: Screening of different solvents, temperatures, concentrations and amounts of lipase.

time	solvent	temperature	concentration	amount of lipase	alcohol (*3S,4R*)-(5)	
					ee (%)	exp. yield (%)
141 h	MTBE	rt	20 mM	100 wt.%	98	38
141 h	MTBE	15 °C	50 mM	100 wt.%	91	39
141 h	DIPE	rt	20 mM	100 wt.%	95	36
141 h	DIPE	15 °C	50 mM	100 wt.%	72	40
44 h	MTBE	rt	20 mM	200 wt.%	97	41

As shown in **Table 2**, the best selectivity was observed at room temperature using MTBE as solvent. In contrast, the reaction in DIPE resulted in a lower selectivity. Additionally no desirable temperature effect was observed. In order to shorten the reaction time of 141 h (approx. 6 d), there exist two possible options for the acceleration.

Either a higher amount of lipase can be used or the concentration can be increased. In case of previous work[6] both options were combined in one experiment (200 wt.% lipase, 50 mM) resulting in an unsatisfactory outcome (18%, 94% ee) as discussed before. Furthermore, the results of the screening (**Table 2**) showed that a concentration of 20 mM was a good choice.

Accordingly, the double amount of lipase (200 wt.%) was used in order to accelerate the reaction. The reaction in MTBE resulted in a satisfactory yield of 41% and 97% ee after 44 h.

With these optimized conditions in hand, a scale-up to a 5 g scale (Lit.[6]: 0.5 g) was performed.

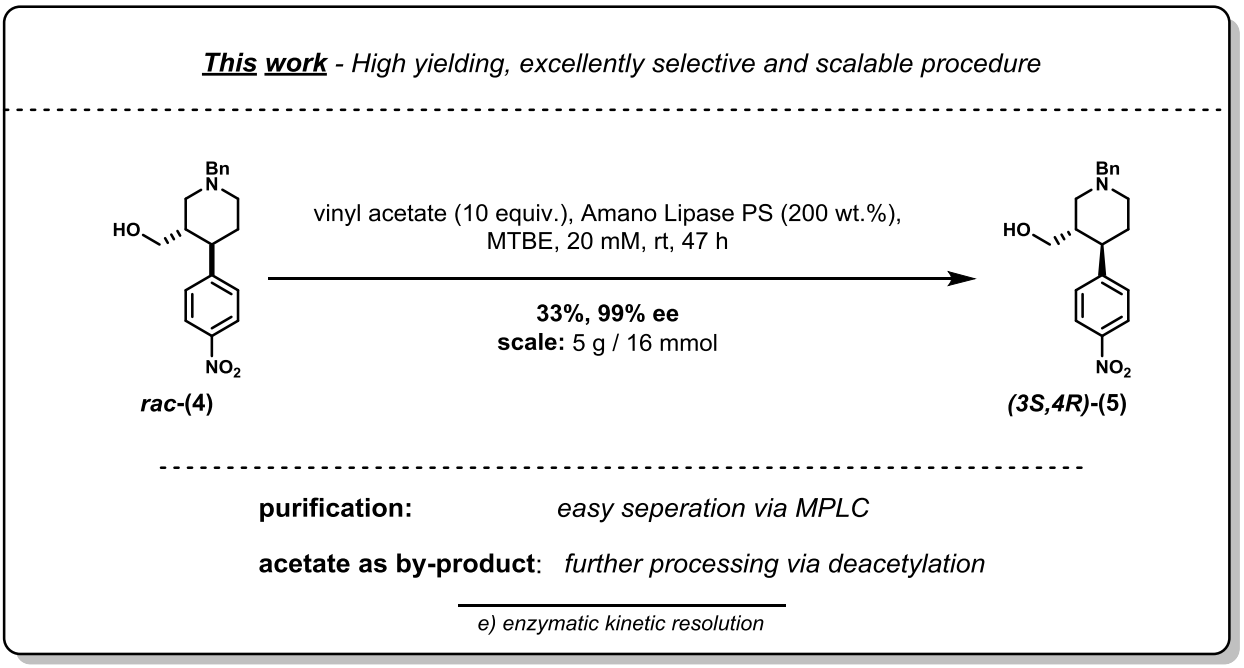

The scale-up of the reaction to a 5 g scale resulted in a very good isolated yield of 33% and an excellent selectivity of 99% ee. Furthermore, the reaction was completed in 47 h.

Alcohol **(*3S,4R*)-(5)** was dissolved in MTBE (concentration: 20 mM) and an excess of vinyl acetate and 200 wt.% Amano Lipase were added. The reaction was monitored via optimized chiral HPLC measurements. After reaching the excellent enantiomeric excess of 99% ee, the lipase was removed via filtration through a pad of celite. DCM was used for washing due to availability issues. After removal of the solvent, alcohol **(*3S,4R*)-(5)** was separated from acetate **(*3R,4S*)-(7)** via MPLC.

Acetate **(*3R,4S*)-(7)** (3.7 g, 60%, 71% ee) was deacetylated in the next step in order to allow further processing of the (*3R,4S*)-enantiomer as model compound instead of wasting it.

3.2.7 Deacetylation: Alcohol (*3R,4S*)-(6) for Further Test Reactions

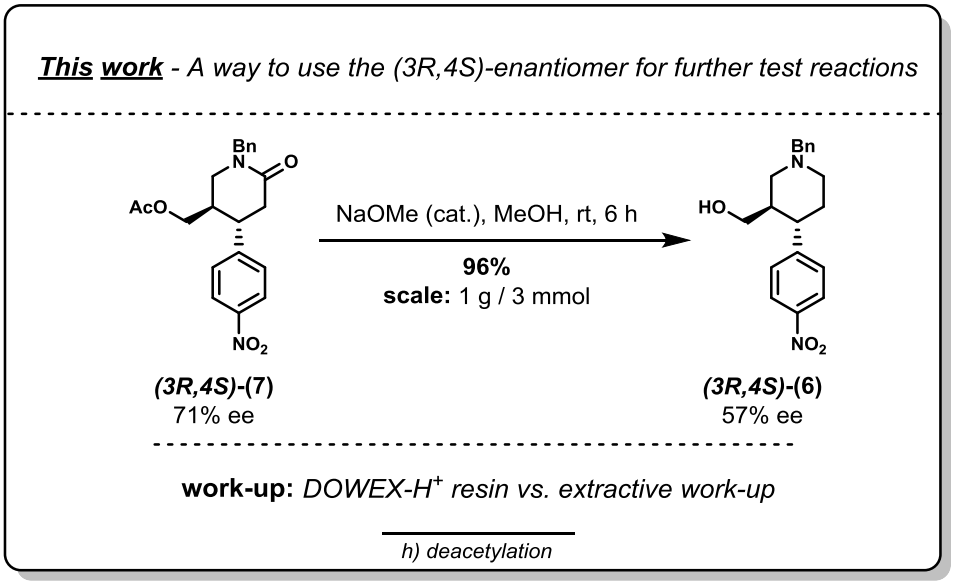

The deacetylation was performed according to a modified literature protocol[28].

The procedure was developed in this work in order to convert acetate **(*3R,4S*)-(7)** to alcohol **(*3R,4S*)-(6)** and use the high amounts of the opposite enantiomer for further test reactions of the following steps before up-scaling these steps.

The deacetylation was performed, using NaOMe as base. The solution of NaOMe in dry MeOH ((30% (w/v)) was added in catalytic amounts to a solution of acetate **(*3R,4S*)-(7)** in dry MeOH, until a pH value of 10 was reached. The reaction was stirred at room temperature and after 6 h TLC analysis indicated full conversion.

In the literature protocol[28], DOWEX-H^+ resin was used after complete conversion to neutralize the reaction mixture. This work-up was not feasible due to a strong interaction of the nitro substituent with the resin, whereby alcohol **(*3R,4S*)-(6)** could not be recovered from the resin.

Accordingly, an extractive work-up was performed with DCM and a satd. aqu. solution of NH_4Cl. Without further purification, pure alcohol **(*3R,4S*)-(6)** in nearly quantitative yield of 96% was obtained.

Concluding, acetate **(*3R,4S*)-(7)** was converted successfully to alcohol **(*3R,4S*)-(6)**, a valuable compound for further test reactions of the following reaction steps in order to be able to convert the whole amount of desired alcohol **(*3S,4R*)-(5)** via the optimized and scaled process.

3.2.8 Etherification: Synthesis of Ether (8)

Previous work *- The etherification with sesamol via the formation of a mesylate*

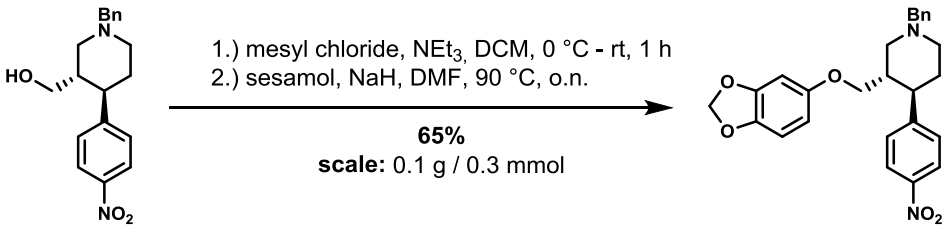

(3S,4R)-(5) (8)

f) etherification

In the previous work[6], the etherification was performed referring to a modified literature procedure[29].

In the first step, the mesylate was formed by the addition of mesyl chloride to a solution of alcohol ***(3S,4R)*-(5)** in dry DCM. During the reaction HCl was formed, which formed a salt in presence of NEt_3. After stirring for 1 h, the reaction was quenched with water followed by extractive work-up. After removal of the solvent in vacuo, the mesylate was used directly for the etherification with sesamol.

Sesamol, dissolved in dry DMF, was deprotonated using NaH. After the addition of a solution of the mesylate in dry DMF, the reaction was stirred over night at 90 °C. After extractive work-up and further purification via MPLC, ether **(8)** was obtained in a yield of 65%.

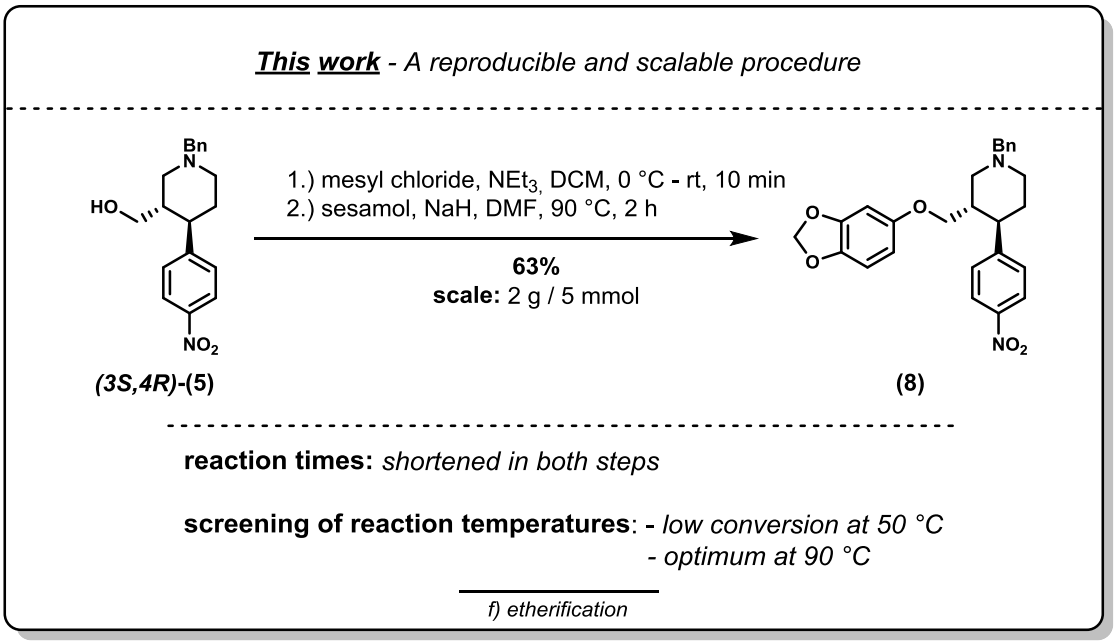

In this work, the scale-up to a 2 g scale (Lit.[6]: 0.1 g) was performed. Additionally, a thorough investigation of reaction times and reaction temperatures led to shorter reaction times in both steps.

The mesylation of alcohol **(*3S,4R*)-(5)** with mesyl chloride in dry DCM was finished after stirring for 10 min at room temperature according to TLC analysis. In contrast, the reaction would be finished after stirring for 1 h at room temperature according to previous work[6].

Also the etherification of the mesylate with sesamol in dry DMF was finished in a shorter time. The reaction was completed after stirring for 2 h at 90 °C according to TLC analysis. In contrast, the reaction mixture had to be stirred over night at 90 °C according to previous work[6].

Because of the short reaction time of the second step, the reaction temperature was lowered to 50 °C. Unfortunately, the reaction was not finished after 25 h at 50 °C. According to this, the scale-up was performed at 90 °C.

After stirring for 2 h at 90 °C, the reaction mixture was diluted with EtOAc and the organic phase was washed with water and 1 N NaOH thereby removing the excess of sesamol. In order to ensure that no loss of product and therefore decrease in yield proceeded while washing the organic phase, re-extracts of the washing phases were analyzed via TLC. After removal of the solvent, further purification was performed via MPLC. Ether **(8)** was obtained in 2 g scale in a satisfying yield of 63% (Lit.[6]: 65%, 0.1 g scale).

This work *- Identification of side products formed during the mesylation step*

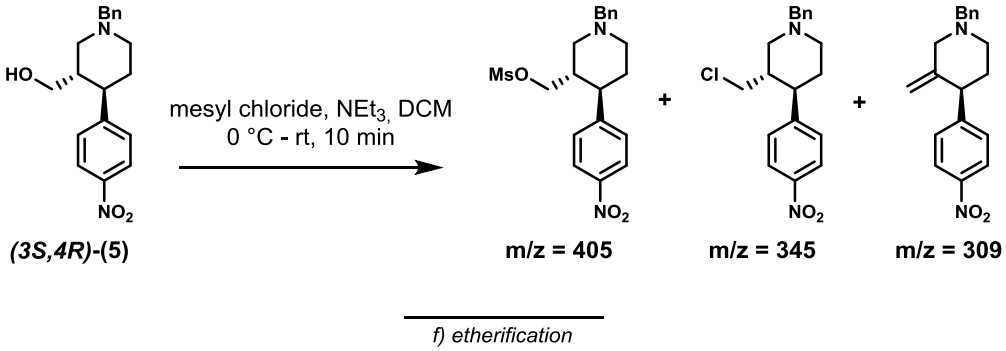

***(3S,4R)*-(5)**

f) etherification

The review of HPLC/MS data of a side fraction, obtained via MPLC, resulted in the conclusion that in the first step, the mesylation, also the chlorinated species (m/z = 345) was formed besides the desired mesylate (m/z = 405). This chlorinated species underwent an elimination in the second step at 90 °C, thereby forming the corresponding alkene (m/z = 309).

In order to avoid the formation of the chlorinated species, a higher amount of NEt_3 can be used in the first step. This will lead to an approximately 10% higher yield.

3.2.9 Reduction and Deprotection: Synthesis of Aniline (9)

Previous work *- The final step to the azo precursor*

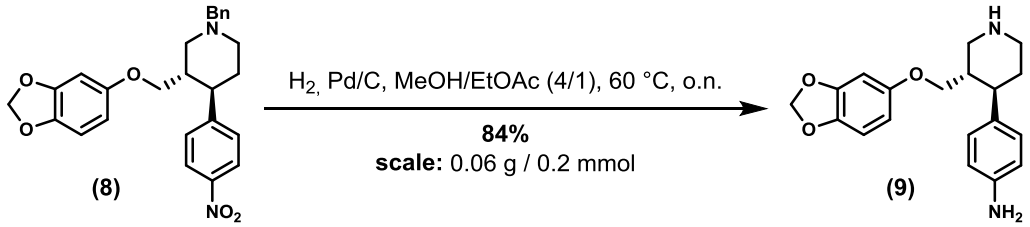

g) reduction and deprotection

In the final step to the azo precursor, the nitro group had to be converted to the aniline. Furthermore, the benzyl group was cleaved off under these conditions.

In the previous work[6], 10% Pd/C was added to a solution of ether **(8)** in a mixture of MeOH and EtOAc. After stirring for 16 h at 60 °C under hydrogen atmosphere, the catalyst was removed via filtration through a pad of celite. MeOH, which was used for washing, was removed in vacuo. After purification via flash column chromatography, aniline **(9)** was obtained in a yield of 84%.

This work *- Proof of the reproducibility in a mg-scale due to expectable stability issues*

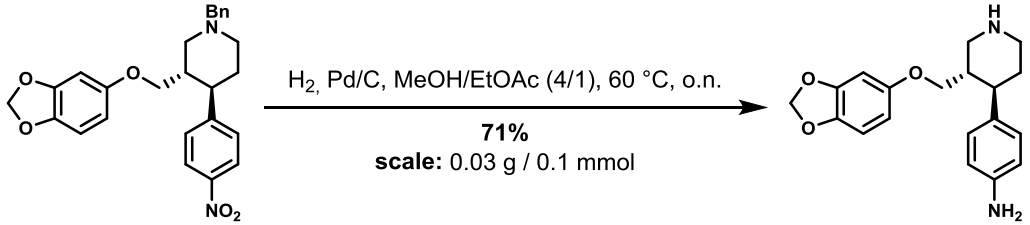

screening of the reaction temperatures: *- low conversion at room temperature*
- best conditions: 60 °C / over night

g) reduction and deprotection

According to the expected instability of aniline **(9)** compared to tits oxidized form **(8)**, no scale-up was performed for this step. However, the reproducibility of the conditions was confirmed. In addition, a thorough investigation of the reaction temperature was performed.

Unfortunately, the reduction at room temperature instead of 60 °C resulted in a low conversion. The reaction was not finished after 22 h. Concluding, 60 °C were necessary to convert compound **(8)** over night.

After stirring over night at 60 °C, the catalyst was removed via filtration through a pad of celite. MeOH was used for washing and was removed in vacuo. The crude material was purified via MPLC instead of flash column chromatography due to easier purification in case of a g-scale.

After purification a yield of 71% (Lit.[6]: 84%) was obtained. The lower yield can be explained by the smaller scale of 0.03 g ((Lit.[6]: 0.06 g) and the purification via MPLC. Especially for such small quantities a higher loss of material had to be expected as compared with flash column chromatography.

3.2.10 Conclusion and Outlook

Azo precursor *- The door opener for photoswitchable azo-paroxetine based SSRIs*

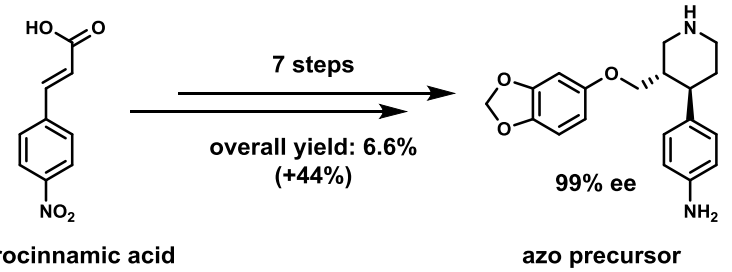

4-nitrocinnamic acid **azo precursor**

optimization: *- reproducible and high yielding conditions*
- optimized work-flow

scale-up: *- synthesis of high quantites (g-scale)*
- feasible purification methods

outlook: *- synthesis of various azo-paroxetine derivatives*
- discovery of potential photoswitchable azo-paroxetine based SSRIs

conclusion and outlook

In summary, the 7-step synthesis to the azo precursor was optimized and scaled successfully resulting in an overall yield of 6.6%, an increase of 44% in comparison to previous work[6] (4.6%, 94% ee), and an excellent enantiomeric excess of 99% ee.

With 1.3 g of the azo-paroxetine precursor with an excellent enantiomeric excess of 99% ee in hand, it is now possible to synthesize various azo-paroxetine derivatives either via Mills reaction, or via azo coupling in order to find more potent photoswitchable azo-paroxetine based SSRIs.

Furthermore, the optimization of all 7 steps led to reproducible and high yielding procedures with an optimized work-flow. Additionally the optimized conditions also resulted in easier purification protocols, which were feasible even and especially for higher quantities.

Concluding, the optimization as well as the scale-up of the 7-step synthesis to the azo precursor with an excellent enantiomeric excess was an important milestone for the future discovery of more potent photoswitchable azo-paroxetine based SSRIs being used as photopharmacological tools in the field of neuroscience.

3.3 HTI Series

3.3.1 Synthesis: The Enantiopure HTI Key Intermediate

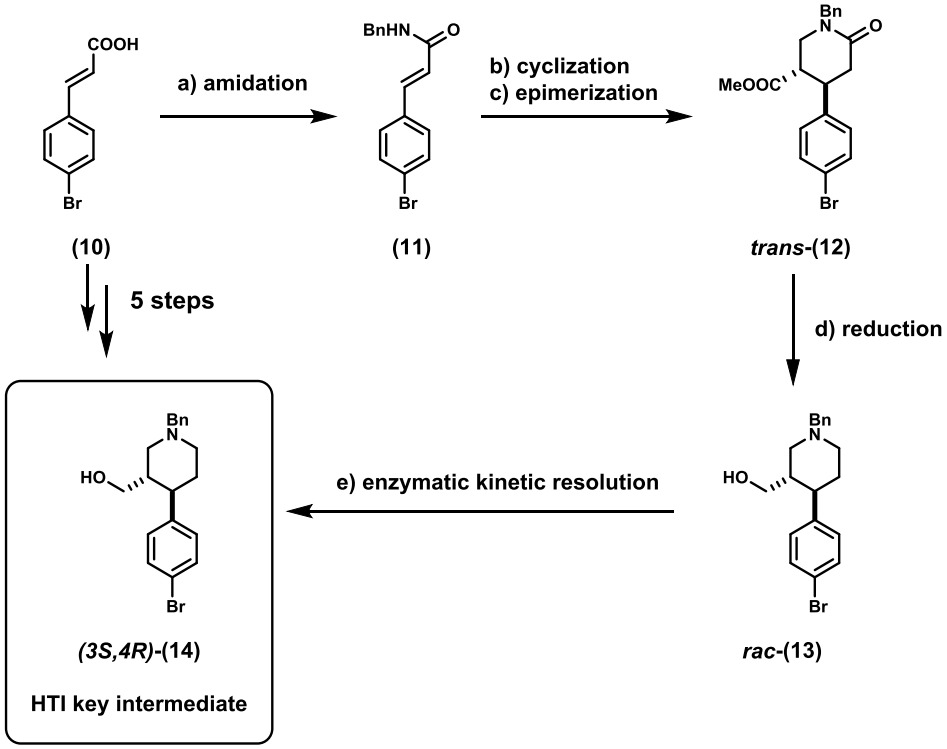

Figure 16: The synthesis of the HTI key intermediate for the HTI-paroxetine based SSRIs

The synthesis of the enantiopure HTI key intermediate was performed via 5-step synthesis starting from commercially available 4-bromocinnamic acid **(10)**.

In the first step, 4-bromocinnamic acid **(10)** was converted to the *N*-benzyl protected intermediate **(11)** via amidation. The cyclization via double Michael addition led to a diastereomeric mixture of piperidinones **(12)**. An enrichment of the desired *trans*-piperidinone ***trans*-(12)** was achieved via epimerization. The reduction of the ester and the amide functionality resulted in racemic alcohol ***rac*-(13)**. The enzymatic kinetic resolution was performed in order to obtain the enantiopure HTI key intermediate **(*3S,4R*)-(14).**

3.3.2 Amidation: Applicability to *N*-Benzyl Protected Brominated Amide (11)

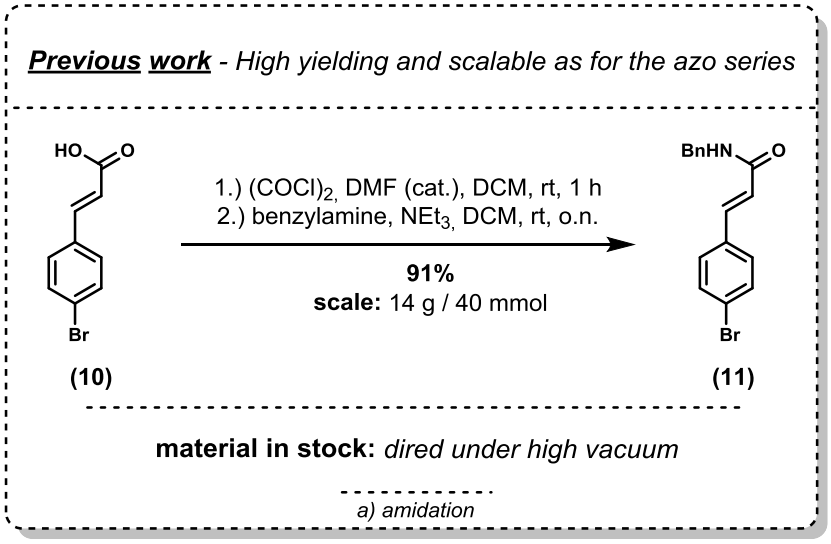

The applicability of the high yielding and scalable procedure developed for the azo series to the HTI series was already performed in the previous work[6].

Due to this fact and the availability of enough material, it was not necessary to synthesize *N*-benzyl protected amide **(11)** in this work.

However, the material was dried under high vacuum in order to ensure anhydrous conditions in the following step, which were necessary for reproducibility being elaborated in detail in the chapter regarding the azo series.

3.3.3 Cyclization: Applicability to Brominated Piperidinones *cis*-(12) and *trans*-(12)

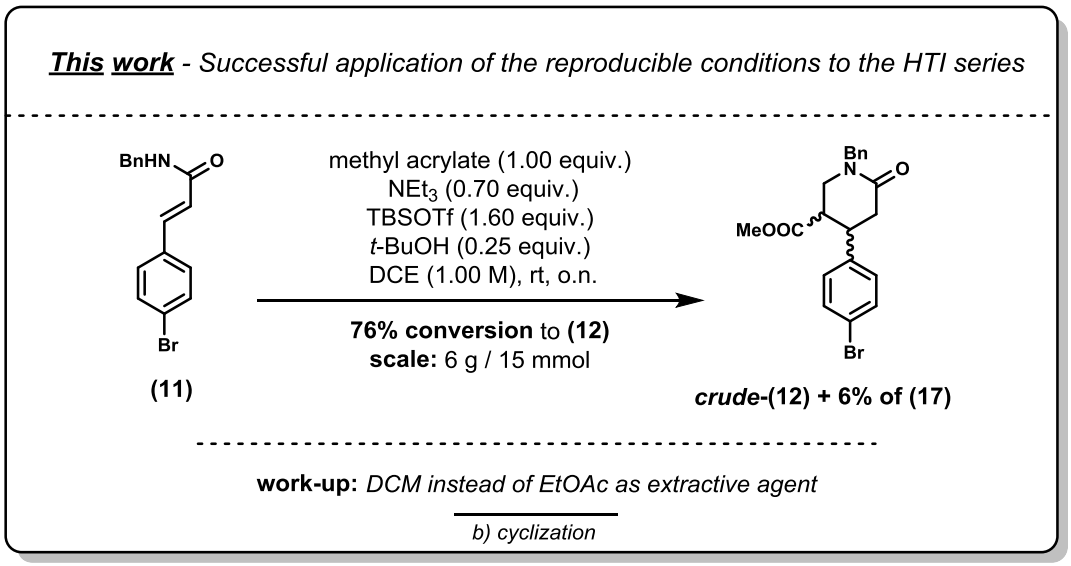

The cyclization in the HTI series was performed according to a modification of the optimized procedure developed for the azo series with an effect on the work-up.

Amide **(11)** was suspended in dry 1,2-DCE and freshly distilled methyl acrylate, dry NEt_3, TBSOTf and dry *t*-BuOH were added via syringe and under argon atmosphere. The immediate addition of *t*-BuOH was necessary in order to suppress the formation of triple Michael adduct **(17)**, which was formed in an amount of 6% according to ^{1}H-NMR measurements. The reaction mixture, which became homogeneous in course of the reaction, was stirred over night in order to ensure the maximum conversion of 76%.

The reaction was monitored as for the azo series via TLC (LP/EtOAc = 1/2; R_f = 0.71 **(11)**, 0.63 **(17)**, 0.57 ***trans*-(12)**, 0.37 ***cis*-(12)**; stained with $KMnO_4$), and GC/MS (Note: Triple Michael adduct **(17)** was also not detectable via GC/MS). The conversion to the piperidinones ***cis*-(12)** and ***trans*-(12)** was calculated by comparison of the integrals of the ^{1}H-NMR measurement of the crude mixture (**Table 3**).

Table 3: Calculations of the conversion using the ^{1}H-NMR measurements of the crude mixture

parameters	**(11)**	***cis*-(12)**	**(17)**	***trans*-(12)**
protons	Ar-C<u>H</u>=CH-	H2' & H6'	-OCH_3	H5
δ [ppm]	7.61	6.89	3.60	2.62
integral	1	2	3	1

For the work-up, the reaction was quenched with a satd. aqu. solution of NH_4Cl. DCM was used as extracting agent, because the extraction with EtOAc, being used in case of the azo series, resulted in the formation of an inseparable three-phase system. After a washing step with brine and drying over $MgSO_4$, volatiles were removed in vacuo. The oily supernatant, coming from degradation of reagents used in excess, was removed via Pasteur pipette and a drying step under high vacuum followed. As elaborated for the azo series, the crude mixture was used directly for the epimerization in order to avoid a time and solvent consuming separation via MPLC.

Concluding, the optimized and scalable conditions developed for the azo series were successfully applied for the HTI series.

3.3.4 Epimerization: Applicability to Brominated *trans*-Piperidinone *trans*-(12)

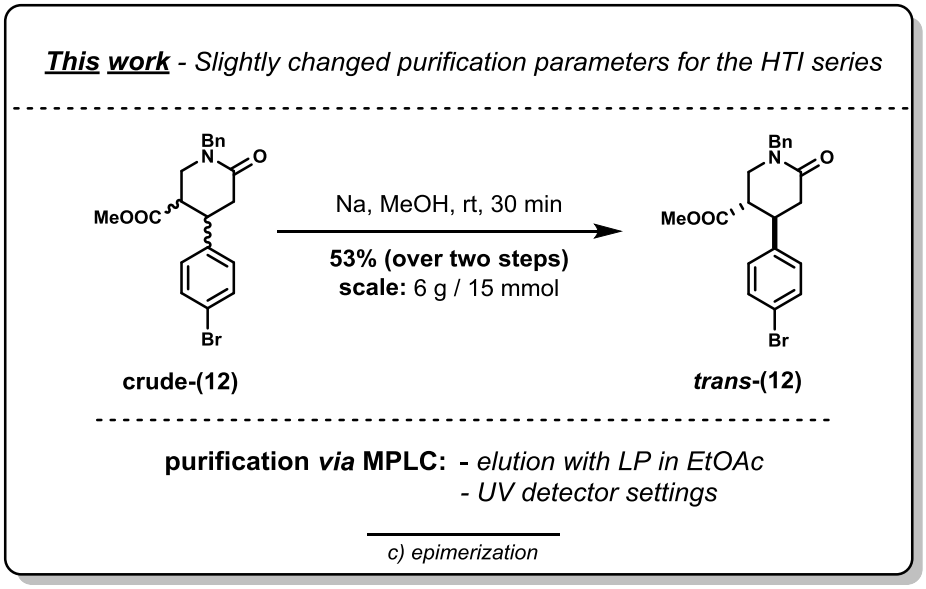

The epimerization in the HTI series was performed according to a modification of the optimized procedure developed for the azo series with an effect on the purification parameters.

Crude mixture **crude-(12)** was added to a solution of freshly prepared NaOMe in dry MeOH. The equilibrium (*cis*/*trans* = 15/85 according to ^{1}H-NMR analysis) was reached, like in case of the azo series, after stirring for 30 min at room temperature. After extractive work-up, further purification was performed via MPLC. The eluent and the UV detector settings were adapted accordingly.

In contrast to the azo series, where a mixture of acetone in LP was used as eluent, TLC analysis indicated a better separation for the HTI series using a mixture of EtOAc in LP. Because of a low absorbance of piperidinones **(12)** at 254 nm, the wavelength of the UV detector was set to 266 nm. This wavelength represented the absorbance maximum of ***trans*-(12)** according to a measured spectrum. Additionally the selectivity of the UV detector was increased to a value of 5xe^{-1}

With these optimized settings of the MPLC, the scale-up to a 6 g scale resulted in a yield of 53% over two steps. In comparison, a 7% higher yield over two steps was obtained in the previous work[6]. According to that, the direct epimerization of the crude is highly recommended, especially for a g-scale.

3.3.5 Reduction: Applicability to Brominated Alcohol *rac*-(13)

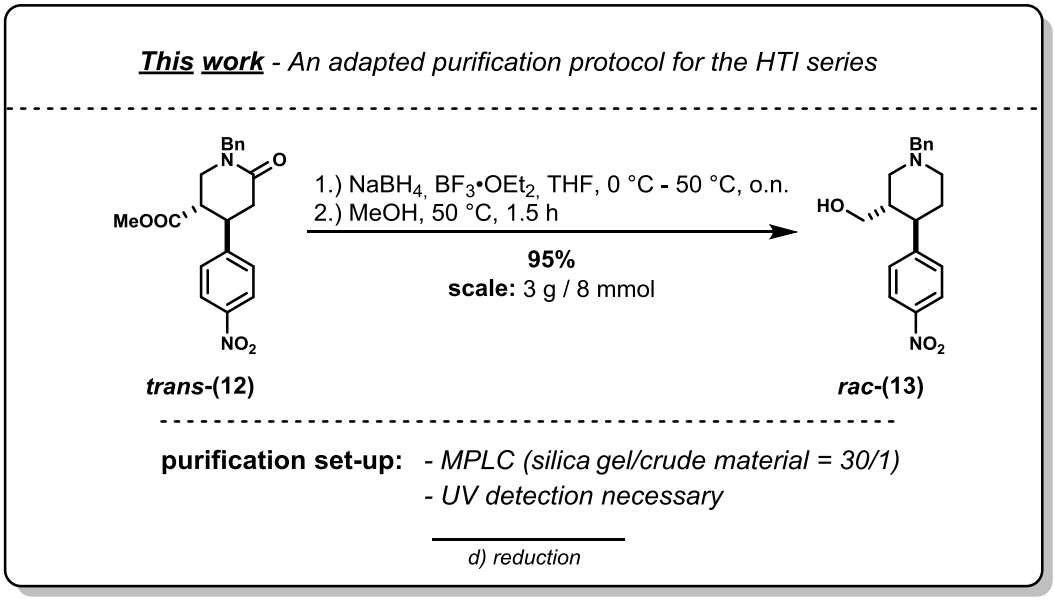

In the previous work[6], the first attempt using $LiAlH_4$ resulted in the formation of debrominated species. Therefore, the reduction was performed according to a modification of the optimized conditions, developed for the azo series with an effect on the purification set-up.

In the procedure, developed for the azo series, $NaBH_4$ and BF_3•OEt_2 formed the reducing species in situ in dry THF. A solution of piperidinone ***trans*-(12)** in dry THF was added and the reaction mixture was stirred over night at 50 °C.

The reaction was monitored via TLC (DCM/MeOH = 100/5; R_f = 0.50 ***trans*-(12)**, 0.70 **complex-(13)**, 0.22 ***rac*-(13)**; stained with $KMnO_4$), a monitoring via HPLC/MS was not possible due to undetectable compounds.

After extractive work-up and methanolysis, the crude mixture was purified via MPLC (silica gel/crude material = 30/1). The purification via MPLC with UV-detection was more suitable than the purification via vacuum filtration according to the UV absorption of the compounds

With this adapted purification set-up, alcohol ***rac*-(13)** was obtained in a higher yield of 95% (Lit.[6]: 84%).

3.3.6 Enzymatic Kinetic Resolution: The Enantiopure Synthesis of Key Intermediate (*3S,4R*)-(14)

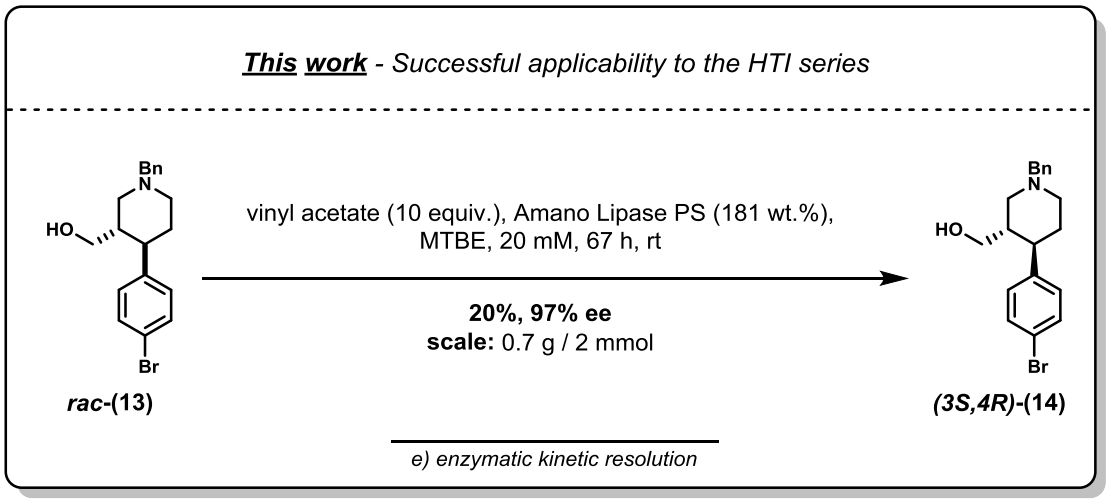

In the previous work[6], only a screening on analytic scale was performed but no preparative scale was conducted. However, the assignment of the absolute configuration of the alcohol was already performed indirectly via debromination of the alcohol to the corresponding paroxetine analog.

Therefore, enantiomerically enriched alcohol (80% ee), using CAL-B as lipase for the preceding enzymatic kinetic resolution, was converted to the corresponding paroxetine analog (**Figure 17**).

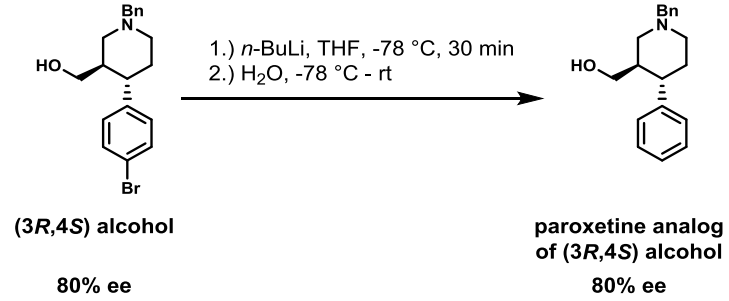

Figure 17: Determination of the absolute configuration of the alcohol.

The comparison of literature values[26] for the (*3R*,*4S*)-enantiomer of the paroxetine analog of (*3S,4R*)-(5) alcohol ($[\alpha]_D^{23}$ = +15.1, c = 1.0, $CHCl_3$, 90% ee), with the determined values[6] ($[\alpha]_D^{23}$ = +13.4, c = 1.0, $CHCl_3$, 80% ee), led to the conclusion that the undesired (*3R,4S*)-enantiomer of the alcohol was formed in case of using CAL-B as catalyst for the enzymatic kinetic resolution.

However, further experiments indicated that, in contrast to CAL-B, CAL-A and Amano Lipase PS show the desired acetylation of the *(3R,4S*)-enantiomer and led to the desired alcohol **(*3S,4R*)-(14)** .

According to the significantly higher selectivity of Amano Lipase PS as compared with CAL-A, Amano Lipase PS was used for the optimization of the enzymatic kinetic resolution in this work. Additionally MTBE and DIPE were used for a further screening as they were found to be the solvents of choice regarding selectivity and reaction time.

A screening (**Table 4**) of the solvents (100 wt.% lipase, 20 mM, rt) led to the conclusion that MTBE leads to higher selectivities and a faster reaction than DIPE. According to the long reaction time of 141 h, a higher amount of Amano Lipase PS was necessary for the acceleration of the reaction.

The use of 181 wt.% Amano Lipase PS, the same stoichiometric amount as having been used for the azo series, resulted in satisfying yield of 30% and 94% ee after 72 h.

Table 4: Results of the screening of the HTI series.

time	solvent	temperature	concentration	amount of lipase	alcohol (*3S,4R*)-(14)	
					ee (%)	exp. yield (%)
141 h	MTBE	rt	20 mM	100 wt.%	96	33
141 h	DIPE	rt	20 mM	100 wt.%	91	29
72 h	MTBE	rt	20 mM	181 wt.%	94	30

The monitoring of the reaction (enantiomeric excess and expectable yield of alcohol **(*3S,4R*)-(14)**) was performed with the optimized HPLC method, developed for the azo series (**Figure 18**). Due to a lower absorbance of the bromo species than the nitro species, the injection volume was increased from 3 µL to 10 µL (for details see chapter **4.1.8**).

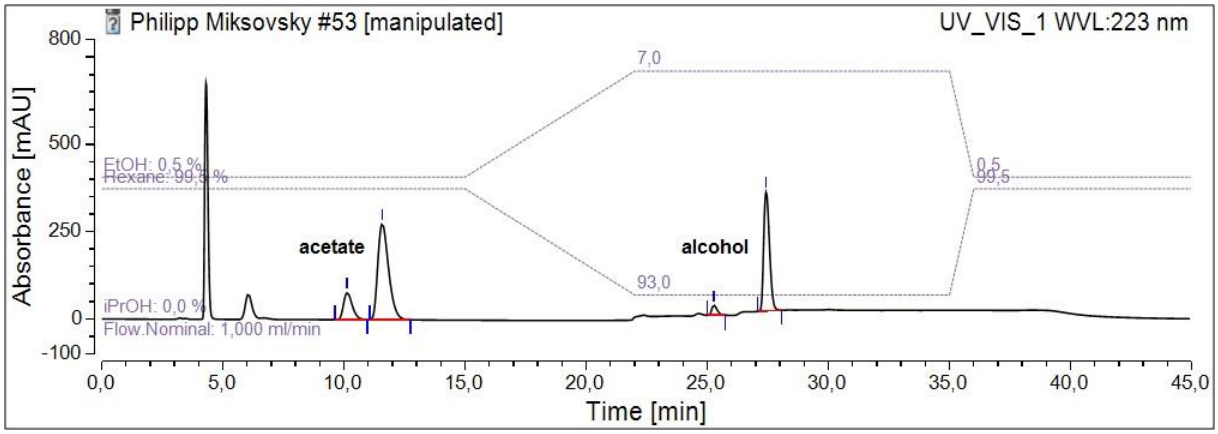

Figure 18: The optimized HPLC method was also suitable for the reaction monitoring in the HTI series.

With the results of the screening (30%, 94% ee, 72 h) and the optimized HPLC method in hand, a preparative scale (0.7 g) was prepared.

Alcohol **(*3S,4R*)-(14)** was dissolved in MTBE (concentration: 20 mM) and an excess of vinyl acetate and 181 wt.% Amano Lipase were added. After 67 h, the lipase was removed via filtration through a pad of celite and DCM was used for washing. After removal of the solvent, alcohol **(*3S,4R*)-(14)** was separated from acetate **(*3R,4S*)-(15)** via MPLC.

Alcohol **(*3S,4R*)-(14)** was obtained in a yield of 20% and 97% ee. Acetate **(*3R,4S*)-(15)** (60%, 54% ee) can be further converted to the alcohol via deacetylation protocol, developed for the azo series.

3.3.7 Conclusion and Outlook

Enantiopure HTI key intermediate *- Pharmacologically valuable HTI-paroxetine based SSRIs*

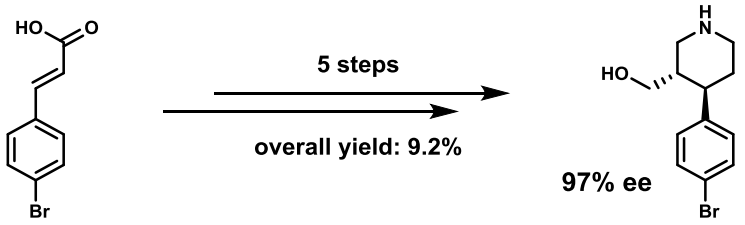

4-bromocinnamic acid **HTI key intermediate**

enantioselective synthesis: **-** *HTI key intermediate with 97% ee*

optimization & scale-up: *- modified and adapted procedures*
- scaled procedure with adapted purification protocols

outlook: **-** *synthesis of various enantiopure HTI-paroxetine derivatives*
- screening for potent HTI-paroxetine based SSRIs

conclusion and outlook

The first-time performed enantioselective synthesis of the HTI key intermediate resulted in an overall yield of 9.2% and a very good enantiomeric excess of 97% ee.

With such a high enantiomeric excess, the door is open for pharmacologically more valuable HTI-paroxetine based SSRIs. Furthermore, in combination with the optimization and the successful scale-up, various HTI-paroxetine derivatives can be synthesized and screened in order to find potent photoswitchable HTI-paroxetine based SSRIs.

Concluding, the development of the enantioselective synthesis to the enantiopure HTI key intermediate was an important milestone for the future discovery of more potent photoswitchable HTI-paroxetine based SSRIs being used as photopharmacological tools in the field of neuroscience.

4 Experimental Part

4.1 General Notes

4.1.1 Chemicals

Chemicals were purchased from several chemical suppliers. Oxalyl chloride, benzyl amine, methyl acrylate and mesyl chloride were distilled prior to use. NEt_3 and *t*-BuOH, used for reactions which required anhydrous conditions, were refluxed over CaH_2, distilled off and stored over molecular sieves in pre-dried flasks. Amano Lipase PS (immobilized on diatomite) was purchased from Sigma-Aldrich (product No. 708011).

4.1.2 Dry solvents

DCM, THF and MeOH, used for reactions which required anhydrous conditions, were pre-distilled and dried over Al_2O_3 columns (PURESOLV, Innovative Technology). Dry 1,2-DCE was purchased from Sigma-Aldrich. Dry DMF was purchased from ACROS Organics (AcroSeal and stored over molecular sieves).

4.1.3 Reactions under an inert atmosphere

Flasks were pre-dried in a drying cabinet at 80 °C, evacuated and flushed with argon on a Schlenk line three times. Reagents and solvents were added to the reaction via syringe under argon atmosphere. Syringes were purged with argon prior to use.

4.1.4 Specific rotation

For determining the specific rotation $[\alpha]_D^{20}$ of chiral compounds, a modular circular polarimeter (MCP 500) from Anton Paar and a cuvette of 100 mm length and 3 mm diameter was used. For calculations, the following equation was used:

$[\alpha]_D^{20} = (100 \cdot \alpha) / (c \cdot l)$; c in [g/100 mL]; l in [dm^3]

4.1.5 Medium pressure liquid chromatography (MPLC)

Column chromatography was carried out with a Büchi Sepacore MPLC system, comprised of two Büchi Pump Modules C-605, a Büchi pump manager C-615, a Büchi fraction collector C-660 and a Büchi UV photometer C-635. Cartridges (5 g – 90 g) and glass columns (500 g) were packed with silica gel 60 from Merck (mesh 40 – 60 µm). Mixtures of EtOAc or acetone in LP as well as MeOH and NH_4OH in DCM were used as eluents. The UV detector was set to a wavelength of 254 nm or 266 nm

and sensitivities between $2xe^{-0}$ and $5xe^{-1}$. The crude materials were loaded either by dissolving them in a minimum amount of eluent or, in case of insolubility, by adsorbing them on celite by dissolving the crude material in an appropriate solvent followed by the evaporation of the solvent. In case of using gradients, eluent volumes were indicated as multiples of the respective column volumes (CV).

5 g column = 6 mL CV

9 g column = 12 mL CV

50 g column = 60 mL CV

90 g column = 120 mL CV

500 g column = 720 mL CV

4.1.6 Thin layer chromatography (TLC)

TLC analysis was performed on silica gel 60 F_{254} aluminum plates containing a fluorescent indicator from Merck using solvent mixtures of EtOAc and acetone in LP as well as mixtures of DCM, MeOH and NH_4OH as eluents. Spots were visualized using ultraviolet light (254 nm) or were stained with potassium permanganate solution (3.0 g $KMnO_4$, 20.0 g K_2CO_3, 250 mg KOH, 300 mL H_2O) followed by heating.

4.1.7 High performance liquid chromatography – mass spectrometry hyphenation (HPLC/MS)

HPLC/MS was carried out with a Nexera Prominence UHPLC system from Shimadzu (system controller: CBM 20A; solvent delivery unit: 2 x LC - 30AD (dual gradient pump); degasser: DGU - 20A3, DGU - 20A5; autosampler: SIL -3 0AC; column oven: CTO - 20AC (temperature 40 °C); detectors: SPD - M20A, RF - 20Axs, ELS-2041, LCMS – 2020) using a Waters XSelect CSH C18 XP column (2.5 µm; 3x50 mm). The measurements were performed with mixtures of acetonitrile in H_2O under acidic conditions (0.1% formic acid) over 3.01 min (gradient: 5% (kept for 0.15 min) – 98% (gradient for 2.05 min; kept for 0.30 min) - 5% (gradient for 0.01 min; kept for 0.5 min); flow rate: 1.7 mL/min; injection volume: 0.1 - 1 µL).

4.1.8 High performance liquid chromatography (HPLC)

HPLC, used for the determination of the enantiomeric excess, was carried out with a Dionex UltiMate 3000 HPLC system from Thermo Fisher Scientific (pump: LPG-3400 SD; auto sampler: WPS-3000 SL analytic; column compartment: TCC-3000 SD;

detector: DAD-3000 RS) using a ChiralPak AS-H column (250 mm x 4.6 ID). The measurements were performed with mixtures of EtOH in hexane (gradient: 0.5% – 7%, 15.22.35.36.45; flow rate: 1mL/min; temperature: 25 °C; injection volume: 3 µL (azo series) – 10 µL (HTI series); wavelength UV detector: 269 nm (azo series), 223 nm (HTI series). For data analysis the software Chromeleon 7 was used.

Azo series

Injection Name:	**PM-090_51 h_grad_Hex_EtOH_0.5to7_1ml_3µL_2**	*Run Time (min):*	**45,00**
Vial Number:	**RA1**	*Report Template:*	**Report 4 Spectra**
Injection Volume:	**3,00**	*Channel:*	**UV_VIS_1**
Column:	**ASH**	*Wavelength:*	**269,0**
Instrument Method:	**grad_Hex_EtOH_0.5to7_1ml_25°_45min_15.22.35.36.45**	*B %:*	**0,0**
Processing Method:	**Long alcohol**	*C %:*	**99,5**
Injection Date/Time:	**17.Okt.18 17:16**	*D %:*	**0,5**
Operator:	**Irena Jelenkovic - Didic**		

Chromatogram

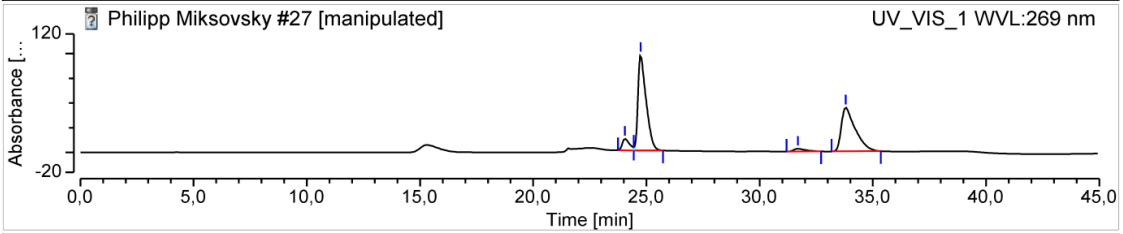

Integration Results

No.	Peak Name	Retention Time	Area	Height	Relative Area	Relative Height
		min	mAU*min	mAU	%	%
1	(*3S,4R*) acetate	24,050	4,282	11,714	5,50	7,52
2	(*3R,4S*) acetate	24,743	40,202	96,750	51,60	62,15
3	(*3R,4S*) alcohol	31,687	1,721	2,826	2,21	1,82
4	(*3S,4R*) alcohol	33,800	31,700	44,386	40,69	28,51

HTI series

Injection Name:	**PM-101_47h_grad_Hex_EtOH_0.5to7_45_1ml_10µL_1**	*Run Time (min):*	**45,00**
Vial Number:	**RD3**	*Report Template:*	**Report 4 Spectra**
Injection Volume:	**10,00**	*Channel:*	**UV_VIS_1**
Column:	**ASH**	*Wavelength:*	**223,0**
Instrument Method:	**grad_Hex_EtOH_0.5to7_1ml_25°_45min_15.22.35.36.45**	*B %:*	**0,0**
Processing Method:	**Long alcohol**	*C %:*	**99,5**
Injection Date/Time:	**23.Jän.19 14:58**	*D %:*	**0,5**
Operator:	**Irena Jelenkovic - Didic**		

Chromatogram

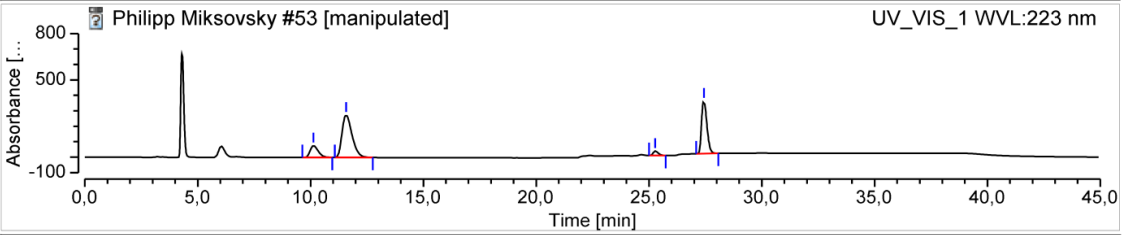

Integration Results

No.	Peak Name	Retention Time	Area	Height	Relative Area	Relative Height
		min	mAU*min	mAU	%	%
1	(*3S,4R*) acetate	10,133	32,471	77,106	11,73	10,67
2	(*3R,4S*) acetate	11,580	142,184	274,975	51,35	38,06
3	(*3R,4S*) alcohol	25,270	7,511	28,769	2,71	3,98
4	(*3R,4S*) alcohol	27,430	94,701	341,608	34,20	47,28

4.1.9 Melting point

Melting points were determined using a Büchi Melting Point B-545.

4.1.10 Gas chromatography – mass spectrometry hyphenation (GC/MS)

A Thermo Trace 1300 / ISQ LT (single quadrupole MS (EI)) containing a standard capillary column BGB 5 (30 m x 0.25 mm ID) was used for GC/MS measurements.

The following signals were reported:

all fragment peaks at/over mass (m/z) 100 and at/over 10% relative intensity
all molecular ions
all peaks with 100% intensity

4.1.11 Nuclear magnetic resonance spectroscopy (NMR spectroscopy)

^{1}H-NMR, ^{13}C-NMR spectra were recorded from $CDCl_3$ solutions on a Bruker Avance UltraShield *400* (^{1}H: 400 MHz, ^{13}C: 101 MHz) spectrometer. Chemical shifts are reported in ppm and were calibrated to the residual solvent signal[30] ($CDCl_3$, ^{1}H: 7.26 ppm, ^{13}C: 77.16 ppm). Coupling constants are reported in Hz (Hertz). The assignments are based on COSY, HSQC, HMBC and NOESY experiments as well as on the comparison with reported spectra.

The assignments of protons and carbon atoms in the NMR codes were carried out as follows:

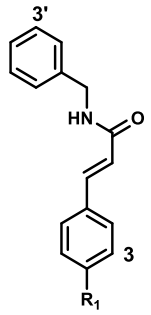

2, 11

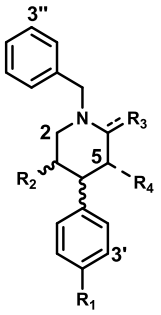

3-7, 12-17

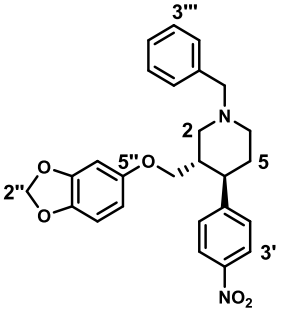

8

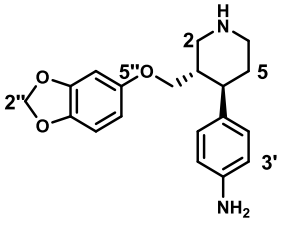

9

4.2 Azo Series

4.2.1 *N*-Benzyl-3-(4-nitrophenyl)acrylamide (2)

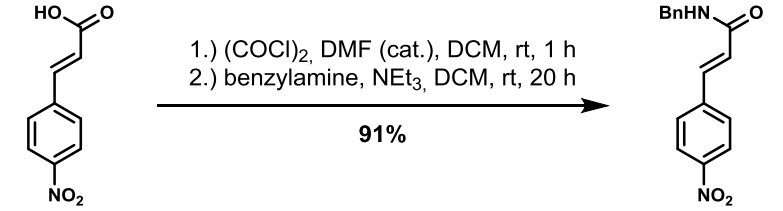

(1)
193.16 g/mol

(2)
282.30 g/mol

The protected amide was synthesized via optimization of a procedure, developed in previous work[6].

4-Nitrocinnamic acid **(1)** (13.52 g, 70.0 mmol, 1.00 equiv.) was suspended in dry DCM (230 mL, 0.30 M relative to starting material **(1)**). Dry DMF (1 drop) and freshly distilled oxalyl chloride (18.0 mL, 210 mmol, 3.00 equiv.) were added dropwise under argon via syringe. The mixture was stirred at room temperature. After stirring for 1 h, TLC analysis (MeOH quench) showed full conversion to the acid chloride. Volatiles were removed in vacuo.

After dissolving the isolated acid chloride in dry DCM (230 mL), dry NEt_3 (9.7 mL, 70.0 mmol, 1.00 equiv.) and freshly distilled benzylamine (7.50 g, 70.0 mmol, 1.00 equiv.) were added while cooling with a NaCl/ice bath to maintain the temperature at 25 °C. The mixture was stirred over night (20 h) at room temperature. The formed precipitate was collected and washed with 1 N HCl (400 mL) and 1 N NaOH (400 mL). Due to the low solubility of product **(2)** in DCM, the mother liquor was concentrated in vacuo and the precipitate was recrystallized from toluene. The combined fractions were dried under high vacuum, which was necessary for the following step.

Yield	91% (18.05 g, 63.9 mmol) (Lit.[6]: 93%, 120 mmol)
Appearance	pale yellow crystals
Melting point	189.0 – 189.5 °C (Lit.[6]: 189.5 - 190.0 °C)
TLC analysis	R_f = 0.71 (LP/EtOAc = 1/2)
Sum formula	$C_{16}H_{14}N_2O_3$

GC/MS	282 (30, M^+), 160 (21), 130 (26), 106 (100), 104 (24), 103 (17), 102 (46)
^{1}H-NMR (400 MHz, $CDCl_3$)	δ = 4.59 (d, *J* = 5.7 Hz, 2H, N-CH_2), 6.00 (br s, 1H, NH), 6.53 (d, *J* = 15.6 Hz, 1H, Ar-CH=C<u>H</u>-), 7.28 – 7.49 (m, 5H, H2' & H3' & H4' & H5' & H6'), 7.63 (d, *J* = 8.7 Hz, 2H, H2 & H6), 7.72 (d, *J* = 15.6 Hz, 1H, Ar-C<u>H</u>=CH-), 8.23 (d, *J* = 8.8 Hz, 2H, H3 & H5) ppm.
^{13}C-NMR (101 MHz, $CDCl_3$)	δ = 44.2 (t, N-CH_2), 124.3 (d, 2C, C3 & C5), 124.7 (d, Ar-CH=<u>C</u>H-), 128.0 (d, C4'), 128.1 & 128.5 & 129.0 (d, 6C, C2 & C6 & C2' & C3' & C5' & C6'), 137.9 (s, C1'), 139.0 (d, Ar-<u>C</u>H=CH-), 141.2 (s, C1), 148.3 (s, C4), 164.7 (s, amide) ppm.

Comment: Spectral data are in accordance with the literature[6].

4.2.2 Methyl 1-benzyl-4-(4-nitrophenyl)-6-oxopiperidine-3-carboxylate (3)

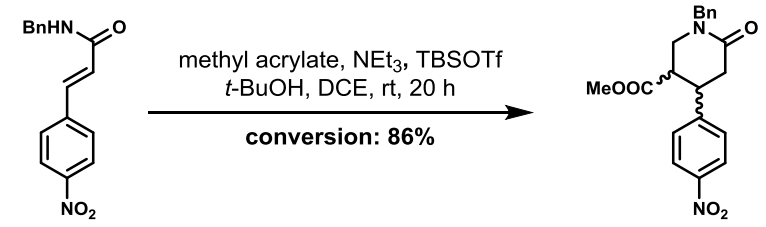

(2)
282.30 g/mol

crude-(3)
368.39 g/mol

A crude mixture of cyclized piperidinone products ***cis*-(3)** and ***trans*-(3)** was synthesized via optimization of a procedure, developed in the previous work[6], which referred to a literature protocol toward the synthesis of paroxetine[22].

A 50 mL oven-dried three necked flask was charged with amide **(2)** (4.80 g, 17.0 mmol, 1.00 equiv., dried under high vacuum) and evacuated and flushed with argon three times. After suspending the starting material in dry 1,2-DCE (17.0 mL, 1.00 M relative to amide **(2)**), freshly distilled methyl acrylate (1.47 g, 17.0 mmol, 1.00 equiv.) and dry NEt_3 (1.65 mL, 11.9 mmol, 0.70 equiv.) were added via syringe. TBSOTf (6.25 mL, 27.2 mmol, 1.60 equiv.) was added dropwise via syringe. After full addition, dry *t*-BuOH (0.40 mL, 4.25 mmol, 0.25 equiv.) was added immediately via syringe in order to suppress the formation of triple Michael adduct **(16)** (R_f = 0.49 (LP/EtOAc = 1/2)). The reaction mixture, which became homogenous in course of the reaction, was stirred at room temperature. After stirring over night (20 h), the maximum of conversion was observed according to GC/MS analysis as GC/MS data indicated no further change in the amount of unconverted starting material. The reaction mixture was quenched with 20 mL of a satd. aqu. solution of $NaHCO_3$.

The quenched mixture was poured into 200 mL satd. aqu. solution of $NaHCO_3$. The aqu. layer was extracted with EtOAc (3 x 80 mL). The combined organic phases were washed with brine (1 x 100 mL) and dried over $MgSO_4$. Volatiles were removed in vacuo. Removing the oily supernatant (degradation products of reagents used in excess) of via Pasteur pipette followed by a drying step under high vacuum resulted in the crude material (7.14 g), which was directly used for the epimerization. In case of a smaller scale (2.00 mmol), MPLC was suitable for further purification (silica gel/crude material = 100/1, 90 g silica gel, flow rate: 60 mL/min, EtOAc in LP = 40% - 100%, solid loading: crude/celite = 1/5, UV detector: sensitivity = $2xe^{-0}$, λ = 254 nm).

Conversion to piperidinones (3)	86% (scale: 6 g / 17 mmol)
Amount of triple Michael adduct	5%
Yield (mg-scale)	69% (506 mg, 1.38 mmol, *cis*/*trans* = 36/33)
	(Lit.[6]: 78%, 1.55 mmol, *cis*/*trans* = 46/32)
Appearance of the crude mixture	dark orange oil

Analysis of purified *cis*-(3) and *trans*-(3):

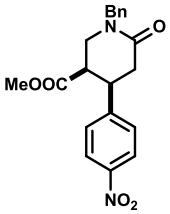

***cis*-(3)**

Appearance	colorless crystals
Melting point	116.5 – 117.0 °C (Lit.[6]: 117.5 - 118.0 °C)
TLC analysis	R_f = 0.25 (LP/EtOAc = 1/2)
Sum formula	$C_{20}H_{20}N_2O_5$
GC/MS	368 (11, M^+), 191 (10), 176 (20), 132 (12), 119 (21), 118 (15), 115 (14), 106 (13), 104 (12), 91 (100)
^{1}H-NMR (400 MHz, $CDCl_3$)	δ = 2.97 (d, *J* = 5.7 Hz, 1H, H5), 3.18 – 3.25 (m, 1H, H3), 3.27 – 3.37 (m, 1H, H2), 3.44 (dd, *J* = 12.8, 5.1 Hz, 1H, H2), 3.58 (s, 3H, O-CH_3), 3.75 – 3.84 (m, 1H, H4), 4.54 (d, *J* = 14.3 Hz, 1H, N-CH_2), 4.82 (d, *J* = 14.3 Hz, 1H, N-CH_2), 7.20 (d, *J* = 8.7, 2H, H2' & H6'), 7.30 – 7.39 (m, 5H, H2'' & H3'' & H4'' & H5'' & H6''), 8.08 (d, *J* = 8.8 Hz, 2H, H3' & H5') ppm.
^{13}C-NMR (101 MHz, $CDCl_3$)	δ = 36.0 (t, C5), 39.6 (d, C4), 43.6 (d, C3), 45.1 (t, C2), 50.6 (t, N-CH_2), 52.2 (q, O-CH_3), 123.9 (d, 2C, C3' & C5'), 128.0 (d, C4''), 128.7 & 128.7 & 128.9 (d, 6C, C2' & C6' & C2'' & C3'' & C5'' & C6''), 136.4 (s, C1''), 146.9 (s, C1'), 147.4 (s, C4'), 167.9 (s, C6), 170.6 (s, ester) ppm.

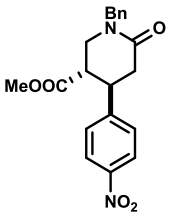

***trans*-(3)**

Appearance	colorless crystals
Melting point	131.0 – 131.5 °C (Lit.[6]: 132.5 - 132.5 °C)
TLC analysis	R_f = 0.45 (LP/EtOAc = 1/2)
Sum formula	$C_{20}H_{20}N_2O_5$
GC/MS	368 (25, M^+), 191 (10), 176 (22), 132 (12), 119 (13), 118 (13), 106 (13), 104 (12), 92 (13), 91 (100)
^{1}H-NMR (400 MHz, $CDCl_3$)	δ = 2.65 (dd, *J* = 17.7, 10.7 Hz, 1H, H5), 2.86 (dd, *J* = 17.7, 5.7 Hz, 1H, H5), 3.05 (td, *J* = 9.8, 5.3 Hz, 1H, H3), 3.42 (dd, *J* = 12.5, 5.3 Hz, 1H, H2), 3.47 (s, 3H, O-CH_3), 3.49 – 3.62 (m, 2H, H2 & H4), 4.56 (d, *J* = 14.5 Hz, 1H, N-CH_2), 4.76 (d, *J* = 14.5 Hz, 1H, N-CH_2), 7.27 – 7.44 (m, 7H, H2' & H6' & H2'' & H3'' & H4'' & H5'' & H6''), 8.18 (d, *J* = 8.7 Hz, 2H, H3' & H5') ppm.
^{13}C-NMR (101 MHz, $CDCl_3$)	δ = 38.0 (t, C5), 41.6 (d, C4), 46.3 (d, C3), 47.9 (t, C2), 50.2 (t, N-CH_2), 52.4 (q, O-CH_3), 124.3 (d, 2C, C3' & C5'), 128.0 (d, C4''), 128.2 & 128.4 & 128.9 (d, 6C, C2' & C6' & C2'' & C3'' & C5'' & C6''), 136.4 (s, C1''), 147.4 (s, C4'), 148.6 (s, C1'), 167.6 (s, C6), 171.5 (s, ester) ppm.

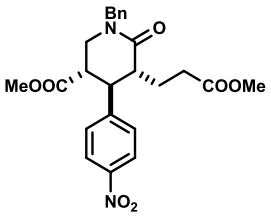

(16)

Appearance	colorless oil
TLC analysis	R_f = 0.49 (LP/EtOAc = 1/2)
Sum formula	$C_{24}H_{26}N_2O_7$
HPLC/MS	455.3 (100, M+H)
^{1}H-NMR (400 MHz, $CDCl_3$)	δ = 1.99 - 2.32 (m, 2H, C$\underline{H}_2$-CH_2-COOMe), 2.57 - 2.73 (m, 2H, CH_2-C$\underline{H}_2$-COOMe), 2.84 - 3.00 (m, 1H, H5), 3.19 - 3.30 (m, 2H, H2 & H3), 3.41 (dd, *J* = 12.1, 4.1 Hz, 1H, H2), 3.50 – 3.57 (m, 4H, H4 & OCH_3), 3.66 (s, 3H, OCH_3), 4.48 (d, *J* = 14.2 Hz, 1H, N-CH_2), 4.79 (d, *J* = 14.2 Hz, 1H, N-CH_2), 7.16 (d, *J* = 8.8 Hz, 2H H2' & H6'), 7.29 – 7.45 (m, 5H, H2'' & H3'' & H4'' & H5'' & H6''), 8.04 (d, *J* = 8.7 Hz, 2H, H3' & H5') ppm.
^{13}C-NMR (101 MHz, $CDCl_3$)	δ = 28.5 (t, $\underline{C}H_2$-CH_2-COOMe), 32.2 (t, CH_2-$\underline{C}H_2$-COOMe), 41.1 (d, C3), 44.5 (d, C5), 44.9 (t, C2), 45.3 (d, C4), 50.8 (t, NCH_2), 51.9 (q, O-CH_3), 52.2 (q, O-CH_3), 123.9 (d, 2C, C3' & C5'), 128.1 & 128.7 & 128.9 & 129.1 (d, 7C, C2' & C6' & C2'' & C3'' & C4'' & C5'' & C6''), 136.3 (s, C1''), 146.9 & 147.4 (s, 2C, C1' & C4'), 170.4 & 170.8 (s, 2C, C6 & ester), 173.6 (s, ester) ppm.

Comment: Spectral data are in accordance with the literature[6].

4.2.3 Methyl (±)-*trans*-1-benzyl-4-(4-nitrophenyl)-6-oxopiperidine-3-carboxylate *trans*-(3)

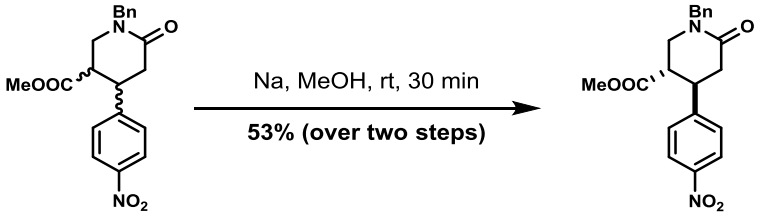

crude-(3)
368.39 g/mol

***trans*-(3)**
368.39 g/mol

The epimerization was performed via optimization of a procedure, developed in the previous work[6], which referred to a literature protocol toward the synthesis of paroxetine[22].

Sodium (1.23 g, 53.4 mmol) was added to dry MeOH (180 mL) in a 500 mL three necked flask under argon counter stream, while cooling with a NaCl/ice bath. After stirring for 10 min at room temperature, mixture **crude-(3)** (7.14 g, dissolved in 65 mL dry MeOH by means of ultrasound) was added dropwise via syringe. After stirring for 30 min at room temperature, the equilibrium between the diastereomers was reached according to TLC and GC/MS analysis (sample dissolved in DCM). The reaction mixture was quenched with a satd. aqu. solution of NH_4Cl (300 mL). To dissolve the precipitate, 150 mL H_2O was added. The aqu. layer was extracted with DCM (4 x 100 mL). The combined organic phases were washed with a satd. aqu. solution of $NaHCO_3$ (1 x 250 mL) and brine (1 x 250 mL) and were dried over $MgSO_4$. Volatiles were removed in vacuo to afford the crude material (*cis*/*trans* = 16/84 according to ^{1}H-NMR analysis).

T*rans*-piperidinone ***trans*-(3)** was obtained after purification via MPLC (silica gel/crude material = 70/1, 500 g silica gel, flow rate: 120 mL/min, acetone in LP = 20% (2 CV) - 27% (10 CV gradient), solid loading: crude/celite = 1/5, UV detector: sensitivity = $2xe^{-0}$, λ = 254 nm).

For a smaller scale (0.54 mmol), the epimerization was performed with purified ***cis*-(3)**.

Yield (over two steps)	starting from **crude-(3)**:	53% (3.37 g, 9.15 mmol)
	starting from ***cis*-(3)**:	57% * (Lit.[6]: 61% *)
Yield (epimerization)	starting from ***cis*-(3)**:	68% (135 mg, 0.37 mmol) (Lit.[6]: 62%, 0.66 mmol)

Characterization of trans-(3)*:* see section regarding the preparation of mixture **crude-(3)**

* The yield was calculated from two independently performed mg-scales for the cyclization and the epimerization.

4.2.4 (±)-*trans*-(1-Benzyl-4-(4-nitrophenyl)piperidin-3-yl)methanol *rac*-(4)

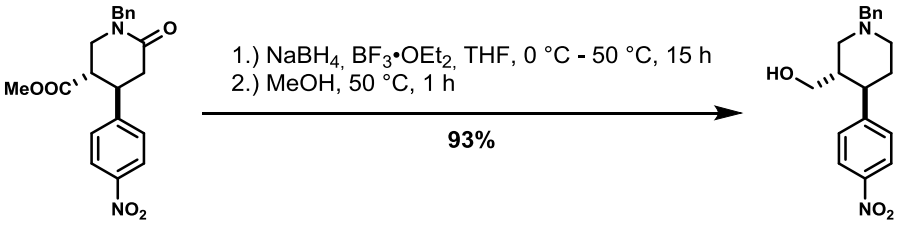

***trans*-(3)**
368.39 g/mol

***rac*-(4)**
326.40 g/mol

The reduced species ***rac*-(4)** was synthesized via optimization of a procedure, developed in the previous work[6], which referred to a modified literature protocol[23].

BF_3•OEt_2 (2.97 mL, 24.1 mmol, 4.00 equiv.) was added dropwise to a suspension of $NaBH_4$ (912 mg, 24.1 mmol, 4.00 equiv.) in dry THF (20 mL, 0.30 M relative to ***trans*-(3)**) while cooling to 0 °C with a NaCl/ice bath. The mixture was stirred for 1 h at 0 °C.

A solution of ***trans*-(3)** (2.22 g, 6.03 mmol, 1.00 equiv.) in dry THF (30.2 mL, 0.2 M relative to ***trans*-(3)**, final concentration: 0.1 M) was added via syringe at 0 °C. After full addition, the reaction mixture was heated to 50 °C (oil bath was set to 60 °C). The reaction mixture was stirred over night (15 h). The starting material was fully converted (TLC analysis) to the appropriate borane complex (R_f = 0.69 (DCM/MeOH = 100/10)) and the reaction was quenched carefully with 40 mL 1 N NaOH while cooling with a NaCl/ice bath to maintain the temperature at 25 °C. The reaction mixture was poured into 1 N NaOH (350 mL) and was extracted with EtOAc (400 mL). The aqu. layer was extracted with EtOAc (4 x 70 mL). The combined organic phases were washed with brine (1 x 250 mL) and dried over $MgSO_4$.

After removing the volatiles in vacuo, MeOH (43 mL, 0.14 M relative to ***trans*-(3)**) was added to the isolated amine-borane complex and heated to 50 °C (oil bath was set to 60 °C) in order to convert the amine-borane complex to alcohol ***rac*-(4)**. After 1 h, the conversion was completed according to TLC analysis. Volatiles were removed in vacuo. For further purification, vacuum filtration was used (silica gel/crude material = 15/1, washing step with DCM, eluent: DCM/MeOH = 100/10). After suspending the obtained oil in DIPE followed by the removal of solvent in vacuo, orange crystals were obtained.

Yield	93% (1.83 g, 5.61 mmol) (Lit.[6]: 83%, 5.21 mmol)
Appearance	orange crystals
Melting point	99.0 – 100.0 °C (Lit.[6]: 104.0 - 105.0 °C)
TLC analysis	R_f = 0.52 (DCM/MeOH = 100/10)
Sum formula	$C_{19}H_{22}N_2O_3$
^{1}H-NMR (400 MHz, $CDCl_3$)	δ = 1.25 (br s, 1H, OH), 1.75 – 1.95 (m, 2H, H5), 2.01 – 2.22 (m, 3H, H2 & H3 & H6), 2.54 (td, *J* = 11.2, 4.5 Hz, 1H, H4), 2.95 – 3.06 (m, 1H, H6), 3.17 – 3.28 (m, 2H, O-CH_2 & H2), 3.37 (dd, *J* = 10.7, 2.7 Hz, 1H, O-CH_2), 3.56 (d, *J* = 13.1 Hz, 1H, N-CH_2), 3.62 (d, *J* = 13.1 Hz, 1H, N-CH_2), 7.27 – 7.36 (m, 5H, H2'' & H3'' & H4'' & H5'' & H6''), 7.39 (d, *J* = 8.7 Hz, 2H, H2' & H6'), 8.16 (d, *J* = 8.7 Hz, 2H, H3' & H5') ppm.
^{13}C-NMR (101 MHz, $CDCl_3$)	δ = 34.2 (t, C5), 44.0 (d, C3), 44.9 (d, C4), 53.8 (t, C6), 57.2 (t, C2), 63.6 & 63.7 (t, 2C, N-CH_2 & O-CH_2), 124.0 (d, 2C, C3' & C5'), 127.3 (d, C4''), 128.4 & 128.5 & 129.3 (d, 6C, C2' & C6' & C2'' & C3'' & C5'' & C6''), 138.2 (s, C1''), 146.8 (s, C4'), 152.7 (s, C1') ppm.

Comment: Spectral data are in accordance with the literature[6].

4.2.5 (*3S*,*4R*)-(1-Benzyl-4-(4-nitrophenyl)piperidin-3-yl)methanol (*3S*,*4R*)-(5); (3R,4S)-(1-benzyl-4-(4-nitrophenyl)piperidin-3-yl)methyl acetate (*3R*,*4S*)-(7)

***rac*-(4)**
326.40 g/mol

(3*S*,4*R*)-(5)
326.40 g/mol

33%
99% ee

(3*R*,4*S*)-(7)
368.43 g/mol

60%
71% ee

The enzymatic kinetic resolution was performed via optimization of a procedure, developed in the previous work[6].

Alcohol ***rac*-(4)** (5.27 g, 16.2 mmol, 1.00 equiv.) was dissolved in MTBE* (808 mL, 20 mM relative to ***rac*-(4)**). Vinyl acetate (15.0 mL, 161 mmol, 10.00 equiv.) and Amano Lipase PS (10.54 g, 200 wt.%, 653 mg catalyst per mmol ***rac*-(4)**, from Sigma-Aldrich product No. 708011) were added. The orange reaction mixture was stirred at room temperature. The reaction (expected yield and enantiomeric excess of **(*3S,4R*)-(5)**) was monitored via chiral HPLC (1 mg sample / 1 mL HPLC grade hexane, for further details see chapter **4.1.8**).

After 47 h, the catalyst was removed via filtration through a pad of celite and washing with DCM (1600 mL). Volatiles were removed in vacuo. In order to separate alcohol **(*3S,4R*)-(5)** from acetate **(*3R,4S*)-(7)**, MPLC was used (silica gel/crude material = 75/1, 500 g silica gel, flow rate: 120 mL/min, EtOAc in LP = 0% (3 CV) - 100% (gradient for 30 CV), solid loading: crude/celite = 1/5, UV detector: sensitivity = $2xe^{-0}$, λ = 254 nm).

* The solvent (quality: reagent grade) should be equilibrated with water prior to use due to its hygroscopy and the thereby arising damage for the catalyst.

Alcohol (*3S,4R*)-(5) 33% (1.72 g, 5.27 mmol), 99% ee

$[\alpha]_D^{20}$ = -19.2 (c = 1.0, $CHCl_3$)

(Lit.[6]: 18% (94% ee), 0.28 mmol;

$[\alpha]_D^{20}$ = -18.3 (c = 1.0, $CHCl_3$))

Acetate (*3R,4S*)-(7) 60% (3.67 g, 9.96 mmol), 71% ee

$[\alpha]_D^{20}$ = +21.6 (c = 1.0, $CHCl_3$)

Characterization of (*3S,4R*)-(5): see section regarding the preparation of ***rac*-(4)**

Characterization of (*3R,4S*)-(7):

Appearance	orange oil
TLC analysis	R_f = 0.54 (LP/EtOAc = 1/2)
Sum formula	$C_{21}H_{24}N_2O_4$
^{1}H-NMR (400 MHz, $CDCl_3$)	δ = 1.76 – 1.88 (m, 2H, H5), 1.87 - 1.97 (m, 4H, H2 & CH_3), 2.05 (td, *J* = 11.2, 3.7 Hz, 1H, H6), 2.22 – 2.36 (m, 1H, H3), 2.48 (td, *J* = 11.3, 4.9 Hz, 1H, H4), 2.94 – 3.05 (m, 1H, H6), 3.09 – 3.16 (m, 1H, H2), 3.53 (d, *J* = 13.1 Hz, 1H, N-CH_2), 3.59 – 3.69 (m, 2H, N-CH_2 & O-CH_2), 3.80 (dd, *J* = 11.3, 3.7 Hz, 1H, O-CH_2), 7.28 – 7.41 (m, 5H, H2′ & H6′ & H2″ & H3″ & H4″ & H5″ & H6″), 8.17 (d, *J* = 8.8 Hz, 2H, H3′ & H5′) ppm.
^{13}C-NMR (101 MHz, $CDCl_3$)	δ = 20.8 (q, CH_3), 34.4 (t, C5), 41.0 (d, C3), 45.6 (d, C4), 53.6 (t, C6), 57.2 (t, C2), 63.4 (t, N-CH_2), 65.2 (t, O-CH_2), 124.1 (d, 2C, C3′ & C5′), 127.3 (d, C4″), 128.4 & 128.5 & 129.3 (d, 6C, C2′ & C6′ & C2″ & C3″ & C5″ & C6″), 138.1 (s, C1″), 146.9 (s, C4′), 152.0 (s, C1′), 170.9 (s, ester) ppm.

Comment: Spectral data are in accordance with the literature[6].

4.2.6 (*3R*,*4S*)- (1-Benzyl-4-(4-nitrophenyl)piperidin-3-yl)methanol (*3R*,*4S*)-(6)

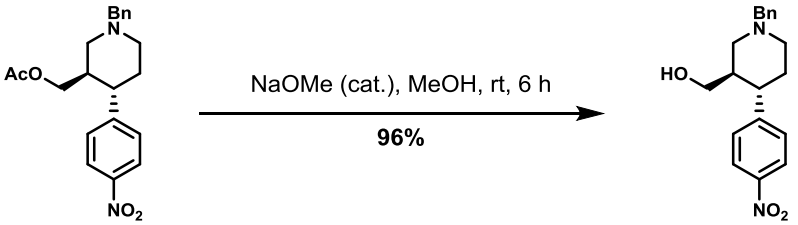

***(3R,4S)*-(7)**
368.43 g/mol

(3*R*,4*S*)-(6)
326.40 g/mol

The deacetylation of acetate **(*3R,4S*)-(7)** was performed according to a modified literature procedure[28] in order to use the opposite enantiomer for further test reactions of the following reaction steps.

A solution of NaOMe in dry MeOH ((30% (w/v)) was added in catalytic amounts (approx. 0.1 mL) to a solution of acetate **(*3R,4S*)-(7)** (1.01 g, 2.74 mmol) in dry MeOH (40 mL, 0.07 M relative to **(*3R,4S*)-(7)**) until a pH value of 10 was reached (controlled via pH paper). After 6 h (TLC analysis) the reaction was quenched with 50 mL of a satd. aqu. solution of NH_4Cl and poured into additional 250 mL satd. aqu. solution of NH_4Cl. To dissolve the formed precipitate, H_2O (70 mL) was added. The aqu. layer was extracted with DCM (6 x 70 mL). The combined organic phases were washed with a satd. aqu. solution of $NaHCO_3$ (1 x 100 mL) and brine (1 x 100 mL) and were dried over $MgSO_4$. Volatiles were removed in vacuo. Product **(*3R,4S*)-(6)** was obtained in high purity without further purification.

Yield 96% (859 mg, 2.63 mmol), 57% ee

Specific rotation $[\alpha]_D^{20}$ = +10.8 (c = 1.0, $CHCl_3$)

Characterization of (*3R,4S*)-(6): see section regarding the preparation of ***rac*-(4)**

4.2.7 *(3S,4R)*-3-((Benzo[*d*][1,3]dioxol-5-yloxy)methyl)-1-benzyl-4-(4-nitrophenyl)piperidine (8)

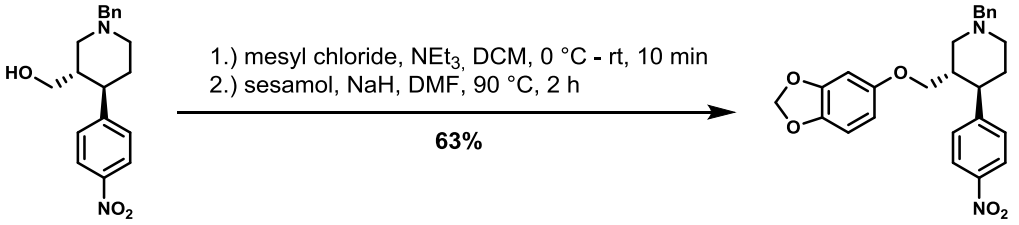

(3*S*,4*R*)-(5)
326.40 g/mol

(8)
446.50 g/mol

Ether **(8)** was synthesized via optimization of a procedure, developed in the previous work[6], which referred to a literature protocol toward the synthesis of paroxetine[31].

Dry NEt_3 (0.92 mL, 6.63 mmol, 1.44 equiv.) and freshly distilled mesyl chloride (0.51 mL, 6.63 mmol, 1.44 equiv.) were added via syringe and under argon atmosphere to a solution of alcohol **(*3S,4R*)-(5)** (1.50 g, 4.60 mmol, 1.00 equiv.) in dry DCM (23 mL, 0.20 M relative to **(*3S,4R*)-(5)**) while cooling with a NaCl/ice bath to 0 °C. After full addition, the reaction was warmed to room temperature. After 10 min, full conversion (TLC analysis) was observed. The reaction was quenched with water (100 mL). The quenched mixture was poured into a satd. aqu. solution of $NaHCO_3$ (100 mL). The aqu. layer was extracted with DCM (8 x 50 mL). The combined organic phases were washed with brine (1 x 100 mL) and dried over $MgSO_4$. Volatiles were removed in vacuo in order to obtain the crude mesylate, which was used without further purification for the second step.

In the second step, sesamol (1.27 g, 9.20 mmol, 2.00 equiv.) was dissolved in dry DMF (38 mL, 0.24 M relative to sesamol) and NaH (368 mg, 60% dispersion in mineral oil, 9.20 mmol, 2.00 equiv.) was added under argon counter stream while cooling to 0 °C with a NaCl/ice bath. The suspension was stirred for 20 min at room temperature. A solution of crude mesylate in dry DMF (19 mL, 0.24 M relative to mesylate) was added dropwise, whereby the reaction mixture got dark red to black. The reaction mixture was heated to 90 °C (oil bath set to 96 °C). After 2 h, the mesylate was converted completely according to TLC and GC/MS analysis. The reaction mixture was diluted with EtOAc (200 mL). The organic phase was washed with H_2O (1 x 100 mL), 1 N NaOH (3 x 100 mL) and brine (1 x 100 mL). TLC analysis of re-extracts of the washing solutions ensured no loss of product while washing the organic layer.

Volatiles were removed in vacuo. For further purification, MPLC was used (silica gel/crude material = 100/1,180 g silica gel, flow rate: 50 mL/min, EtOAc in LP = 0% (8 CV) - 40% (gradient for 20 CV), solid loading: crude/celite = 1/10), UV detector: sensitivity = $2xe^{-0}$, λ = 254 nm).

Yield	63% (1.29 g, 2.89 mmol) (Lit.[6]: 65%, 0.18 mmol)

Characterization of (8):

Appearance	orange oil
Specific rotation	$[\alpha]_D^{20}$ = -74.2 (c = 1.0, $CHCl_3$)
	(Lit.[6]: $[\alpha]_D^{20}$ = -63.0 (c = 1.0, $CHCl_3$))
TLC analysis	R_f = 0.65 (LP/EtOAc = 1/2)
Sum formula	$C_{26}H_{26}N_2O_5$
^{1}H-NMR (400 MHz, $CDCl_3$)	δ = 1.76 – 2.01 (m, 2H, H5), 2.05 – 2.20 (m, 2H, H2 & H6), 2.23 – 2.38 (m, 1H, H3), 2.62 – 2.79 (m, 1H, H4), 2.98 – 3.07 (m, 1H, H6), 3.18 – 3.28 (m, 1H, H2), 3.43 (dd, *J* = 9.4, 6.1 Hz, 1H, -O-CH_2-), 3.51 – 3.54 (m, 1H, -O-CH_2-), 3.57 (d, *J* = 13.4 Hz, 1H, benzyl), 3.64 (d, *J* = 13.1 Hz, 1H, N-CH_2), 5.88 (s, 2H, H2″), 6.08 (dd, *J* = 8.5 Hz, *J* = 2.5 Hz, 1H, H6″), 6.29 (d, *J* = 2.5 Hz, 1H, H4″), 6.61 (d, *J* = 8.5 Hz, 1H, H7″), 7.27 – 7.41 (m, 7H, H2′ & H6′ & H2″ & H3″ & H4″ & H5″ & H6″), 8.14 (d, *J* = 8.8 Hz, 2H, H3′ & H5′) ppm.
^{13}C-NMR (101 MHz, $CDCl_3$)	δ = 34.1 (t, C5), 42.1 (d, C3), 45.0 (d, C4), 53.7 (t, C6), 57.3 (t, C2), 63.5 (t, N-CH_2), 69.5 (t, -O-CH_2-), 98.0 (d, C4″), 101.3 (t, C2″), 105.6 (d, C6″), 108.0 (d, C7″), 124.0 (d, 2C, C3′ & C5′), 127.3 (d, C4‴), 128.4 & 128.5 & 129.3 (d, 6C, C2′ & C6′ & C2‴ & C3‴ & C5‴ & C6‴), 138.2 (s, C1‴), 141.9 (s, C7a″), 146.9 (s, C4′), 148.3 (s, C3a″), 152.4 (s, C1′), 154.3 (s, C5″) ppm.

Characterization of the crude mesylate:

Appearance	orange oil
TLC analysis	R_f = 0.66 (DCM/MeOH = 100/10)
Sum formula	$C_{20}H_{24}N_2O_5S$
^{1}H-NMR (400 MHz, $CDCl_3$)	δ = 1.80 – 1.92 (m, 2H), 2.13 (t, *J* = 10.8 Hz, 2H), 2.59 (td, *J* = 11.1, 5.0 Hz, 1H), 2.85 (s, 3H), 2.97 – 3.33 (m, 3H), 3.58 – 4.05 (m, 4H), 7.29 – 7.61 (m, 7H), 8.19 (d, *J* = 8.7 Hz, 2H) ppm.

Comment: Spectral data are in accordance with the literature[6].

4.2.8 4-((*3S*,*4R*)-3-((Benzo[*d*][1,3]dioxol-5-yloxy)methyl)piperidin-4-yl)aniline (9)

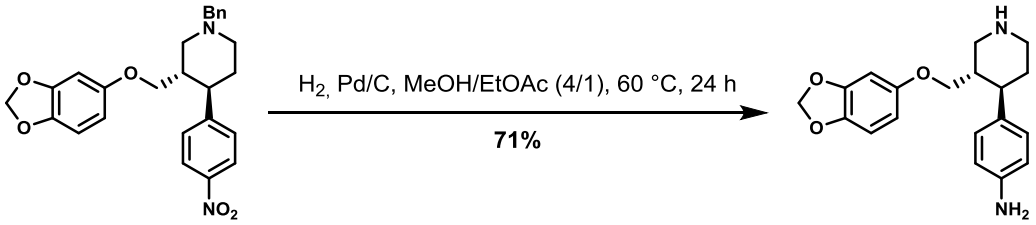

(8)
446.50 g/mol

(9)
326.40 g/mol

Aniline **(9)** was synthesized according to a procedure, developed in the previous work[6].

10% Pd/C (10 mg cat., 9.6 µmol Pd, 0.10 equiv.) was added to a solution of ether **(8)** (43 mg, 96 µmol, 1.00 equiv.) in a mixture of MeOH/EtOAc (1 mL, 4/1). The reaction mixture was flushed with argon and then stirred under an atmosphere of hydrogen (using a H_2-ballon).

After stirring over night (24 h) at 60 °C, the reaction mixture was diluted with 5 mL of MeOH and filtered through a pad of celite (MeOH was used for washing). Volatiles were removed in vacuo. For further purification MPLC was used (silica gel/crude material = 130/1, 5 g silica gel, flow rate: 12 mL/min, DCM to DCM/MeOH/NH_4OH (80/20/1) = 0% (6 CV) - 100% (gradient for 20 CV), sample dissolved in 2 mL DCM, UV detector: sensitivity = $2xe^{-0}$, λ = 254 nm).

Yield	71% (22 mg, 67 µmol) (Lit.[6]: 84%, 147 µmol)
Appearance	pale yellow oil
Specific rotation	$[\alpha]_D^{20}$ = -72.1 (c = 1.0, $CHCl_3$)
	(Lit.[6]: $[\alpha]_D^{20}$ = -81.8 (c = 1.0, $CHCl_3$)
TLC analysis	R_f = 0.27 (DCM/MeOH/NH_4OH = 80/20/1)
Sum formula	$C_{19}H_{22}N_2O_3$

^{1}H-NMR (400 MHz, $CDCl_3$) δ = 1.70 – 1.89 (m, 2H, H5), 2.05 – 2.16 (m, 1H, H3), 2.47 (td, *J* = 11.4, 4.5 Hz, 1H, H4), 2.67 (t, *J* = 11.6 Hz, 1H, H2), 2.74 (td, *J* = 12.0, 3.5 Hz, 1H, H6), 3.20 (d, *J* = 12.3 Hz, 1H, H6), 3.35 – 3.53 (m, 2H, H2 & O-CH_2-), 3.61 (dd, *J* = 9.4 & 3.0 Hz, 1H, O-CH_2-), 5.87 (s, 2H, H2″), 6.13 (dd, *J* = 8.5, 2.5 Hz, 1H, H6″), 6.34 (d, *J* = 2.5 Hz, 1H, H4″), 6.56 – 6.72 (m, 3H, H3′ & H5′ & H7″), 6.99 (d, *J* = 7.9 Hz, 2H, H2′ & H6′) ppm.

^{13}C-NMR (101 MHz, $CDCl_3$) δ = 35.0 (t, C5), 42.7 (d, C3), 44.3 (d, C4), 47.0 (t, C6), 50.2 (t, C2), 69.7 (t, O-CH_2-), 98.1 (d, C4″), 101.2 (t, C2″), 105.8 (d, C6″), 107.9 (d, C7″), 115.5 (d, 2C, C3′ & C5′), 128.3 (d, 2C, C2′ & C6′), 134.1 (s, C1′), 141.6 (s, C7a″), 145.0 (s, C4′), 148.2 (s, C3a″), 154.6 (s, C5″) ppm.

Comment: Spectral data are in accordance with the literature[6].

4.3 HTI Series

4.3.1 N-Benzyl-3-(4-bromophenyl)acrylamide (11)

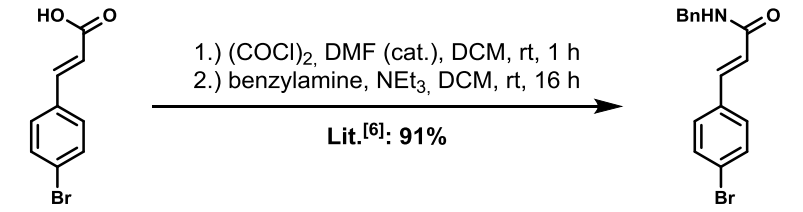

(10)
227.06 g/mol

(11)
316.20 g/mol

Protected amide **(11)** was already synthesized in the previous project[6] according to a reproducible and high yielding procedure in g-scale. Amide **(11)**, which was still available, was used for the next step of this work. However, a summary of the procedure and the analytic data are given below.

The protected amide **(11)** was synthesized, starting from 4-bromocinnamic acid **(10)** (10.00 g, 44.0 mmol, 1.00 equiv.), which was suspended in dry DCM (147 mL, 0.30 M relative to starting material **(10)**). The reaction with freshly distilled oxalyl chloride (11.3 mL, 132 mmol, 3.00 equiv.) and dry DMF (1 drop) resulted after 1 h in the formation of the appropriate acid chloride. After work-up, the acid chloride was dissolved in dry DCM (147 mL). Benzylamine (4.72 g, 44.0 mmol, 1.00 equiv.) and NEt_3 (4.46 g, 44.0 mmol, 1.00 equiv.) were added under cooling with a NaCl/ice bath. After stirring over night (16 h), the conversion was completed according to TLC analysis. After washing with 1 N HCl (100 mL) and 1 N NaOH (100 mL), the recrystallization of the concentrated mother liquor in toluene and a drying step under high vacuum, intermediate **(11)** was used for the following step.

Yield	91% (12.64 g, 39.9 mmol)
Appearance	colorless crystals
Melting point	170.0 – 171.5 °C
TLC analysis	R_f = 0.71 (LP/EtOAc = 1/2) (stained with $KMnO_4$)
Sum formula	$C_{16}H_{14}BrNO$
GC/MS	317 (7, M^+), 315 (7, M^+), 131 (24), 107 (13), 106 (68), 104 (15), 103 (23), 102 (100), 101 (16)

^{1}H-NMR (400 MHz, $CDCl_3$) δ = 4.57 (d, *J* = 5.7 Hz, 2H, N-CH_2), 5.92 (s, 1H, NH), 6.39 (d, *J* = 15.6 Hz, 1H, Ar-CH=C<u>H</u>-), 7.27 – 7.38 (m, 7H, H2 & H6 or H3 & H5 & benzyl), 7.49 (d, *J* = 8.5 Hz, 2H, H2 & H6 or H3 & H5), 7.61 (d, *J* = 15.6 Hz, 1H, Ar-C<u>H</u>=CH-) ppm.

^{13}C-NMR (101 MHz, $CDCl_3$) δ = 44.1 (t, N-CH_2), 121.2 (d, Ar-CH=<u>C</u>H-), 124.0 (s, C4), 127.8 (d, C4′), 128.1 & 128.9 & 129.3 (d, 6C, C2, C6, C2′, C3′, C5′, C6′), 132.2 (d, 2C, C3 & C5), 133.8 (s, C1), 138.2 (s, C1′), 140.3 (d, Ar-<u>C</u>H=CH-), 165.5 (s, amide) ppm.

Comment: Melting point and spectral data were taken from the literature[6] for the reason mentioned above.

4.3.2 Methyl 1-benzyl-4-(4-bromophenyl)-6-oxopiperidine-3-carboxylate (12)

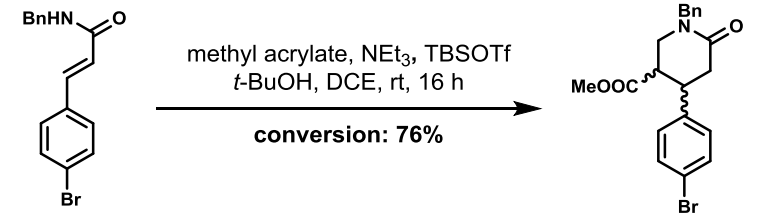

(11)
316.20 g/mol

crude-(12)
402.29 g/mol

A crude mixture of cyclized piperidinone products ***cis*-(12)** and ***trans*-(12)** was synthesized according to the optimized procedure developed for the azo series. The procedure was slightly modified with an effect on the work-up.

A 25 mL oven-dried three necked flask was charged with amide **(11)** (4.74 g, 15.0 mmol, 1.00 equiv., dried under high vacuum), which was suspended in dry 1,2-DCE (15.0 mL, 1.00 M relative to amide **(11)**). Freshly distilled methyl acrylate (1.29 g, 15.0 mmol, 1.00 equiv.), dry NEt_3 (1.46 mL, 10.5 mmol, 0.70 equiv.), TBSOTf (5.52 mL, 24.0 mmol, 1.60 equiv.) were added via syringe. After full addition, dry *t*-BuOH (0.35 mL, 3.75 mmol, 0.25 equiv.) was added immediately via syringe in order to suppress the formation of triple Michael adduct **(17)** ((R_f = 0.63 (LP/EtOAc = 1/2)). The reaction mixture, which became homogenous in course of the reaction, was stirred at room temperature. After stirring over night (16 h), the maximum of conversion was observed according to GC/MS analysis as GC/MS data indicated no further change in the amount of unconverted starting material. The reaction mixture was quenched with 10 mL of a satd. aqu. solution of $NaHCO_3$. The extractive work-up was performed according to the azo series with the modification that DCM (4 x 80 mL) was used as extractive agent instead of EtOAc because of better phase separation. After removal of the solvent in vacuo, the removal of the oily supernatant (degradation products of reagents used in excess) via Pasteur pipette and a drying step under high vacuum, compound mixture **crude-(12)** was used directly for the epimerization.

Conversion to piperidinones (12)	76%
Amount of triple Michael adduct	6%
Appearance of the crude mixture	colorless oil

Analysis of purified *cis*-(12)[6] and *trans*-(12):

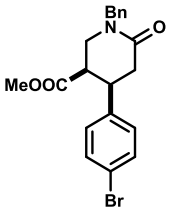

***cis*-(12)**

Appearance	colorless oil
TLC analysis	R_f = 0.37 (LP/EtOAc = 1/2) (stained with $KMnO_4$)
Sum formula	$C_{20}H_{20}BrNO_3$
GC/MS	403 (4, M^+), 401 (4, M^+), 118 (10), 116 (14), 115 (13), 106 (10), 104 (14), 103 (13), 102 (15), 91 (100)
^{1}H-NMR (400 MHz, $CDCl_3$)	δ = 2.84 – 2.97 (m, 2H, H5), 3.09 – 3.16 (m, 1H, H3), 3.28 (dd, *J* = 12.9, 9.4 Hz, 1H, H2), 3.37 (dd, *J* = 12.8, 5.3 Hz, 1H, H2), 3.58 (s, 3H, O-CH_3), 3.67 (m, 1H, H4), 4.60 (d, *J* = 14.4 Hz, 1H, N-CH_2), 4.71 (d, *J* = 14.4 Hz, 1H, N-CH_2), 6.89 (d, *J* = 8.5 Hz, 2H, H2' & H6'), 7.27 – 7.37 (m, 7H, H3' & H5' & H2'' & H3'' & H4'' & H5'' & H6'') ppm.
^{13}C-NMR (101 MHz, $CDCl_3$)	δ = 36.5 (t, C5), 39.3 (d, C4), 43.7 (d, C3), 44.8 (t, C2), 50.6 (t, N-CH_2), 52.0 (q, O-CH_3), 121.6 (s, C4′), 127.9 (d, C4″), 128.6 & 128.8 & 129.4 (d, 6C, C2′ & C6′ & C2″ & C3″ & C5″ & C6″), 131.8 (d, 2C, C3′ & C5′), 136.6 (s, C1″), 138.4 (s, C1′), 168.4 (s, C6), 170.9 (s, ester) ppm.

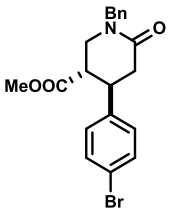

***trans*-(12)**

Appearance	colorless crystals
Melting point	157.5 – 158.0 °C (Lit.[6]: 154.5 - 155.0 °C)
TLC analysis	R_f = 0.57 (LP/EtOAc = 1/2) (stained with $KMnO_4$)
Sum formula	$C_{20}H_{20}BrNO_3$
GC/MS	403 (14, M^+), 401 (14, M^+), 211 (13), 209 (15), 191 (16), 132 (11), 116 (19), 115 (18), 106 (11), 104 (12), 102 (13), 91 (100)
^{1}H-NMR (400 MHz, $CDCl_3$)	δ = 2.62 (dd, *J* = 17.8, 10.5 Hz, 1H, H5), 2.82 (dd, *J* = 17.8, 5.7 Hz, 1H, H5), 2.96 (td, *J* = 9.6, 5.2 Hz, 1H, H3), 3.37 (dd, *J* = 12.4, 5.2 Hz, 1H, H2), 3.32 – 3.44 (m, 1H, H4), 3.46 (s, 3H, CH_3), 3.51 (dd, *J* = 12.3, 9.5 Hz, 1H, H2), 4.55 (d, *J* = 14.4 Hz, 1H, N-CH_2), 4.74 (d, *J* = 14.4 Hz, 1H, N-CH_2), 7.06 (d, *J* = 8.4 Hz, 2H, H2′ & H6′), 7.27 – 7.36 (m, 5H, H2″ & H3″ & H4″ & H5″ & H6″), 7.43 (d, *J* = 8.4 Hz, 2H, H3′ & H5′) ppm.
^{13}C-NMR (101 MHz, $CDCl_3$)	δ = 38.1 (t, C5), 41.2 (d, C4), 46.6 (d, C3), 47.9 (t, C2), 50.2 (t, N-CH_2), 52.2 (q, CH_3), 121.4 (s, C4′), 127.7 (d, C4″), 128.4 & 128.9 & 128.9 (d, 6C, C2′ & C6′ & C2″ & C3″ & C5″ & C6″), 132.1 (d, 2C, C3′ & C5′), 136.6 (s, C1″), 140.1 (s, C1′), 168.2 (s, C6), 171.9 (s, ester) ppm.

Comment: Spectral data of **trans-(12)** are in accordance with the literature[6]. Compound **cis-(12)** was not isolated, analytic data were taken from the literature[6].

4.3.3 Methyl (±)-*trans*-1-benzyl-4-(4-bromophenyl)-6-oxopiperidine-3-carboxylate trans-(12)

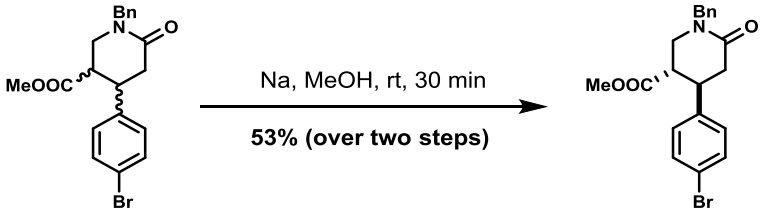

crude-(12)
402.29 g/mol

***trans*-(12)**
402.29 g/mol

The epimerization was performed according to the optimized procedure developed for the azo series. The procedure was slightly modified with an effect on the purification via MPLC.

A solution of NaOMe was prepared from sodium (1.02 g, 44.6 mmol) in dry MeOH (180 mL). Compound mixture **crude-(12)** (6.52 g, dissolved in 60 mL dry MeOH by means of ultrasound) was added under argon atmosphere. After stirring the reaction mixture at room temperature for 30 min, GC/MS analysis indicated that the equilibrium between the diastereomers was reached (*cis*/*trans* = 15/85). The reaction was quenched with a satd. aqu. solution of NH_4Cl (300 mL). H_2O was added (150 mL) to dissolve the precipitate followed by the extraction with DCM (6 x 100 mL), washing steps with a sat. aqu. solution of $NaHCO_3$ (1 x 250 mL) and brine (1 x 250 mL) and a drying step over $MgSO_4$. Volatiles were removed in vacuo.

The crude material was purified via MPLC (silica gel/crude material = 90/1, 500 g silica gel, flow rate: 120 mL/min, EtOAc in LP = 15% (10 CV) - 20% (15 CV) - 30% (12 CV), solid loading: crude/celite = 1/5, UV detector: sensitivity = $5xe^{-1}$, λ = 266 nm).

In contrast to the azo series, where a mixture of acetone in LP was used as eluent, TLC analysis indicated a better separation for the HTI series using a mixture of EtOAc in LP. Due to a low absorbance of piperidinones **(12)** at 254 nm, the settings of the UV detector were adapted to a wavelength of 266 nm and a higher selectivity of $5xe^{-1}$.

Yield (over two steps) starting from **crude-(12)** 53% (3.21 g, 7.98 mmol)

starting from ***cis*-(12)**: (Lit.[6]: 60%*)

Characterization of trans-(12): see section regarding the preparation of mixture **crude-(12)**

* The yield was calculated from two independently performed mg-scales for the cyclization and the epimerization.

4.3.4 (±)-*trans*-(1-Benzyl-4-(4-bromophenyl)piperidin-3-yl)methanol *rac*-(13)

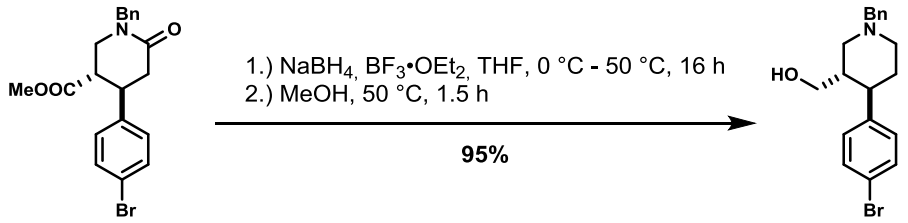

***trans*-(12)**
402.29 g/mol

***rac*-(14)**
360.30 g/mol

The reduction was performed referring to the optimized procedure developed for the azo series. The procedure was slightly modified with an effect on the purification set-up.

BF_3•OEt_2 (3.9 mL, 31.9 mmol, 4.00 equiv.) was added to a suspension of $NaBH_4$ (1.21 g, 31.9 mmol, 4.00 equiv.) in dry THF (27 mL, 0.30 M relative to ***trans*-(12)**) at 0 °C. After stirring the mixture for 1 h at 0 °C, a solution of ***trans*-(12)** (3.21 g, 7.97 mmol, 1.00 equiv.) in dry THF (40 mL, 0.20 M relative to ***trans*-(12)**, final concentration: 0.10 M) was added at 0 °C. After stirring over night (16 h) at 50 °C, full conversion to the borane-amine complex (R_f = 0.70 (DCM/MeOH = 100/5)) was observed (TLC analysis). The reaction was quenched with 100 mL 1 N NaOH while cooling with a NaCl/ice bath. After the extraction with EtOAc (5 x 70 mL), washing with brine (1 x 250 mL) and drying over $MgSO_4$, volatiles were removed.

For the conversion of the amine-borane complex, the crude material was dissolved in MeOH (57 mL, 0.14 M relative to ***trans*-(12)**). After stirring for 1.5 h at 50 °C, TLC analysis indicated full conversion to alcohol ***rac*-(13)**. Volatiles were removed in vacuo. For further purification, MPLC was used in order to make use of the UV absorption of the colorless compound and thereby simplify the purification process (silica gel/crude material = 30/1, 90 g silica gel, flow rate: 50 mL/min, DCM to DCM/MeOH (100/10) = 0% (6 CV) - 100% (gradient for 15 CV), sample dissolved in 6 mL DCM, UV detector settings: λ = 266 nm, sensitivity = $5xe^{-1}$).

Yield	95% (2.73 g, 7.58 mmol) (Lit.[6]: 84%, 0.21 mmol)
Appearance	colorless crystals
Melting point	108.5 – 109.0 °C (Lit.[6]: 109.5 - 110.0 °C)
TLC analysis	R_f = 0.22 (DCM/MeOH = 100/5) (stained with $KMnO_4$)
Sum formula	$C_{19}H_{22}BrNO$
^{1}H-NMR (400 MHz, $CDCl_3$)	δ = 1.72 – 1.89 (m, 2H, H5), 1.95 – 2.14 (m, 3H, H2 & H3 & H6), 2.33 (td, *J* = 10.9, 4.8 Hz, 1H, H4), 2.93 – 3.01 (m, 1H, H6), 3.18 (dd, *J* = 7.5, 1.9 Hz, 1H, H2), 3.23 (dd, *J* = 10.9, 6.2 Hz, 1H, O-CH_2), 3.38 (dd, *J* = 10.9, 2.7 Hz, 1H, O-CH_2), 3.55 (d, *J* = 13.1 Hz, 1H, N-CH_2), 3.61 (d, *J* = 13.1 Hz, 1H, N-CH_2), 7.09 (d, *J* = 8.4 Hz, 2H, H2′ & H6′), 7.27 – 7.36 (m, 5H, H2″ & H3″ & H4″ & H5″ & H6″), 7.41 (d, *J* = 8.4 Hz, 2H, H3′ & H5′) ppm.
^{13}C-NMR (101 MHz, $CDCl_3$)	δ = 34.4 (t, C5), 44.1 (d, C3), 44.6 (d, C4), 54.0 (t, C6), 57.4 (t, C2), 63.6 (t, N-CH_2), 64.1 (t, O-CH_2), 120.2 (s, C4′), 127.2 (d, C4″), 128.4 & 129.4 & 129.4 (d, 6C, C2′ & C6′ & C2″ & C3″ & C5″ & C6″), 131.8 (d, 2C, C3′ & C5′), 138.3 (s, C1″), 143.7 (s, C1′) ppm.

Comment: Spectral data are in accordance with the literature[6].

4.3.5 (*3S*,*4R*)-(1-Benzyl-4-(4-bromophenyl)piperidin-3-yl)methanol (*3S*,*4R*)-(14); (*3R*,*4S*)-(1-Benzyl-4-(4-bromophenyl)piperidin-3-yl)methyl acetate (*3R*,*4S*)-(15)

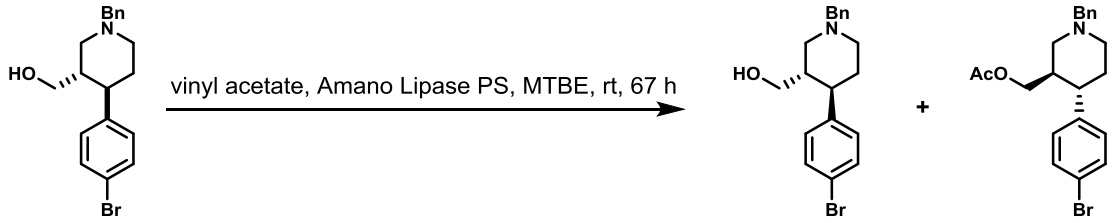

***rac*-(13)**
360.30 g/mol

(3*S*,4*R*)-(14)
360.30 g/mol

20%
97% ee

(3*R*,4*S*)-(15)
402.33 g/mol

50%
54% ee

The enzymatic kinetic resolution was performed according to the optimized procedure, developed for the azo series. The procedure was slightly modified with an effect on the settings of the UV detector of the MPLC.

Alcohol ***rac*-(13)** (737 mg, 2.05 mmol, 1.00 equiv.) was dissolved in MTBE* (102 mL, 20 mM relative to ***rac*-(13)**), vinyl acetate (1.89 mL, 20.5 mmol, 10.00 equiv.) and Amano Lipase PS (1.33 g,181wt.%, 653 mg catalyst per mmol alcohol ***rac*-(13)**, from Sigma-Aldrich product No. 708011) were added and the reaction mixture was stirred at room temperature.

After 67 h (reaction monitoring via chiral HPLC, for further details see chapter **4.1.8**) the catalyst was removed via filtration through a pad of celite. DCM was used for washing. Volatiles were removed in vacuo and the compounds were separated via MPLC (silica gel/crude material = 100/1, 90 g silica gel, flow rate: 50 mL/min, EtOAc in LP = 0% (3 CV) - 100% (gradient for 30 CV), solid loading: crude/celite = 1/5, UV detector settings: λ = 266 nm, sensitivity = $5xe^{-1}$).

* The solvent (quality: reagent grade) should be equilibrated with water prior to use due to its hygroscopy and the thereby arising damage for the catalyst.

Alcohol (*3S,4R*)-(14)	20% (147 mg, 0.42 mmol), 97% ee $[\alpha]_D^{20}$ = -16.2 (c = 1.0, $CHCl_3$)
Acetate (3R,4S)-(7)	50% (413 mg, 1.03 mmol), 54% ee $[\alpha]_D^{20}$ = +12.7 (c = 1.0, $CHCl_3$)

Characterization of (*3S,4R*)-(14): see section regarding the preparation of ***rac*-(13)**

Characterization of (*3R,4S*)-(15):

Appearance	colorless oil
TLC analysis	R_f = 0.66 (LP/EtOAc = 1/2) (stained with $KMnO_4$)
Sum formula	$C_{21}H_{24}BrNO_2$
^{1}H-NMR (400 MHz, $CDCl_3$)	δ = 1.70 – 1.85 (m, 2H, H5), 1.88 – 1.97 (m, 1H, H2 & CH_3), 1.96 – 2.09 (m, 1H, H6), 2.13 – 2.24 (m, 1H, H3), 2.29 (td, *J* = 11.1, 5.1 Hz, 1H, H4), 2.93 – 3.02 (m, 1H, H6), 3.06 – 3.19 (m, 1H, H2), 3.51 (d, *J* = 13.1 Hz, 1H, N-CH_2), 3.57 – 3.69 (m, 2H, N-CH_2 & O-CH_2), 3.80 (dd, *J* = 11.2, 3.5 Hz, 1H, O-CH_2), 7.07 (d, *J* = 8.4 Hz, 2H, H2' & H6'), 7.27 – 7.36 (m, 5H, H2'' & H3'' & H4'' & H5'' & H6''), 7.41 (d, *J* = 8.4 Hz, 2H, H3' & H5') ppm.
^{13}C-NMR (101 MHz, $CDCl_3$)	δ = 20.9 (q, CH_3), 34.5 (t, C5), 41.1 (d, C3), 45.1 (d, C4), 53.8 (t, C6), 57.5 (t, C2), 63.4 (t, N-CH_2), 65.5 (t, O-CH_2), 120.3 (s, C4′), 127.2 (d, C4″), 128.4 & 129.3 & 129.3 (d, 6C, C2′ & C6′ & C2″ & C3″ & C5″ & C6″), 131.9 (d, 2C, C3′ & C5′), 138.2 (s, C1″), 143.1 (s, C1′), 171.0 (s, ester) ppm.

Comment: Spectral data are in accordance with the literature[6]. The assignment of the absolute configuration was performed in the previous work[6] via debromination and comparison of literature values[26] for paroxetine (see chapter **3.3.6**).

5 Appendix

5.1 List of Abbreviations

Ac	acetate
AcOH	acetic acid
approx.	approximately
aqu.	aqueous
Ar	aryl
Bn	benzyl
br	broad (NMR)
CAL-A	lipase A *Candida antarctica*
CAL-B	lipase B *Candida antarctica*
cat.	catalytically
CNS	central nervous system
COSY	correlation spectroscopy
CV	column volumes
d	doublet (NMR)
DAT	dopamine transporter
DCE	1,2- dichloroethane
DCM	dichloromethane
dd	doublet of doublets (NMR)
DIPE	diisopropyl ether
DMF	dimethylformamide
dt	doublet of triplets (NMR)
equiv.	equivalent
Et	ethyl
EtOAc	ethyl acetate
EWG	electron withdrawing group
FGI	functional group interconversion
GABA	γ-aminobutyric acid
GAT	GABA transporter
GC/MS	gas chromatography - mass spectrometry hyphenation
GLYT	glycine transporter
HMBC	heteronuclear multiple bond correlation
HPLC	high-performance liquid chromatography
HPLC/MS	high performance liquid chromatography - mass spectrometry hyphenation
hSERT	human serotonin transporter
HSQC	heteronuclear single quantum coherence
HTI	hemithioindigo
IC_{50}	half maximum inhibitory concentration
J	coupling constant (NMR)
LP	light petroleum (boiling point 40 - 60 °C)
m	multiplet (NMR)
m/z	ratio of mass to charge (GC/MS)
M^+	molecular ion (GC/MS)
MAT	monoamine transporter
Me	methyl

MPLC	medium pressure liquid chromatography
MTBE	methyl *tert*-butyl ether
n-BuLi	*n*-butyllithium
NET	norephinephrine transporter
NMR	nuclear magnetic resonance
NOESY	nuclear Overhauser enhancement spectroscopy
o.n.	over night
pH	quantity of hydrogen
ppm	parts per million
p-TSA	*para*-toluenesulfonic acid
R_f	retention factor (TLC)
rt	room temperature
s	singlet (NMR)
satd.	saturated
SERT	serotonin transporter
SSRI	selective serotonin reuptake inhibitor
TBSOTf	*tert*-butyldimethylsilyl trifluoromethanesulfonate (TBDMS triflate)
t-Bu	*tert*-butyl
tert	tertiary
THF	tetrahydrofuran
TLC	thin layer chromatography
UV	ultraviolet
UV-Vis	ultraviolet-visible
wt.%	weight percent
δ	chemical shift (NMR)

5.2 Reference List of Reactions regarding the Azo Series

Synthesis step	Experiment #	Scale
a)	PM-047	20 g
b)	PM-061	700 mg
c)	PM-068	200 mg
b) + c)	PM-063 + PM-070	6 g
d)	PM-075	2 g
e)	PM-092	5 g
f)	PM-095	2 g
g)	PM-096	30 mg
h)	PM-100	1 g

5.3 Reference List of Reactions regarding the HTI Series

Synthesis step	Experiment #	Scale
a)[6]	PM-078	14 g
b) + c)	PM-084 + PM-086	6 g
d)	PM-091	3 g
e)	PM-101	700 mg

6 References

[1] F. Crick, *Philosophical transactions of the Royal Society of London. Series B, Biological sciences* **1999**, *354*, 2021-2025.

[2] A. S. Kristensen, J. Andersen, T. N. Joergensen, L. Soerensen, J. Eriksen, C. J. Loland, K. Stroemgaard, U. Gether, *Pharmacol. Rev.* **2011**, *63*, 585-640.

[3] T. Fehrentz, M. Schoenberger, D. Trauner, *Angew. Chem., Int. Ed.* **2011**, *50*, 12156-12182.

[4] K. Hüll, J. Morstein, D. Trauner, *Chemical Reviews* **2018**, *118*, 10710-10747.

[5] C. Goudet, X. Rovira, A. Llebaria, *Current Opinion in Pharmacology* **2018**, *38*, 8-15.

[6] D. Dreier, PhD thesis, TU Wien (Wien), **2018**.

[7] S. Jia, W.-K. Fong, B. Graham, B. J. Boyd, *Chemistry of Materials* **2018**, *30*, 2873-2887.

[8] H. M. D. Bandara, S. C. Burdette, *Chem. Soc. Rev.* **2012**, *41*, 1809-1825.

[9] A. A. Beharry, G. A. Woolley, *Chem. Soc. Rev.* **2011**, *40*, 4422-4437.

[10] D. Bléger, S. Hecht, *Angewandte Chemie International Edition* **2015**, *54*, 11338-11349.

[11] M. Dong, A. Babalhavaeji, S. Samanta, A. A. Beharry, G. A. Woolley, *Acc. Chem. Res.* **2015**, *48*, 2662-2670.

[12] M. R. Banghart, M. Volgraf, D. Trauner, *Biochemistry* **2006**, *45*, 15129-15141.

[13] P. Cattaneo, M. Persico, *Phys. Chem. Chem. Phys.* **1999**, *1*, 4739-4743.

[14] H. Fliegl, A. Koehn, C. Haettig, R. Ahlrichs, *J. Am. Chem. Soc.* **2003**, *125*, 9821-9827.

[15] D. H. Waldeck, *Chem. Rev.* **1991**, *91*, 415-436.

[16] C. Petermayer, H. Dube, *Acc. Chem. Res.* **2018**, *51*, 1153-1163.

[17] C. Petermayer, S. Thumser, F. Kink, P. Mayer, H. Dube, *J. Am. Chem. Soc.* **2017**, *139*, 15060-15067.

[18] S. Wiedbrauk, H. Dube, *Tetrahedron Lett.* **2015**, *56*, 4266-4274.

[19] J. A. Coleman, E. M. Green, E. Gouaux, *Nature (London, U. K.)* **2016**, *532*, 334-339.

[20] J. A. Coleman, E. Gouaux, E. Gouaux, *Nat Struct Mol Biol* **2018**, *25*, 170-175.

[21] E. Merino, *Chemical Society Reviews* **2011**, *40*, 3835-3853.

[22] K. Takasu, N. Nishida, A. Tomimura, M. Ihara, *Journal of Organic Chemistry* **2005**, *70*, 3957 - 3962.

[23] T. Norris, T. F. Braish, M. Butters, K. M. DeVries, J. M. Hawkins, S. S. Massett, P. R. Rose, D. Santafianos, C. Sklavounos, *Perkin 1* **2000**, 1615-1622.

[24] H. C. Brown, P. Heim, *The Journal of Organic Chemistry* **1973**, *38*, 912-916.

[25] M. Couturier, J. L. Tucker, B. M. Andresen, P. Dube, J. T. Negri, *Org Lett* **2001**, *3*, 465-467.

[26] S. Brandau, A. Landa, J. Franzen, M. Marigo, K. A. Jorgensen, *Angew. Chem., Int. Ed.* **2006**, *45*, 4305-4309.

[27] G. de Gonzalo, R. Brieva, V. M. Sanchez, M. Bayod, V. Gotor, *Journal of Organic Chemistry* **2001**, *66*, 8947-8953.

[28] M. Draskovits, C. Stanetty, I. R. Baxendale, M. D. Mihovilovic, *The Journal of Organic Chemistry* **2018**, *83*, 2647-2659.

[29] J. F. Bower, T. Riis-Johannessen, P. Szeto, A. J. Whitehead, T. Gallagher, *Chemical Communications* **2007**, 728-730.

[30] G. R. Fulmer, A. J. M. Miller, N. H. Sherden, H. E. Gottlieb, A. Nudelman, B. M. Stoltz, J. E. Bercaw, K. I. Goldberg, *Organometallics* **2010**, *29*, 2176-2179.

[31] J. F. Bower, T. Riis-Johannessen, P. Szeto, A. J. Whitehead, T. Gallagher, *Chemical Communications* **2007**, 728 - 730.